

September
2018



Comparing one and two-dimensional hydraulic modelling of flow on varying spatial scales

IDENTIFYING THE PHYSICAL PROCESSES THAT ARE OF INFLUENCE TO THE MODELLING CHOICE OF A STREAM SYSTEM

MASTER THESIS

M.J. Overduin

Comparing one and two-dimensional hydraulic modelling of flow on varying spatial scales

IDENTIFYING THE PHYSICAL PROCESSES THAT ARE OF INFLUENCE TO THE MODELLING CHOICE OF A STREAM SYSTEM

by

M.J. Overduin

to obtain the degree of Master of Science at the Delft University of Technology,
to be defended publicly on 27-09-2018

| | | |
|-------------------|------------------------------|---|
| Student number: | 4627806 | |
| Thesis committee: | Prof.dr.ir. A.J.H.M. Reniers | TU Delft: Environmental Fluid Mechanics |
| | Dr.ir. C.J. Sloff | TU Delft: Rivers, Ports, Waterways and Dredging Engineering |
| | Dr.ir. M. Zijlema | TU Delft: Environmental Fluid Mechanics |
| | Drs. F. Hoefsloot | LievensCSO |

Preface

Hereby, I would like to present my master thesis “Comparing one and two-dimensional hydraulic modelling of flow on varying spatial scales”. Water systems have had my interest for a very long time. When I was a young boy I was already redirecting little streams in the mountains of the Alps. Growing up, the logical consequence was to study water systems during my Bachelor Civil Engineering at the University of Twente and the Master Hydraulic Engineering at the Delft University of Technology. Part and conclusion of the latter is performing a graduation research. I am glad that LievenseCSO offered me the opportunity and their resources to perform this research. The result of over six months of researching is described in this master thesis.

During the process of this research, I gained a lot of insight in the backgrounds of several simulation models, physical processes that are playing a role in rivers and streams and the considerations one has to make before choosing a certain modelling approach. A lot of people have been part of the process that brought me this far. I would like to thank them in this section, starting with the colleagues at LievenseCSO.

First of all, I would like to thank Walter van Doornik and Frans Hoefsloot. Walter, your experience with numerical modelling has been of incredibly value to me. Frans, your feedback helped me to develop the practical considerations that are of value to the users of simulation models. Furthermore, I would like to thank you for the support and opportunity to perform my research at the office of LievenseCSO in Bunnik, Utrecht.

Secondly, I would like to thank my thesis committee. Especially at the start of the research, I had a hard time specifying the exact research goal and direction. The feedback and suggestions of Ad Reniers, Kees Sloff and Marcel Zijlema helped me to give direction to my research and come to the final product of the research, this master thesis.

Furthermore, I would like to thank my fellow interns at LievenseCSO. It was a pleasure working with you, thanks for the good times we had together. I would like to thank my parents for their unconditional support. Most of all, I would like to thank my lovely wife, Thera. Thank you for your love and the fact that you are always there for me. On the first of August, my beautiful daughter Kate was born. I thank God for her and for the strength I have been given to complete this research.

M.J. Overduin

Delft, September 2018

Abstract

In the past years, climate change has caused an increasing number of extreme weather events. In the Netherlands this is, for instance, reflected by the growing amount of extreme rainfall events. This creates big issues for water management authorities like water boards. Water boards are often responsible for local streams, that cannot handle the peak discharges caused by extreme rainfall. This raises the question whether measures have to be taken, for instance by creating additional storage areas to decrease discharge peaks. For questions like these computational model studies can be used to gain insight in the distribution of discharges and water levels.

During these model studies often one-dimensional models are used. Recent developments made two-dimensional modelling, including for instance the simulation of inundation, possible for regular users like water boards. Two-dimensional modelling is proved to be more accurate for rivers, compared to one-dimensional modelling. Water boards, however, often deal with water systems of smaller scale. This raises the question whether it is worth for authorities like water boards to invest their resources in this new modelling approach. Several physical system properties are of influence on the answer to this question. Therefore, the main question of this research is:

Which physical processes are of influence to the choice of a modelling approach, one or two dimensional, for the modelling of stream systems in particular situations?

The methodology of answering this question consists of three major parts:

- 1) identify possible differences in the model properties of 1D versus 2D modelling;
- 2) analyze the output of test models to see whether the differences in model properties actually influence the effects of physical processes; and
- 3) analyze a case area to see whether these processes are important in practice.

The research scope consists of the hydrodynamics of systems with a length scale of $10^3 - 10^5$ m and a temporal scale of hours to a few days. This range corresponds with a range in discharges of a few cubic meters per second up to a few thousands of cubic meters per second. The choice for this range has been made to be able to analyze the effects between the scales of streams and rivers, as until now mostly rivers have been modelled using 2D modelling approaches.

The starting point of this research has been the analysis of differences in model properties. The used flow equations, numerical methods, computational grids and bathymetry implementation are analyzed and the differences are discussed. Concluding, it can be stated that there are differences, which may be of influence to the model output. The main differences are the number of dimensions on which the flow equations are calculated and the way the bathymetry is schematized by the computational grid.

Using these differences, physical parameters have been specified that were varied in a range of test models. These are mainly the parameters that cause 2D effects, like meandering and varying roughness coefficients. The modelling of flood waves could also cause differences due to the fact that the 1D model is not able to model storage with the used default settings. Lastly, the way the bathymetry is used in the simulations is of great importance, due to the way the bathymetry is discretized in 2D models. The goal of varying these physical properties is to analyze whether these variations would influence the quantity of the effects the differences in model properties are causing. Comparing the output of both a 1D and 2D model, it appeared that there are significant differences in the observed water levels. Generally speaking, the following observations were made:

1. The smaller the simulated spatial scale, the larger the 1D-2D differences are

2. The higher the meandering intensity, the larger the 1D-2D differences are
3. The lower the summer bed roughness, the larger the 1D-2D differences are
4. The larger the 2D grid cell size, the larger the 1D-2D differences are
5. The smaller the flood wave duration, the larger the 1D-2D differences are

The underlying physical processes have been analyzed to see how their influence varies in different situations and for different spatial scales. In the end, six processes were found to be influencing the 1D-2D differences:

1. The effects of grid size on bathymetry discretization
2. The water level and velocity difference in cross-sectional direction for varying roughness
3. The water level and velocity difference in cross-sectional direction for varying meandering intensities
4. The interaction between summer bed and floodplains
5. The Boussinesq approach and consequences for the summer bed – floodplain flow area ratio
6. The effects of storage

When combining the findings of the test models and the analysis of a small scale stream system, it was found that the above processes are of the most influence on the following situations:

1. In situations with a complex bathymetry the process of grid discretization is having the most influence.
2. In situations with a high meandering intensity two physical processes are playing a role: high water level and velocity gradients in lateral direction, and a high summer bed – floodplain interaction.
3. In situations with a very low roughness compared to the surrounding area two physical processes are playing a role: high water level and velocity gradients in lateral direction, and a high summer bed – floodplain interaction.
4. In situations with a lot of elevation changes and open water bodies, a lot of potential storage is present.

In these four situations a 2D approach is preferred, as the physical processes that are present in these situations are all processes that are poorly implemented or represented by a 1D model. Of course, there are also some more practical considerations to be made about the modelling choice. The most important one is the research goal; whether inundation modelling is desired and what the required model output is. Another important consideration is the available time for running the simulations; 2D models have a significantly longer simulation time compared to 1D models.

All things considered, this research provides an overview of the differences in model properties between 1D and 2D modelling approaches, an analysis of the important physical processes that determine the choice of a modelling approach and some recommendations about practical issues one could encounter when performing a modelling study.

Table of contents

| | |
|--|-----|
| Preface | iii |
| Abstract..... | v |
| List of figures..... | ix |
| List of tables | xi |
| List of symbols..... | xii |
| 1. Introduction | 1 |
| 2. Research questions and scope | 2 |
| 3. Comparing modelling approaches..... | 6 |
| 3.1 Methodology..... | 6 |
| 3.2 Flow equations | 6 |
| 3.3 D-Flow 1D | 8 |
| 3.4 D-Flow FM | 10 |
| 3.5 Comparison and conclusions..... | 12 |
| 4. Comparing model output | 14 |
| 4.1 Methodology..... | 15 |
| 4.2 Simulation results and observations..... | 28 |
| 4.3 Explaining theories | 41 |
| 4.4 Conclusions | 59 |
| 5. Practical application | 65 |
| 5.1 Case area background | 65 |
| 5.2 Methodology..... | 67 |
| 5.3 Results..... | 74 |
| 5.4 Conclusions | 84 |
| 6. Practical usability..... | 86 |
| 7. Discussion..... | 88 |
| 8. Conclusions | 90 |
| 9. Recommendations | 93 |
| Bibliography | 95 |
| Appendices..... | 98 |
| A. Secondary flow..... | 98 |
| B. Dimensionless numbers | 99 |
| C. Grid criteria | 101 |

List of figures

| | |
|---|-----|
| Figure 0-1: Schematization of basic parameters (Deltares, 2017a) | xii |
| Figure 1-1: Location of the Smakterbroek area | 1 |
| Figure 2-1: Increasing spatiotemporal scales associated with the complexity of flow equations, based on 179 studies (Cheviron & Moussa, 2016)..... | 4 |
| Figure 3-1: Staggered grid (Zijlema, 2015)..... | 9 |
| Figure 3-2: Grid schematization SOBEK-model (Deltares, 2017a) | 9 |
| Figure 3-3: Unstructured grid (Deltares, 2017b) | 11 |
| Figure 4-1: SOBEK D-Flow 1D – upper figure is total model, bottom figure is zoom on single meander in red square – eye icons = observation point locations, blue line = summer bed, grey lines = cross sections, white dots = grid points..... | 14 |
| Figure 4-2: D-HYDRO D-Flow FM – upper figure is total model, bottom figure is zoom on single meander in red square – eye icons = observation point location, pink line = observation cross section locations, yellow part = summer bed, green part = floodplains, purple line = summer bed/floodplain division, orange lines (quadrilaterals and triangles) = computational grid..... | 14 |
| Figure 4-3: Power laws for water depth and flow width – orange laws are of Dury (1976), blue laws are newly developed | 15 |
| Figure 4-4: Profile schematizations, with increasing scale from top to bottom - Main = summer bed, Section001 = flood plains. To give an example: in the upper figure a discharge of 5 m ³ /s fills the summer bed, a discharge of 15 m ³ /s fills the summer bed and both flood plains. | 16 |
| Figure 4-5: Meandering profiles, yellow parts are summer bed, green parts are flood plains | 18 |
| Figure 4-6: River meander characteristics (Williams, 1986) | 18 |
| Figure 4-7: Discharge-time graph of flood waves, for scale Q = 5 m ³ /s..... | 19 |
| Figure 4-8: Default grid used in simulations - 10 curvilinear cells in cross-sectional direction..... | 20 |
| Figure 4-9: Grid used for analysis of influence of bathymetry discretization – 5, 10 and 20 curvilinear cells in cross sectional direction | 21 |
| Figure 4-10: SOBEK D-Flow 1D (Q5000, extensive meandering) – upper figure is total model, bottom figure is zoom on single meander in red square – the eye icons represent the observation point locations..... | 24 |
| Figure 4-11: D-HYDRO D-Flow FM (Q5000, extensive meandering) – upper figure is total model, bottom figure is zoom on single meander in red square – the eye icons represent the observation point locations - the pink lines represent the observation cross section locations..... | 24 |
| Figure 4-12: Location and numbering of observation locations of flood wave models - top figure is 1D, bottom figure is 2D | 24 |
| Figure 4-13: Conveyance view SOBEK Suite | 26 |
| Figure 4-14: Hydraulic radius and polynomial regression relations for scale Q = 5000 m ³ /s..... | 26 |
| Figure 4-15: Average water depths of all simulations | 28 |
| Figure 4-16: Average flow velocities of all simulations..... | 29 |
| Figure 4-17: Differences in water level for varying meandering intensities | 30 |
| Figure 4-18: Differences in water level for varying roughness coefficients | 32 |
| Figure 4-19: Results of grid size analysis (5 vs. 1D means: difference between 2D simulation with 5 grid cells in lateral direction and 1D simulation) | 34 |
| Figure 4-20: Numbering of observation points (left side is upstream) – top figure is 1D, bottom figure 2D..... | 35 |
| Figure 4-21: Root mean square error of discharge differences of flood wave over entire flood wave period, at observation point #10 (logarithmic y-axis) | 35 |

| | |
|--|----|
| Figure 4-22: Relative (absolute differences divided by peak discharge of flood wave) difference flood wave (cf. Figure 4-20 for the observation locations) | 36 |
| Figure 4-23: Q-t graphs flood waves (1_1D means first observation point, 1D model output, cf. Figure 4-20) | 37 |
| Figure 4-24: Cross sections for varying grid sizes (Q=5 scale) - the green dots indicate the data points on which the bathymetry is based | 41 |
| Figure 4-25: Cross sections for varying grid sizes (Q = 5000) | 42 |
| Figure 4-26: Flow velocity in cross-sectional direction in different situations | 44 |
| Figure 4-27: Flow velocity in cross section for varying roughness, derived from plots above (n = 0.02 causes lower water levels, therefore the outer two grid cells are not flooded, so no flow velocity is present there) | 45 |
| Figure 4-28: Water level gradients in cross section for varying roughness coefficients | 45 |
| Figure 4-29: Flow velocity in cross-sectional direction for scale 5000 with varying meandering intensities | 47 |
| Figure 4-30: Flow velocity in cross-sectional direction for scale 5000 with varying meandering intensities | 47 |
| Figure 4-31: Location of the vector plot | 49 |
| Figure 4-32: Flow vectors for varying roughness coefficients over floodplain, scale Q = 5000, floodplain flow | 49 |
| Figure 4-33: Ratio of summer bed flow area over total flow area | 53 |
| Figure 4-34: Froude numbers for floodplain flow, averaged over meandering intensity | 54 |
| Figure 4-35: Location of vector plots | 55 |
| Figure 4-36: Q-t graph of analyzed situation | 55 |
| Figure 4-37: Flow velocity vectors on three moments in time | 56 |
| Figure 4-38: Water level slopes during rising and falling flood (Fox, 2015) | 57 |
| Figure 4-39: Flow velocity vectors, Q = 5000 | 57 |
| Figure 4-40: Q-t graphs of flood waves | 58 |
| Figure 4-41: Relative difference, scale comparison | 61 |
| Figure 4-42: Change in relative difference for several changes in model schematizations, summer bed flow | 62 |
| Figure 4-43: Change in relative difference for several changes in model schematizations, floodplain flow | 63 |
| Figure 4-44: Average Reynolds and Froude number for all scales, averaged over all simulations | 64 |
| Figure 5-1: Location of the case area | 65 |
| Figure 5-2: Elevation data of the Molenbeek catchment | 66 |
| Figure 5-3: Modelled areas - the black square is an enlargement of the area of the most interest | 69 |
| Figure 5-4: Example of the implemented grid structure – enlargement of the purple square | 70 |
| Figure 5-5: Observation locations | 71 |
| Figure 5-6: Area of interest for observation 1 | 72 |
| Figure 5-7: Three examples of simulated bathymetries in 1D and 2D | 74 |
| Figure 5-8: Flow velocity at discharge of 6.5 m ³ /s | 76 |
| Figure 5-9: Water level at discharge of 6.5 m ³ /s | 76 |
| Figure 5-10: Flow velocity and water depth of indicated cross section in previous figure | 77 |
| Figure 5-11: Flow vectors (colored by magnitude) in meander, at discharge of 6.5 m ³ /s, example 1 | 78 |
| Figure 5-12: Flow vectors (colored by magnitude) in meander, at discharge of 6.5 m ³ /s, example 2 | 78 |
| Figure 5-13: Water depth at discharge of 6.5 m ³ /s, part 1 – dark blue is not flooded | 80 |
| Figure 5-14: Water depth at discharge of 6.5 m ³ /s, part 2 – dark blue is not flooded | 80 |
| Figure 5-15: Locations of all observation points used for this section | 81 |

| | |
|---|-----|
| Figure 5-16: Discharge time of all observation points during small flood wave | 81 |
| Figure 5-17: Discharge time of all observation points during large flood wave | 83 |
| Figure 5-18: Relation dimensionless numbers and relative 1D-2D water level difference + case area indication (red dots) | 84 |
| Figure A-1: River bend processes (Graf & Blanckaert, 2002) | 98 |
| Figure C-1: Examples of smoothness and orthogonality (Deltares, 2017b) | 101 |
| Figure C-2: Example of perfect smoothness and orthogonality (Deltares, 2017b) | 101 |

List of tables

| | |
|---|----|
| Table 3-1: Comparison of modelling modules | 12 |
| Table 4-1: Schematization properties | 17 |
| Table 4-2: Simulations overview (see Table 4-1 for more information) – HW = high water (cf. Figure 4-7) | 22 |
| Table 4-3: Output parameters | 25 |
| Table 4-4: Wave celerities on varying scales | 38 |
| Table 4-5: Flow areas, for scale Q = 5 and varying schematizations (cf. Figure 4-19) | 42 |
| Table 4-6: Grid size variation for no meandering situations | 43 |
| Table 4-7: Water level gradients for varying roughness coefficients, scale Q = 5 | 46 |
| Table 4-8: Water level gradients for varying roughness coefficients, scale Q = 5000 | 46 |
| Table 4-9: Water level gradients for varying meandering intensities | 48 |
| Table 4-10: Discharges and flow velocities of floodplains 1 and 2 (Figure 4-31) - Q = discharge, U = velocity = FP1 = floodplain 1, SB = summer bed | 50 |
| Table 4-11: Alpha calculation method, default (the computation is written out below) | 52 |
| Table 4-12: Alpha calculation method, accurate method | 52 |
| Table 4-13: Alpha values and difference in area ratio | 53 |
| Table 4-14: Concluding table of coupling between observations and processes | 59 |
| Table 4-15: Average values of changes in relative difference, summer bed flow | 62 |
| Table 4-16: Average values of changes in relative difference, floodplain flow | 63 |
| Table 5-1: System characteristics of stream system Molenbeek | 67 |
| Table 5-2: Simulation overview case area | 73 |
| Table 5-3: Comparison case area to theoretical models (Q = 5 scale) | 77 |
| Table 5-4: Distances and travel times between observation points | 82 |
| Table 5-5: Distance and travel time of flood wave | 83 |
| Table 6-1: Computer characteristics | 86 |
| Table 6-2: Simulation times 1D versus 2D | 86 |
| Table 6-3: Simulation time of case area parts | 87 |

List of symbols

x, y, z = directions in Cartesian coordinate system

u, v, w = flow velocity in x, y, z directions [m/s]

NAP = Amsterdam Ordnance Datum or Normaal Amsterdams Peil (in Dutch)

ρ = density [kg/m^3]

p = pressure [N/m^2]

ν = kinematic viscosity [m^2/s]

g = gravitational acceleration [m/s^2]

A = cross sectional flow area [m^2]

C = Chézy coefficient [$\text{m}^{1/2}/\text{s}$]

ζ = water level [$\text{m} + \text{NAP}$]

L_x = length of resistant branch segment

Q = discharge [m^3/s]

R = hydraulic radius [m]

ω_f = water surface width [m]

τ_{wind} = wind shear stress [N/m^2]

ξ = extra resistance coefficient [s^2/m^5]

P_w = wetted perimeter [m]

D = hydraulic depth [m]

B = average flow width [m]

k_m = manning coefficient (Bos – Bijkerk) [$\text{m}^{1/3}/\text{s}$]

γ = roughness parameter [$1/\text{s}$]

h = water depth [m]

z_b = bed level [$\text{m} + \text{NAP}$]

n_m = manning coefficient [$\text{s}/\text{m}^{1/3}$]

$Q_{T=1}$ = discharge occurring once every year [m^3/s]

P = precipitation [m], [m^3/s]

E = evaporation [m], [m^3/s]

q = specific discharge [m^2/s]

F, M = external momentum contributions in the Navier – Stokes equations [m/s^2]

f = Coriolis parameter [rad/s]

T = return period [1/year]

c = wave celerity [m/s]

i_b = bed slope [m/m]

L_m = wave length meander [m]

K = conveyance [m^3/s]

In this research, the parameters water depth, water level and bed level are defined as schematized in the figure below.

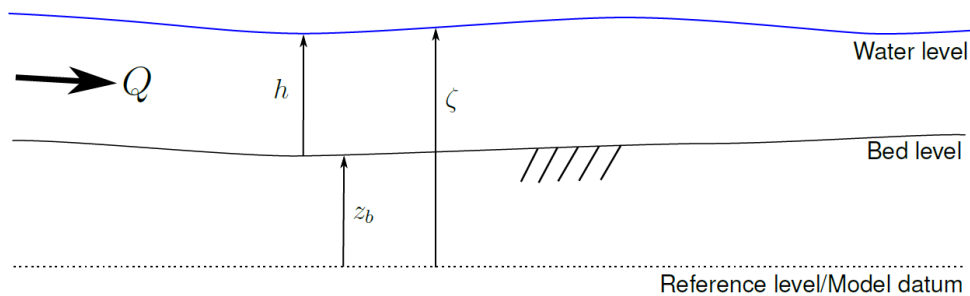


Figure 0-1: Schematization of basic parameters (Deltares, 2017a)

1. Introduction

Extreme rainfall in the summer of the year 2016 has caused flooding of an area in the Netherlands, called Smakterbroek. This area is located in the management area of the water board *Aa en Maas*. The location of the area is given in Figure 1-1. Especially at the stream Molenbeek near the village of Vierlingsbeek the problems were severe and led to a lot of compensation claims. Engineering firm LievenseCSO was asked by the water board to determine the causes of this problem and whether measures have to be taken.

Research projects like the one mentioned above are often carried out using simulation models. Basically, these models contain information about the water courses, water in and outflows and boundary conditions. When running these models, one can gain information about local discharges, water levels and flow velocities. The modelling approach often applied by LievenseCSO is using the one-dimensional flow modelling suite SOBEK. As the stream Molenbeek ends up in the river Meuse, a water level of this river would be the boundary condition of the simulation.



Figure 1-1: Location of the Smakterbroek area

Recent developments of more advanced modelling suites raised the question at LievenseCSO whether these are more suited to model an area like the one described above. One of these suites is the D-HYDRO Suite, developed by Deltares, a research institute in the Netherlands (Deltares, 2017b). This suite can be used to run a flow module called D-Flow FM, which is able to model flow in two dimensions, instead of only one. Because the D-Flow FM module is until now mainly used to model systems of larger scale, mostly rivers, the question emerges whether it is practically and technically suited for the modelling of small-scale water systems, which have a natural discharge of a few cubic meters per second instead of hundreds or even thousands of cubic meters per second.

Besides the comparison of both modelling approaches, 1D versus 2D, the comparison can also be made between these different scales to see whether the models perform differently on varying scales. Comparing different scales can point out whether a certain modelling approach is indeed more suited to model rivers, or is very much able to model smaller scale systems. If the differences between both approaches are significant, it may also be possible to determine what the causes of these differences are.

Of course, 2D modelling approaches have a clear advantage: the ability of modelling more than just the main channel, for instance flood inundation. The goal of this research is purely to compare both approaches on differences in this main channel flow modelling. This is in the end the most important part and starting point of the model.

2. Research questions and scope

The previous chapter introduced the general subject of the research: the comparison of modelling approaches on varying spatial scales. In this case, this will be a 1D approach versus a 2D approach. Besides 1D and 2D modelling approaches, another option is to use a coupled 1D/2D approach. Fernández-Nieto et al. (2010) show that 1D/2D-modelling can also be relevant to modelling studies, but that there are often problems for curvilinear 1D channels and mismatching 2D grids. 2D models avoid arbitrary 1D-2D links and human errors in defining the model parameters (Néelz & Pender, 2013). Of course, human errors in model parameters are always possible, both in 1D and 2D modelling. However, in 1D/2D-coupled modelling more parameters have to be specified, and therefore this type of modelling is more vulnerable to these kind of errors. Besides, when comparing 1D and 2D, a 1D/2D-coupled model would introduce errors which are very hard to identify in the model output. Therefore, this research will not incorporate 1D/2D-coupled models.

Dimitriadis et al. (2016) state that the most important question, based on their research on the comparison of several modelling approaches, is whether more advanced modelling has more advantages than simple approaches. The more sophisticated the approach, the more demanding in terms of data and computational resources it becomes. Therefore, they say, *“the recognition and quantification of the multiple sources of uncertainty will certainly help towards establishing an acceptable compromise between accuracy and parsimony”*. This research will in the first place look for these sources of uncertainty by analyzing the model properties of the modelling suites and the effects of these properties on the simulation of physical processes in the water systems. The other part will consist of a practical application on a case area, to see whether the sources of uncertainty play a role in practical situations.

The considerations as posed in the introduction lead to the following main question:

Which physical processes are of influence to the choice of a modelling approach, one or two dimensional, for the modelling of stream systems in particular situations?

Because of availability, experience and convenience, the D-Flow 1D (SOBEK) module is used to simulate the 1D models, whereas the 2D models are simulated in the D-Flow FM (D-HYDRO) module. There are also a 1D and 3D solver available in FM, but this will not be incorporated in this research. To give a thorough answer to the main question, the following sub questions will be answered:

1. How do the model properties of the simulation models D-Flow 1D and D-Flow FM differ?

The first sub question suggests a bottom-up approach. The reasoning behind this is to be able to establish important parameters that differ between the simulation models. These parameters will be the input for variations in physical parameters, used in the next question, where the sensitivity of the model properties on the model performance will be tested. From this, conclusions can be drawn about the situations in which the modelling approaches will perform better. This will be tested in theoretical models, which will answer the second sub question:

2. What are the differences in model output for varying physical properties of the systems and which processes are causing these differences?

A case study of a small-scale stream system will be analyzed to see whether the problems encountered in sub question 2 actually play a role in practice. This will answer the third sub question:

3. What physical processes are particularly important in a practical case of a small-scale system?

The scope of this research is to identify differences in model properties, which could influence the effects of physical parameters. Analyzing these model properties can be performed on an advanced level, where processes like numerical diffusion and errors in propagation come into play. This would require an extensive analysis of the applied numerical schemes, which is out of the scope of this research. The analysis of model properties will be on a basic level, dealing with issues like flow equations¹ and computational grid² structures. The focus will be on the physical processes, which effects could be influenced by the differences in model properties. The next chapter will explain this in more detail.

Based on the three sub questions an answer can be formulated to the main question. To summarize, this research will;

- 1) identify possible differences in the model properties of 1D versus 2D modelling;
- 2) analyze the output of test models to see whether the differences in model properties actually influence the effects of physical processes; and
- 3) analyze a case area to see whether these processes are important in practice.

An example might help to understand the scope of the research. When comparing model A (1D) to model B (2D), one could find out that there is a difference in the flow equations that are used. Model B solves also equations in lateral direction³, model A does not. A physical system property, which effect could be influenced by this, is meandering⁴, for instance. Meandering may cause gradients in water level and velocities in lateral direction, so model B should be more capable of simulating this, compared to model A. Test models will be generated of streams or rivers with varying meandering intensities, to analyze the effects. This is an example of a process that will be dealt with in this research. Furthermore, this research will analyze the processes behind the meandering to find out why some situations or spatial scales are more influenced by this process than others. Lastly, this research will analyze a case area. In this case area, one could again look for meanders, to see whether they have the same shape and intensity, and to see whether the same processes are going on. In this way, some useful remarks can be given about the issues one can encounter during modelling studies and some tips can be provided.

Generally speaking, there are a few ways in which simulation models or modelling approaches can be compared to each other (Cheviron & Moussa, 2016):

- Scale; domain length, flow depth, meandering wave length and amplitude
- Flow typology; bed topography, morphology, extreme events
- Dimensionless numbers; Reynolds number, Froude number
- Model refinement; Navier-Stokes vs. Saint-Venant, grid, assumptions, areas of application

¹ In most river or stream modelling activities the so-called flow equations are used to be able to calculate water depths, discharges or other parameters one could be interested in. Basically, these equations are on the basis of the simulation models.

² A computational grid consists of nodes and elements on which the model calculates the parameters and output. A grid is necessary because it is impossible to calculate all parameters at every location in the model, which are infinite. Therefore, a grid has to be constructed where the calculation locations can be specified. More on this will be discussed in the next chapter.

³ Perpendicular direction to the flow direction. Another used term for the same direction is cross sectional direction.

⁴ Meandering is the process of the emergence of curves in a river, often initiated by erosion and sedimentation of the outer and inner bends.

In this research, the model refinement will be dealt with at first. In this section, the model properties of both modelling approaches will be compared. The consideration is made whether the simulation of several physical properties of water systems will be affected by differences in these modelling approaches. These physical properties will be used to generate the model schematizations. These models will be used for several simulations, performed on different scales, where among others physical properties like bed topography and extreme events will be varied to find out what the influence is. Because this research will focus on the hydrodynamics of the systems, the morphology will not be taken into account. The dimensionless numbers are used to be able to describe the systems and explain differences that will follow from the model output.

In the paper of Cheviron & Moussa (2016), the range of spatial scales that are dealt with is quite significant. On that range, the differences in used flow equations – they compared Navier Stokes (NS), Reynolds-averaged Navier Stokes (RANS), Saint-Venant (SV) and approximations to Saint-Venant (ASV) with each other – are clearly visible. The figure below illustrates this. The range of spatial scales is also shown on the horizontal axis.

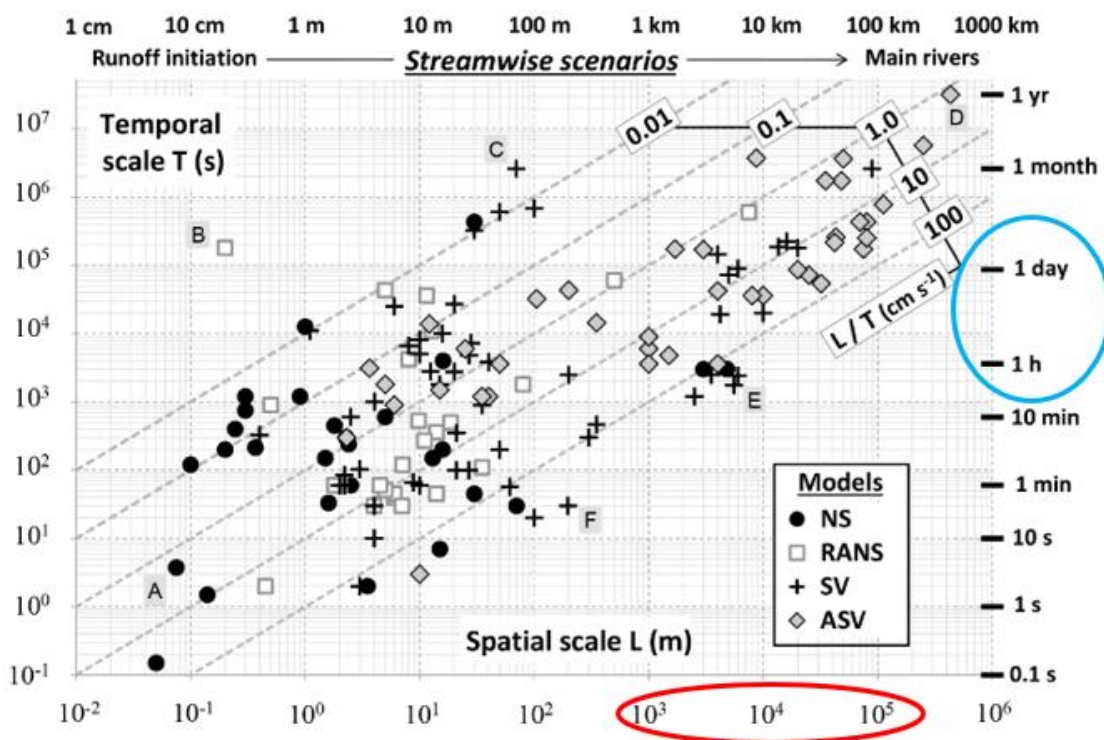


Figure 2-1: Increasing spatiotemporal scales associated with the complexity of flow equations, based on 179 studies (Cheviron & Moussa, 2016)

Obviously, this research will not deal with this large range of scales and flow equations. The precise scales will be based on a range of discharges, as mentioned in the introduction, between a few cubic meters per second towards thousands of cubic meters per second. To illustrate the spatiotemporal scales, one can roughly say that length scale, this research focuses on the range of an hour to a few days (blue circle in the figure). The associated flow velocity (depicted as L/T in the figure) is approximately 1 m/s or 100 cm/s in the analyzed systems, which makes the analyzed length scale between $10^3 - 10^5$ m (red circle).

Teng et al. (2017) summarize the difference between 1D and 2D modelling approaches as follows: “The 1D versions are computationally efficient, but they suffer from a number of drawbacks including

the inability to simulate lateral diffusion of the flood wave, the discretisation of topography as cross sections rather than as a continuous surface and the subjectivity of cross section location and orientation. The 2D versions that solve full shallow water equations have been reported to be able to simulate timing and duration of inundation with high accuracy. Nevertheless they are computationally intensive. The 2D and 3D models are generally considered as unviable for areas larger than 1000 km² when the resolution required is less than 10m and/or in a probabilistic approach requiring multiple simulations as the time taken to run simulations may be prohibitively long.”

This research will find out whether the issues mentioned in the citation above are of actual importance, and whether there are issues that are not mentioned. Furthermore, this research will analyze the differences and discuss whether they are of the same importance on varying spatial scales. The first sub question will be answered by means of literature study, presented in chapter 3. Chapter 4 will answer the second sub question, and chapter 5 the last one. In chapter 6 the practical usability of the models will be discussed. Chapter 7 will analyze some of the uncertainties of the research. Based on the combination of answers, chapter 8 will provide an answer to the main question. The last chapter will elaborate on some recommendations for modelling studies of stream systems or follow-up researches.

3. Comparing modelling approaches

In this chapter, the first sub question will be answered: How do the model properties of the simulation models D-Flow 1D and D-Flow FM differ? This chapter is built up as follows: First of all, the methodology will be discussed. Secondly, to be able to understand the models, it is important to understand the flow equations on which the models are based. These equations will be analyzed in the second paragraph. The third and fourth paragraph will discuss the model characteristics of both D-Flow 1D and D-Flow FM. The last paragraph will compare these characteristics and draw conclusions on what differences may be of influence to possible output differences.

3.1 Methodology

This question will be answered by means of a literature study. The used flow equations, construction methods of the computational grids (1D vs. 2D), the underlying assumptions and the suggested application areas can be compared. After performing this literature study, the most important differences in model properties, that could be of influence to the model performance will be selected. These parameters will be the input to sub question 2.

3.2 Flow equations

In most river or stream modelling activities the so-called flow equations are used to be able to calculate water depths, discharges or other parameters one could be interested in. These flow equations are based on the Navier-Stokes equations. The NS equations are derived from the 3D mass and momentum conservation equations based on Newton's second law. After averaging over a characteristic time period, one can derive the Reynolds-averaged Navier-Stokes (RANS) equations. After doing this, one can continue by spatial averaging over the vertical direction and obtain the two-dimensional Shallow Water Equations (2D SWE or 2DH SWE). The next possible simplification is to average the 2D SWE over the lateral direction and obtain the Saint-Venant equations. These are, in other words, the 1D SWE equations. D-Flow 1D is based on the latter equations. D-Flow FM is based on the depth-averaged RANS equations, i.e. the 2D SWE.

The equations as implemented in D-Flow FM are given below (Deltares, 2017b):

$$\frac{\partial h}{\partial t} + \frac{\partial hu}{\partial x} + \frac{\partial hv}{\partial y} = Q \quad 3.1$$

$$\frac{\partial u}{\partial t} + u \frac{\partial u}{\partial x} + v \frac{\partial u}{\partial y} - fv = -\frac{1}{\rho_0} P_x - \frac{gu\sqrt{u^2 + v^2}}{C_{2D}^2 h} + F_x + F_{sx} + M_x \quad 3.2$$

$$\frac{\partial v}{\partial t} + u \frac{\partial v}{\partial x} + v \frac{\partial v}{\partial y} + fu = -\frac{1}{\rho_0} P_y - \frac{gv\sqrt{u^2 + v^2}}{C_{2D}^2 h} + F_y + F_{sy} + M_y \quad 3.3$$

where

Q = contributions per unit area due to discharge or withdrawal of water, precipitation and evaporation

ρ_0 = reference density [kg/m^3]

P = pressure [N/m^2]

u, v = flow velocity [m/s]

h = water depth [m]

F, M = external momentum contributions [m/s^2]

f = Coriolis parameter [rad/s]

C = Chézy coefficient [$m^{1/2}/s$]

- other symbols are listed in the List of Symbols (on page xii)

These equations are based on the Cartesian coordinate system. Besides Reynolds averaged, the equations are also based on the f-plane, Boussinesq and incompressible fluid assumptions. The f-plane approximation is based on the assumption that the Coriolis parameter is constant with latitude (Pietrzak, 2017). The Boussinesq approximation is based on the assumption that differences in density are small with respect to the density itself. Based on this, it is assumed that density differences do not influence the horizontal momentum. The incompressible fluid assumption assumes that the density is constant when moving with the fluid. The equations include forces, induced by unbalances of horizontal Reynolds stresses, and contributions due to external sinks or sources of momentum (Deltares, 2017b). This could be forces of structures, wind or waves, for instance. Under the shallow water assumption, the vertical momentum equation is reduced to a hydrostatic pressure equation.

The SV equations as implemented in D-Flow 1D are given below (Deltares, 2017a):

$$\frac{\partial A}{\partial t} + \frac{\partial Q}{\partial x} = q_{lat} \quad 3.4$$

$$\frac{\partial Q}{\partial t} + \frac{\partial}{\partial x} \left(\frac{Q^2}{A} \right) + gA \frac{\partial \zeta}{\partial x} + \frac{gQ|Q|}{C^2RA} - \omega_f \frac{\tau_{wind}}{\rho_w} + gA \frac{\xi Q|Q|}{L_x} = 0 \quad 3.5$$

where

A = cross sectional flow area [m^2]

Q = discharge [m^3/s]

R = hydraulic radius [m]

C = Chézy coefficient [$m^{1/2}/s$]

ζ = water level [m + NAP]

- other symbols are listed in the List of Symbols

Here, the x-direction is the stream direction. This is different from the 2D SWE equations. As the SV equations are derived from the RANS equations, the same assumptions apply. Usually, the Saint-Venant momentum equation only consists of the first four terms of equation 3.5, which describe inertia, convection, the water level gradient and the bed friction. This reduced form of the momentum equation, in combination with the continuity equation where q_{lat} (eq. 3.4) is equal to zero, are also called the long wave equations (Battjes & Labeur, 2017). Because these equations are simplified forms of the Navier-Stokes equations, the last two terms have been added to incorporate some effects that could be of influence. In this case these effects are wind force and extra resistance of for instance structures, such as bridges.

3.3 D-Flow 1D

D-Flow 1D is the most known and used module of the SOBEK Suite. A brief introduction of the most important parts will be given in this paragraph.

Model equations

The water flow is computed by solving the complete Saint-Venant equations (Deltares, 2017a). For 1D channel flow, the 1D continuity equation (eq. 3.4) and the 1D momentum equation (eq. 3.5) are solved. The effects of boundary friction and turbulence can be accounted for through resistance laws analogous to those used for steady flow (Deltares, 2018a).

Numerical method

The D-Flow 1D module uses a numerical scheme called the Delft flooding-scheme⁵ (FLS) to solve the SV equations. The most important criterion during the design of this scheme has been the robustness. A robust scheme guarantees a solution for every time step, and can furthermore deal with phenomena as super and subcritical flow, flow transitions (like hydraulic jumps) and drying/flooding (Deltares, 2017a). Although it guarantees a solution for every time step, the actual internal computational timestep can be decreased when required by certain flow conditions (Deltares, 2017a). The numerical accuracy of the solution depends mainly on the grid size. Obviously, smaller grid sizes produce more accurate solutions, but also result in a longer simulation time. The combination of grid size and time step is combined in a criterion called the CFL-condition, which calculates the Courant number (Zijlema, 2015). This number is calculated as follows for 1D-modelling:

$$\sigma = \frac{|u|\Delta t}{\Delta x} \quad 3.6$$

where

u = flow velocity [m/s]

Δt = time step [s]

Δx = grid size [m]

In general, for most schemes, this number should be smaller than 1 to guarantee stability. Usually, in hydraulic modelling a conservative maximum value of the Courant number is chosen, for instance 0.7 (Warner (2010), Sündermann & Holz (2012); Deltares (2017b)). The velocity is usually not varying much, therefore the numerical stability mainly depends on the time step and grid size. As the grid size is most of the time determined before the simulation, the time step will be adjusted during the simulation when stability needs to be guaranteed. For 2D-modelling, the same condition can be used. In this case the Courant number is also calculated for the y-direction.

Computational grid

D-Flow 1D uses a so-called staggered⁶ grid approach (Deltares, 2017a). In this grid arrangement the variables ζ (water level) and u (velocity) are calculated at alternate grid points (Zijlema, 2015). A schematization of a staggered grid is given in Figure 3-1. In general, the network nodes (boundary and connection nodes, see Figure 3-2) of a 1D-model are ζ -calculation points.

⁵ See Duinmeijer (2002) for more information about the Delft FLS.

⁶ For more information on staggered schemes for shallow water flows, see Stelling & Duinmeijer (2003).

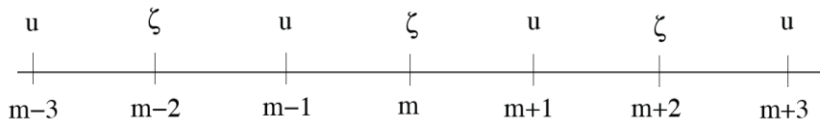


Figure 3-1: Staggered grid (Zijlema, 2015)

In the channels between the nodes the ζ -calculation points are defined. In the D-Flow 1D module, the momentum equation is solved between ζ -calculation points, the continuity equation is solved between the u -calculation points. Generally, the grid size is determined by a typical spatial scale of the problem that is studied. Obviously, the distance between two grid points should not be too small in order to restrain the simulation time. On the other hand, the distance should not be too large, in order to be accurate and represent the physical processes properly. A schematization of calculation points as implemented in D-Flow 1D is given in Figure 3-2.

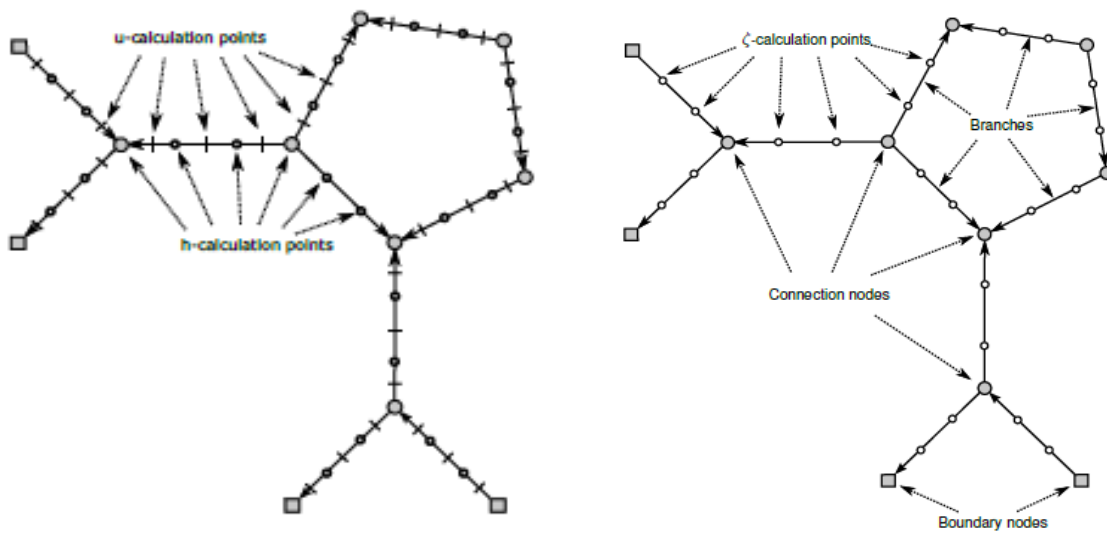


Figure 3-2: Grid schematization SOBEK-model (Deltares, 2017a)

Bathymetry

At arbitrary locations on branches in a model, cross sections can be defined with for instance Y and Z data. D-Flow 1D interpolates the bathymetry of the system between these cross sections. To increase accuracy, it is therefore desirable to have as much data, both measurements per cross section as the number of measured cross sections, available as possible.

3.4 D-Flow FM

D-Flow FM is the most known and used module of the D-HYDRO Suite. In this research, only the 2D solver of this module will be used.

Model equations

The D-Flow FM module solves the depth-averaged, so 2D, continuity equation (eq. 3.1) and momentum equations, see equations 3.2 and 3.3. Also turbulence is modeled by D-Flow FM. In general, the grid sizes and time steps are too large to resolve the turbulent scales of motion (Deltares, 2017b). Assumed is that the horizontal turbulence coefficients are a superposition of three parts: molecular viscosity, 2D-turbulence and 3D-turbulence⁷. Molecular viscosity is already incorporated in the Navier-Stokes equations. The second part cannot be resolved by the horizontal grid of D-Flow FM (Deltares, 2017b). The third part, the 3D part, is solved by a turbulence closure method that uses space and time-averaged variables. For two-dimensional, depth averaged (2DH), simulations, the horizontal eddy viscosity and eddy diffusivity coefficient should also contain a contribution due to the vertical variation of the horizontal flow. In Delft3D-FLOW, another product of Deltares, a sub-grid scale model, called HLES (Horizontal Large Eddy Simulation) is implemented, but this is not yet the case in the D-Flow FM module. Instead, FM contains a simplified horizontal model, so very large grid size variations can be coped with (Deltares, 2017b). The model, used in the turbulence closure method, is called the k - ϵ turbulence closure model. This model solves equations about the dissipation rate (ϵ) and turbulent kinetic energy (k).

Numerical method

D-Flow FM uses a numerical scheme similar to the Delft FLS as used in D-Flow 1D. Also for this numerical scheme, the CFL-condition applies, as explained in the previous sub paragraph about D-Flow 1D. Because of the 2D nature of this module, two separate CFL-conditions have to be applied, both in x and y-direction. The scheme is capable of dealing with all flow types, subcritical or supercritical. Also bore propagation velocities and eddy shedding flows are modelled accurately (Deltares, 2017b).

Computational grid

FM or Flexible Mesh refers to the flexible grid composition in D-Flow FM. Grids can be combinations of multiple types of grid cell shapes, like triangles, quadrilaterals, pentagons and hexagons. An often used type is the curvilinear grid, which exists of quadrilaterals. In Figure 3-3, this grid type is used in the waterways. If a grid contains triangles, it is called unstructured. An example of an unstructured grid is given in Figure 3-3. D-Flow FM uses a staggered grid arrangement comparable to D-Flow 1D. Usually, channel beds are modelled using a standard curvilinear grid containing quadrilaterals, as this is more accurate and less computationally demanding; floodplains and other areas are modelled using other types of grids, mostly triangular ones, as this captures the complex geometries much better, but with the cost of possibly lower numerical accuracy.

⁷ See Uittenbogaard et al. (1992) for more on this subject.

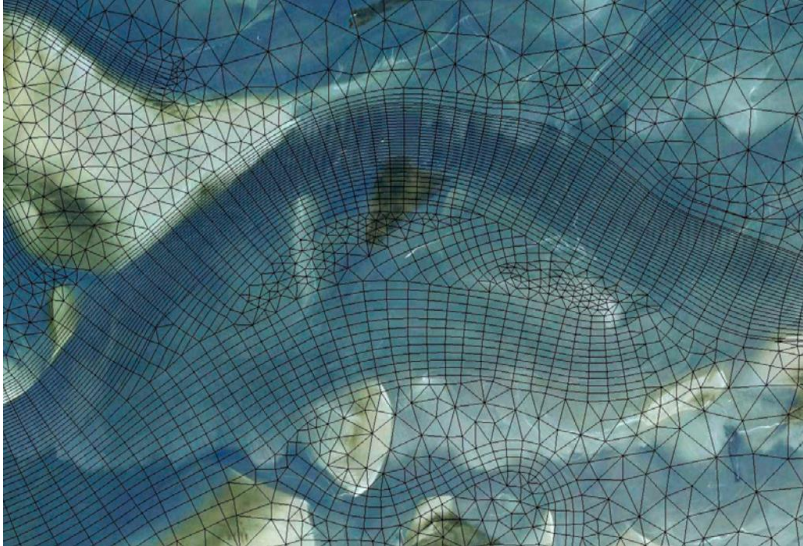


Figure 3-3: Unstructured grid (Deltares, 2017b)

Bathymetry

Unlike D-Flow 1D, D-Flow FM needs the complete bathymetry as input. This can be obtained from direct measurements, or can be manually interpolated from measured cross sections using software like ArcGIS. The fact that, in contrast to a 1D model, grid cells are assigned in cross-sectional direction, means that the bathymetry is discretized. This has as consequence that accuracy may be lost, depending on the number of grid cells.

3.5 Comparison and conclusions

Both modules have a set of underlying assumptions that are on the basis of the simulations. The most important assumptions to this research of the Flow-1D module of the SOBEK Suite and the Flow-FM module of the D-HYDRO Suite are given in the first part of the table below (Deltares, 2018a). The assumptions have often a direct link with the model equations and approaches, therefore they are coupled in the first part of the table. Also, in the previous paragraphs, both modules have been described on the aspects of numerical methods, computational grids and bathymetry construction. An explanation and elaboration of the aspects is given below the table.

Table 3-1: Comparison of modelling modules

| D-Flow 1D (SOBEK) | D-Flow FM (D-HYDRO) |
|---|---|
| Underlying assumptions and model equations | |
| The flow is one-dimensional i.e. the velocity can be represented by an average flow over the cross section and the water level can be assumed to be horizontal across the section. | The flow is two-dimensional, water levels can differ in cross-sectional direction and cause pressure differences. Velocity differs in cross-sectional direction (horizontally). |
| The used model equations are the SV equations with some additions compared to the standard 1D SWE. | The used model equations are the depth-averaged RANS equations under the hydrostatic pressure assumption. |
| The effects of boundary friction and turbulence can be accounted for through resistance laws analogous to those used for steady flow. | The model is capable of resolving the turbulent scales (large eddy simulation), but usually the hydrodynamic grids are too coarse to resolve the fluctuations. |
| 2D/3D dynamic effects in (sharp) bends are not taken into account, i.e., their effect on the global flow behavior is assumed negligible. | In 2DH-simulations, secondary flow is computed post-process (i.e. indirectly) by numerical techniques that calculate streamline curvatures and spiral motion/secondary flow ⁸ (Deltares, 2017b). |
| Numerical method | |
| The CFL-condition (Courant wave number) applies, which can increase the computation time due to time step restrictions. | The CFL-condition (Courant flow number) applies, which can increase the computation time due to time step restrictions. |
| Robust scheme, which is able to generate a solution for every time step, and can furthermore deal with phenomena as super-critical flow, flow transitions (like hydraulic jumps) and drying/flooding. | Robust scheme, which is capable of dealing with all flow types, subcritical or supercritical. Also bore propagation velocities and eddy shedding flows are modelled accurately. |
| Computational grid | |
| Staggered grid | Staggered grid |
| Calculation nodes on the 1D-networks. | Flexible grid arrangement, 2D grid cells. |
| Bathymetry construction | |
| At arbitrary locations on branches in a model cross sections can be defined with Y and Z data. | Requires the complete bathymetry as input. |
| All data points of the cross section are used in the simulations. | Depending on the number of grid cells, not all bathymetry data is used in the simulations. |

In contrast to D-Flow 1D, D-Flow FM takes the effects of cross-sectional variations in water level and velocity and turbulence into account. 1D-modelling has also as drawback that the lateral diffusion of flood waves is not taken into account accurately (Teng, et al., 2017). In D-Flow 1D this is solved by providing an option to schematize a storage part in the cross sections and by allowing to vary

⁸ See Appendix A for more on this subject

roughness over the cross sections. Both modules are bound by the CFL criterion, although D-Flow FM in two directions. Comparing the computational grids, D-Flow 1D has the advantage that constructing a grid is very convenient and does not require much time. D-Flow FM has the advantage of modelling everything with a flexible mesh, which offers optimal flexibility for modelling and makes it convenient to set up new grids and modify existing grids or increase the resolution locally. The disadvantage is the relatively large amount of time it takes to construct a 2D grid. Comparing the bathymetry construction gives both modules an advantage and a disadvantage. D-Flow 1D has the advantage that not on all locations the bathymetry has to be known. The disadvantage of this is that the bathymetry is discretized as cross sections, instead of modelling a continuous surface. Furthermore, the subjectivity of cross section location and orientation is playing a role (Teng, et al., 2017). These aspects cause that the construction of a 1D model often takes a lot of time due to extensive calibration activities. Most of the time this is done by varying the roughness in the summer bed. D-Flow FM, on the other hand, offers more detail and thus more accurate modelling of the complete bathymetry, but requires a lot more input data. This does, however, often save a lot of calibration activities because the initial level of accuracy is higher. The advantage of using a 1D model is that all data points of cross sections are taken into account. When using a 2D model, the bathymetry in cross-sectional direction is discretized depending on the number of assigned grid cells, so data could get lost in the discretization process.

There is, however, a downside to more accuracy. As always in modelling studies, more accuracy goes hand in hand with more simulation time. This is due to a larger number of grid cells and the fact that more physical processes are taken into account. Furthermore, D-Flow FM also solves the momentum equation in cross-sectional direction, which introduces a second CFL-condition, because of the nature of the applied numerical scheme. This may limit the time step even further, which causes a larger simulation time.

The tension between accuracy and costs is always present. Several recent researches on the differences of 1D, 2D or 1D/2D-coupled modelling conclude the following: 1D-modelling is much faster, but cannot model velocity or water level differences within cross sections and velocity or direction differences within floodplains (Finaud-Guyot et al. (2011); Bladé et al. (2012); Morales-Hernández et al. (2016); Anees et al. (2016); Dimitriadis et al. (2016)). Most studies show more than an order of magnitude difference in computation time. The practical question that comes with this, is obvious: is the extra accuracy large enough to make it worth longer simulation times? This research will analyze this question and search for a general answer to whether 1D or 2D-modelling is preferred in particular situations.

Conclusions

From the above analysis, it appears that there are a few physical parameters that could cause differences in model performance. These are mainly the properties that cause 2D effects, like meandering and varying roughness coefficients. These processes are seen as the cause of gradients in water level and velocity in cross-sectional direction and summer bed-floodplain interaction. The modelling of flood waves could also cause differences due to the fact that the 1D model is not able to model storage with the used default settings. Lastly, the way the bathymetry is used in the simulations is of great importance, due to the way the bathymetry is discretized in 2D models.

4. Comparing model output

In this chapter the second sub question will be answered: What are the differences in model output for varying physical properties of the systems and which processes are causing these differences? This will be done by setting up small academic models, in D-Flow 1D and D-Flow FM. In these models, various parameters, like the bed roughness or the meandering intensity, can be varied to find out what the effects are of these variations. First of all, the methodology of the construction of these models will be discussed. This methodology paragraph is built up as follows: Firstly the method of determining the shape, width, depth and slope will be shown. After that, the parameters that were concluded in the previous chapter to probably be of importance are discussed, together with the proposed variations in the models, that may show the influence of these parameters. Thirdly, the model details will be analyzed, for instance the grid characteristics or the implemented boundary conditions. Then, the final models will be shown. Lastly, the process of output generation will be discussed.

The second paragraph shows the simulation output and the observations that are made from the output. The third paragraph will discuss a number of theories that explain the causes of the differences between the 1D and 2D models. The last paragraph will conclude this chapter and try to find the relations between the second and third paragraph.

First of all, an example will be given of the models that are constructed. This gives a first indication of the direction of this chapter.

Visualization models

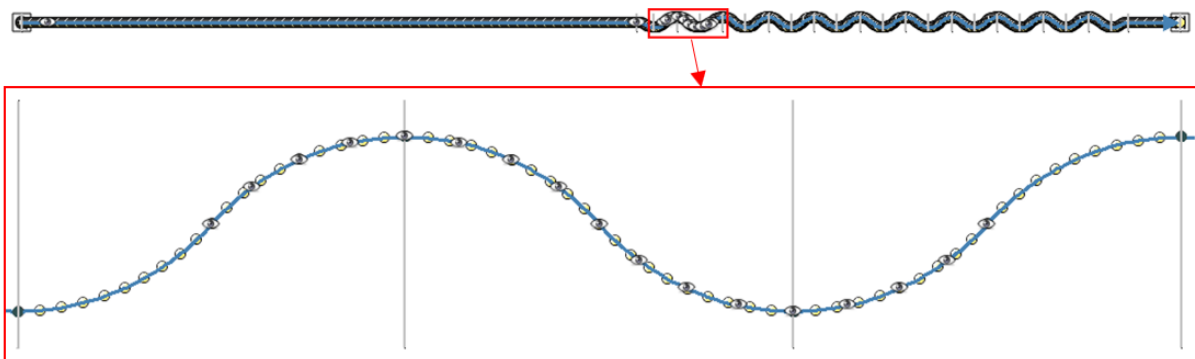


Figure 4-1: SOBEK D-Flow 1D – upper figure is total model, bottom figure is zoom on single meander in red square – eye icons = observation point locations, blue line = summer bed, grey lines = cross sections, white dots = grid points

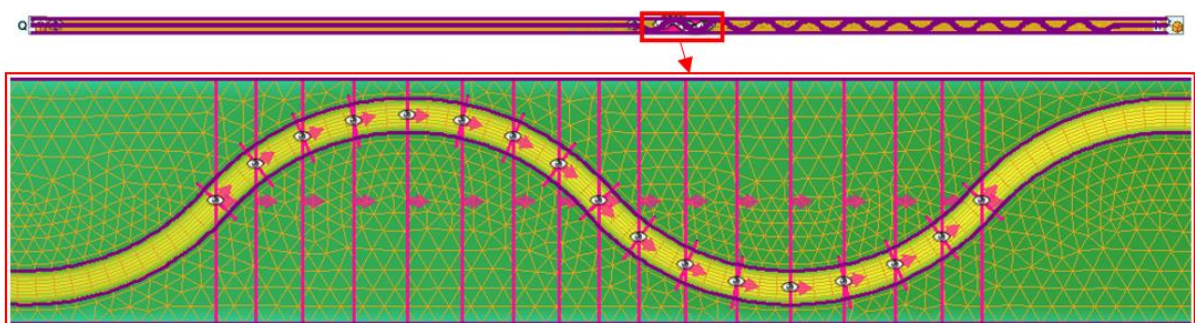


Figure 4-2: D-HYDRO D-Flow FM – upper figure is total model, bottom figure is zoom on single meander in red square – eye icons = observation point location, pink line = observation cross section locations, yellow part = summer bed, green part = floodplains, purple line = summer bed/floodplain division, orange lines (quadrilaterals and triangles) = computational grid

4.1 Methodology

To map the differences, several small models are set up in both 1D and 2D in which certain parameters can be varied. A first look has been given on the previous page. In this paragraph, the construction method of these models will be discussed. The basic approach is as follows: When modelling in 2D, the bathymetry is schematized on the basis of basic cross sections and river courses that have been set up in SOBEK (1D). This data is exported to ArcGIS in order to be able to exactly copy the location of the watercourses to other models. These cross sections (dimensions and slope) are based on the discharge (see below). It has been decided to use four different orders of magnitude of discharge to be simulated; 5, 50, 500 and 5000 m³/s. These discharges represent roughly the magnitude of average Dutch streams and rivers. These are summer⁹ discharges, so the floodplains are not flooded. In order to be able to distinguish summer bed – floodplain interaction, also winter discharges are simulated. These discharges are three times larger in this case; 15, 150, 1500 and 15000 m³/s. With these discharges, the summer bed and floodplains are both flooded.

4.1.1 Profile dimensions and characteristics

The relation of dimensions to discharges is often determined by using so-called 'power laws'¹⁰, of which many publications can be found (Abdelhaleem et al., 2016; Buffington & Montgomery, 2013; Dury, 1976; Rosgen, 1994; Singh, 2003; Williams, 1986). These formulas relate a discharge to a water level and an average width, in this case a summer bed width. However, none of the mentioned relations is directly applicable to the large range of discharges used in this research. For instance, the paper of Abdelhaleem et al. (2016) only shows power laws for the ranges of 90-200 m³/s, 2-200 m³/s and 0.22-4.9 m³/s. Dury (1976) appeared to be the most useful when comparing the laws to the case area dimensions. By adjusting the coefficients of the laws slightly to the cross sections of the stream Molenbeek and the river Meuse, which are within the boundaries of 5 and 5000 m³/s, a power formula has been developed in the form of $y = ax^b$ that can be applied to this range. From both areas, five random cross sections have been chosen on which the laws are based. In Figure 4-3 these laws have been given.

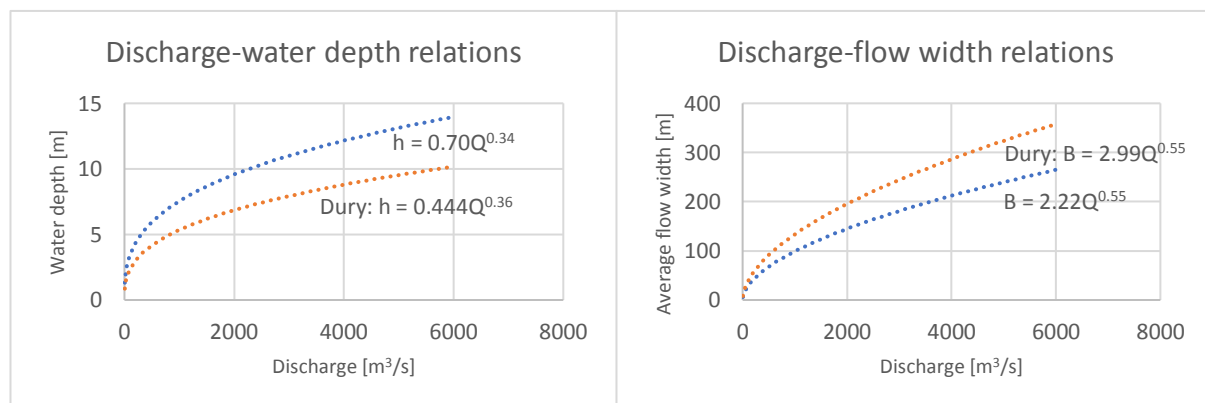


Figure 4-3: Power laws for water depth and flow width – orange laws are of Dury (1976), blue laws are newly developed

⁹ In the flood safety profession, often the terms 'summer' and 'winter' are used. In general, summer discharges are low, so the main part of the river that is flooded is called 'summer bed'. During winter season, often higher discharges occur and the flood plains are flooded. Instead of flood plains, the term 'winter bed' is also used.

¹⁰ A power law has the form of $y = ax^b$. It represents a relationship between x and y , where a relative change of x results in a proportional relative change of y . In this case, these relations are just empirical or statistical regression relations and used to give a rough estimate of river dimensions.

One can derive from the table and the graphs that Dutch rivers are on average a little deeper and less wide compared to the international average. A simplified general cross section from the river Meuse was taken as the basic profile. The sizes of these are adjusted in proportion so that the average width and depth are equal to the dimensions that emerge from the power law. This keeps the shape of the summer bed constant for all scales. This prevents the shape from causing undesired effects. For the floodplain, an average shape and dimensions were also taken from the river Meuse. The cross sections for all scales are given in Figure 4-4.

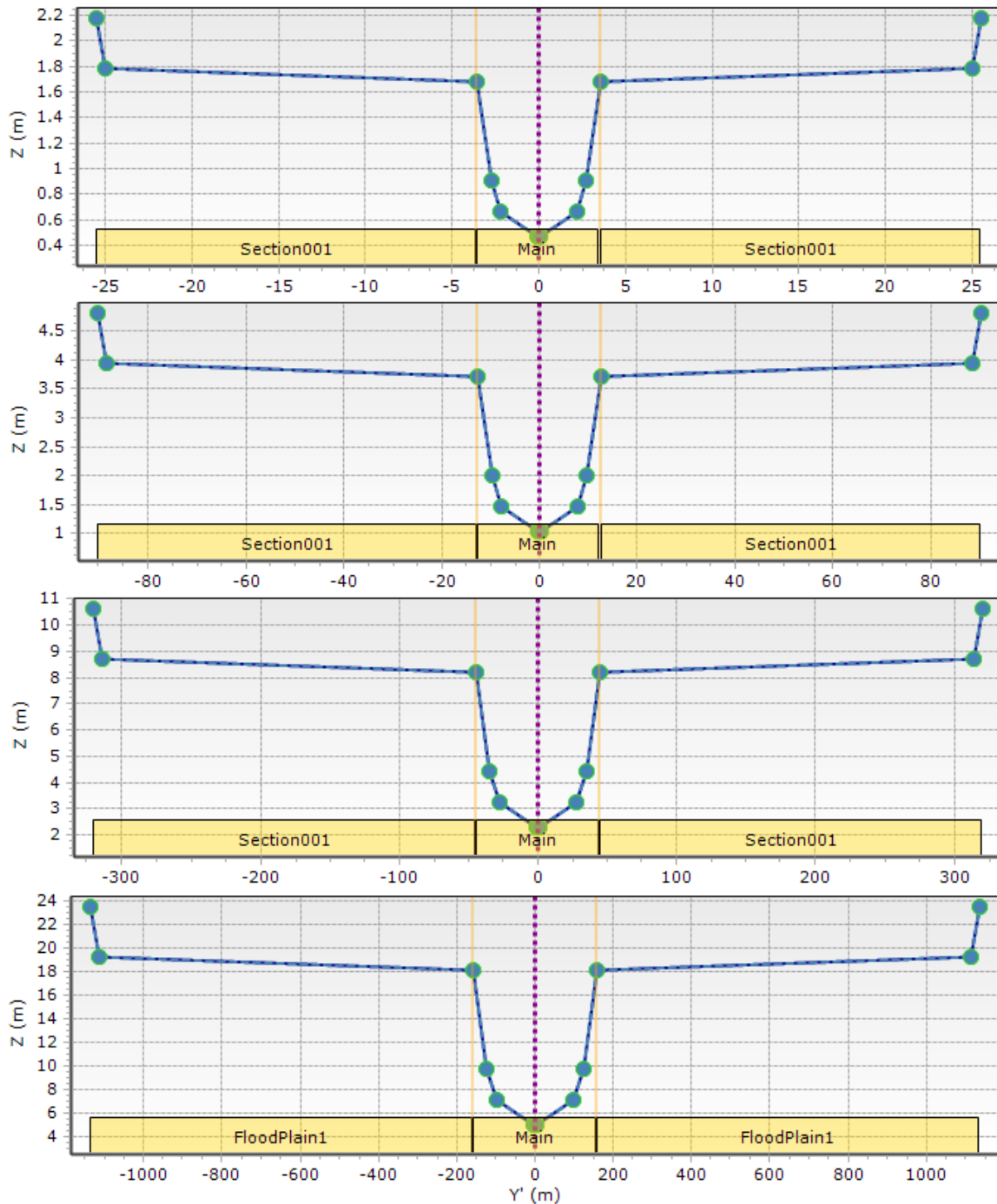


Figure 4-4: Profile schematizations, with increasing scale from top to bottom - Main = summer bed, Section001 = flood plains. To give an example: in the upper figure a discharge of $5 \text{ m}^3/\text{s}$ fills the summer bed, a discharge of $15 \text{ m}^3/\text{s}$ fills the summer bed and both flood plains.

The D-Flow 1D module offers the possibility to specify a certain part of the cross section as storage part, to account for storage effects. In this research, the choice is made not to use this option, for two reasons:

1. The goal of this research is to identify the processes that are going on and give a general idea about the quantity of them. Using this storage possibility would introduce effects that are not directly traceable in the model output, which would therefore be unreliable.
2. Specifying these storage part is a very arbitrary process and would require an extensive analysis to identify the most accurate dimensions. This would be a calibration activity, which is not part of this research.

Besides the water depth and flow width, also the slope is depending on the discharge. Naturally, a smaller scale stream has a larger slope compared to larger scales. Because mainly steady flow will be simulated, the Manning formula can be used to calculate the required slope. The formula, created by Manning (1889), is presently written as

$$u = \frac{1}{n_m} R^{2/3} i_b^{1/2} \quad 4.1$$

where

u = stream flow velocity [m/s]

R = hydraulic radius [m]

n_m = manning coefficient [s/m^{1/3}]

i_b = bed slope [m/m]

In combination with the relation

$$Q = u * A \quad 4.2$$

the discharge can be calculated. The slope i_b can be adjusted to create a certain discharge capacity. With the summer discharge and a manning roughness of 0.04 (maximum in this study, see below) the summer bed is almost completely filled, the same applies to the floodplains with the winter discharge. This applies to all cross sections and associated discharges.

The table below shows the properties of the four scales that are modelled. In combination with Figure 4-4 this gives a complete overview of the model schematizations.

Table 4-1: Schematization properties

| Scale [m ³ /s] | Summer bed depth [m] | Summer bed average width [m] | Slope | Summer discharge [m ³ /s] | Winter discharge [m ³ /s] |
|---------------------------|----------------------|------------------------------|---------|--------------------------------------|--------------------------------------|
| 5 | 1.22 | 5.38 | 1.5e-03 | 5 | 15 |
| 50 | 2.69 | 19.07 | 7.0e-04 | 50 | 150 |
| 500 | 5.94 | 67.59 | 3.5e-04 | 500 | 1500 |
| 5000 | 13.11 | 239.61 | 2.0e-04 | 5000 | 15000 |

4.1.2 Variables

The variables during the simulations have been introduced briefly at the end of the previous chapter, based on the model differences. These variables will be discussed more in detail in this paragraph.

Summer bed – floodplain interaction

By modelling winter discharges for each river profile, the interaction between the summer bed and floodplains can be analyzed by means of analyzing flow patterns, velocities and water levels.

Roughness

To compare roughness values that are only based on the bed topography, it is best to analyze the Manning coefficients of the systems. This parameter is well-known, often used and can directly be linked to the kind of vegetation and bed topography. The roughness of the summer bed will be varied for each profile. The following roughness (Manning) coefficients will be simulated (Battjes & Labeur, 2017):

- 0.02 - very smooth, corresponding to smooth earth without weeds (uncommon in nature, therefore mostly used as calibration roughness)
- 0.03 - common roughness summer bed, corresponding to clean and straight natural river channels
- 0.04 – corresponding to winding natural river channels with pools and shoals

The roughness of the floodplains will be constant, with a Manning coefficient of 0.045.

Channel meandering

Also the channel meandering is of great importance to possible 2D effects. The more severe the meandering, the larger the flow resistance or roughness becomes (Philips & Tadayan, 2006). The following profiles are constructed for all four scales and corresponding cross sections:

1. Straight profile
2. Little meandering profile
3. Extensive meandering profile

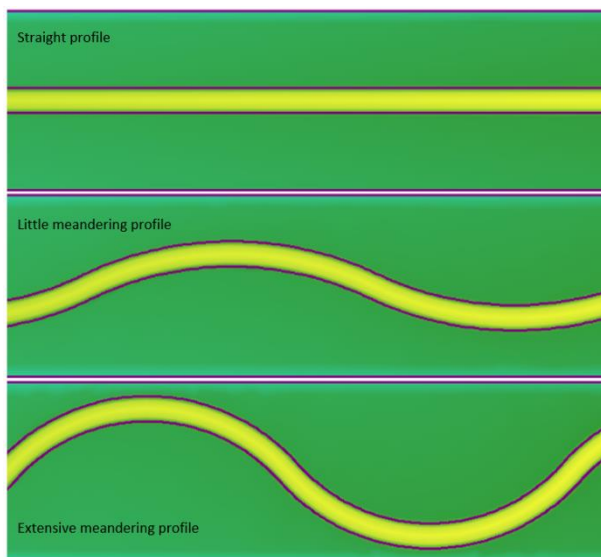


Figure 4-5: Meandering profiles, yellow parts are summer bed, green parts are flood plains

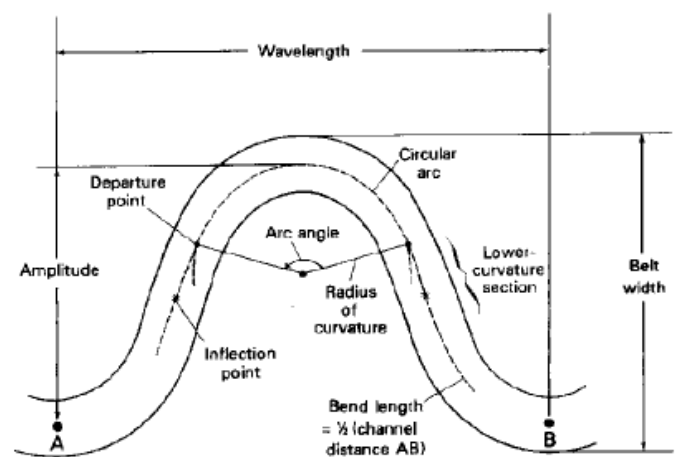


Figure 4-6: River meander characteristics (Williams, 1986)

The wavelength of a meander (see Figure 4-6) can also be derived with a power law (Dury, 1976). In this case, the power law of Dury (1976) has been used: $L_m = 32.857 * Q^{0.55}$. The amplitude of the meanders is based on several practical examples and the available space within the floodplains. The meanders have exactly the same shape for all scales.

Flood waves

A total of three types of flood waves are simulated, with peaks of approximately one day, three days and 12 days. The flood waves will be modelled for all scales, for the situation without meandering and a roughness parameter of 0.03. The flood wave that will be simulated is taken from standard river Meuse simulations and is scaled to the discharge capacities of the four situations. For the smallest scale ($Q = 5 \text{ m}^3/\text{s}$) the flood waves are given below, for 12 days (which is the original wave length) and one day.

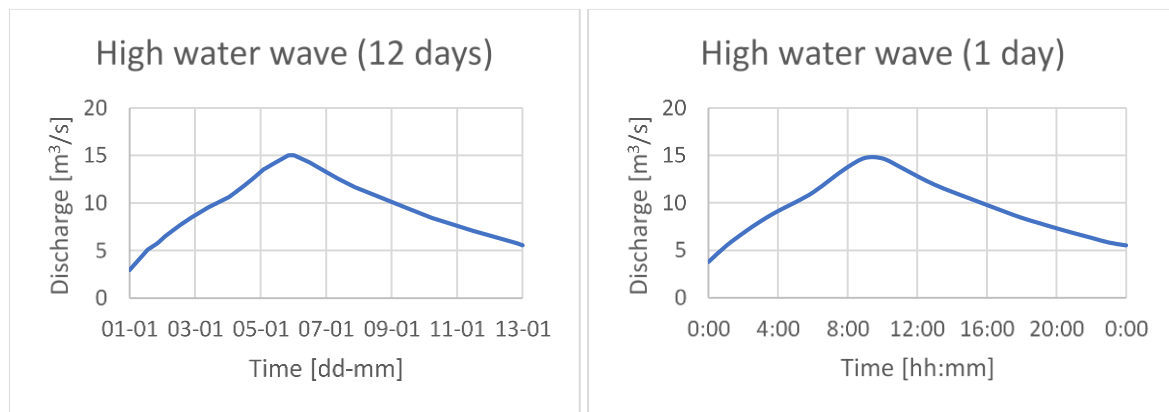


Figure 4-7: Discharge-time graph of flood waves, for scale $Q = 5 \text{ m}^3/\text{s}$

Grid size (bathymetry discretization)

As discussed in the previous paragraph, D-Flow 1D uses a 1D grid, D-Flow FM a 2D grid. To minimize grid effects on the model performance, both grids contain the same amount of grid cells or points in stream direction, i.e. on the summer bed reach. Furthermore, the number of grid cells or points does not differ between the scales. Both the bathymetry and the grid are scaled with the discharge magnitude. This is all done to minimize undesired effects of parameters that are not analyzed in this research.

According to Deltares (2017c), when modelling in 1D, a good first indication of the distance between calculation points is the width of the cross sections. One has to take into account that the distance should not be too large to ensure sufficient accuracy. Besides that, the distance should not be too small to ensure stability and minimize simulation time. However, for the goal of this research, it is important the level of detail is sufficient. The simulation time is not an issue, because the used models are not very large. The final number of grid cells or points in x-direction is approximately 1000 for all simulations. In practice this means that the distance between grid cells is approximately 10 times smaller than the width of a cross section.

For the 2D grids, there are also grid cells in y-direction. In order to be able to represent the meanders sufficiently, the number of grid cells in flow direction should not be too large. For the summer bed, a curvilinear grid has been chosen with 10 cells in y-direction. The floodplain is covered with triangular grid cells. This choice has been made because of the implementation of meandering of the summer bed within the model boundaries, i.e. winter dikes. When implementing a curvilinear grid on the floodplains as well, the number of grid cells in cross-sectional direction cannot vary, which would

create extremely narrow cells on one side of the summer bed and extremely wide cells on the other side of a meander, cf. Figure 4-8. This would decrease the accuracy. When using triangular cells, the number of cells is not predetermined. Furthermore, the grids have to meet certain requirements, in order to be able to run the simulations. These criteria are further discussed in appendix C.

Space discretization and time integration are often of great influence to the model output. Whether these effects are present can be checked by adjusting the grid size and time step combination for both the 1D and 2D model and see whether the differences stay, increase or decrease. The most important issue in this research is the discretization in cross-sectional direction when modelling in 2D. Because of the fact that each grid cell can only have one bed level, the average elevation value is taken of the grid cell area. With this, deviations are created with respect to the actual bottom level. When modelling in 1D, the elevation data of a cross section are not discretized. This means that, when increasing the number of 2D grid cells, especially in cross-sectional direction, the results are more accurate. The default grid is the one presented in the figure below.

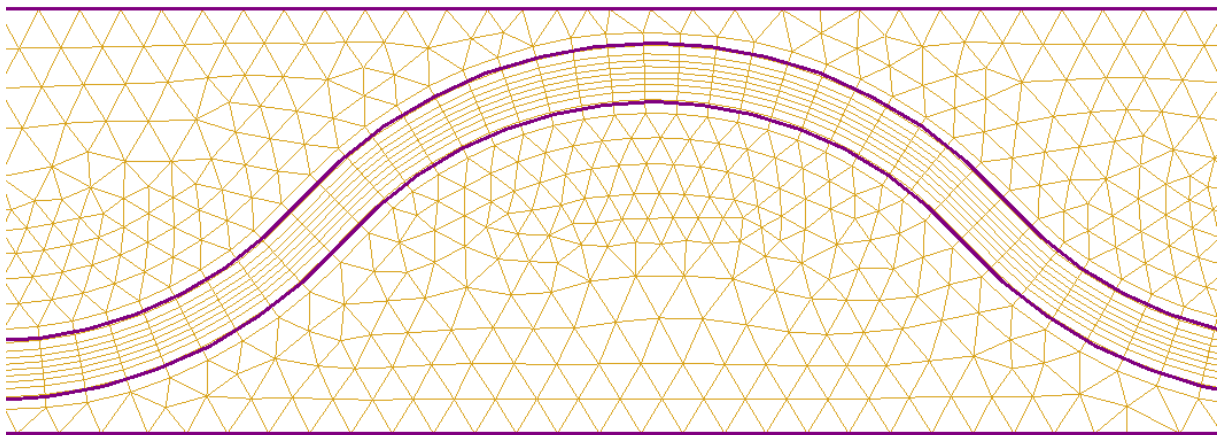


Figure 4-8: Default grid used in simulations - 10 curvilinear cells in cross-sectional direction

Other issues that could play a role are the number of 1D grid points and the used time step, both in 1D and 2D models. A quick scan, by varying these parameters for a number of situations, has been performed to see whether these effects are worth analyzing. This was not the case. Therefore, only variations in the 2D grids have been analyzed.

Because the aspect ratio¹¹ of the grid cells should not be too large, the grid cells in both directions have been doubled, which keeps the aspect ratio constant. The default setting was approximately 1000 grid cells in flow direction and 10 over cross-sectional direction. Simulations were done with a 2000x20 grid, but also with a 500x5 grid, to analyze the differences and the importance of the discretization of the bottom level. It has been chosen to do this for all scales, with the following conditions:

- Roughness coefficient $n = 0.03$ – this is a representative value both in this research as in practical applications
- Both summer bed flow as floodplain flow – both are modelled with different grid types (curvilinear versus triangular), so the effects are expected to differ

¹¹ The aspect ratio is a grid criteria which officially only applies to regular grids, but is still used for irregular grids as a guideline for curvilinear grid cell dimensions. It represents the ratio between the length and width of a grid cell.

- Extensive meandering – as it is expected that this type will be the most sensitive to discretization

As visible in Figure 4-8, the curvilinear grid has been stretched out a little in cross-sectional direction to meet the smoothness criterium¹². The default grid for all simulations has therefore 8 cells in cross-sectional direction in the summer bed. It is partly an arbitrary process to adjust the grid to meet this criterium. In this section, to be able to make an accurate comparison, three new grids have been constructed, with exactly 5, 10 and 20 grid cells in cross-sectional direction in the summer bed, because it is important that the amount of grid cells is exactly doubled or halved. These grids have not been adjusted to meet the smoothness criterium, because then the grids would not have the same shape anymore and the summer bed – floodplain division would not be on the exact same location anymore. The consequence of increasing the number of grid cells in lateral direction is that the grid cells of the floodplains are also smaller.

Using these new grids, an accurate analysis can be performed on the effects of changes in grid size. The grids that will be examined in this section are dimensioned as shown in the figures below.

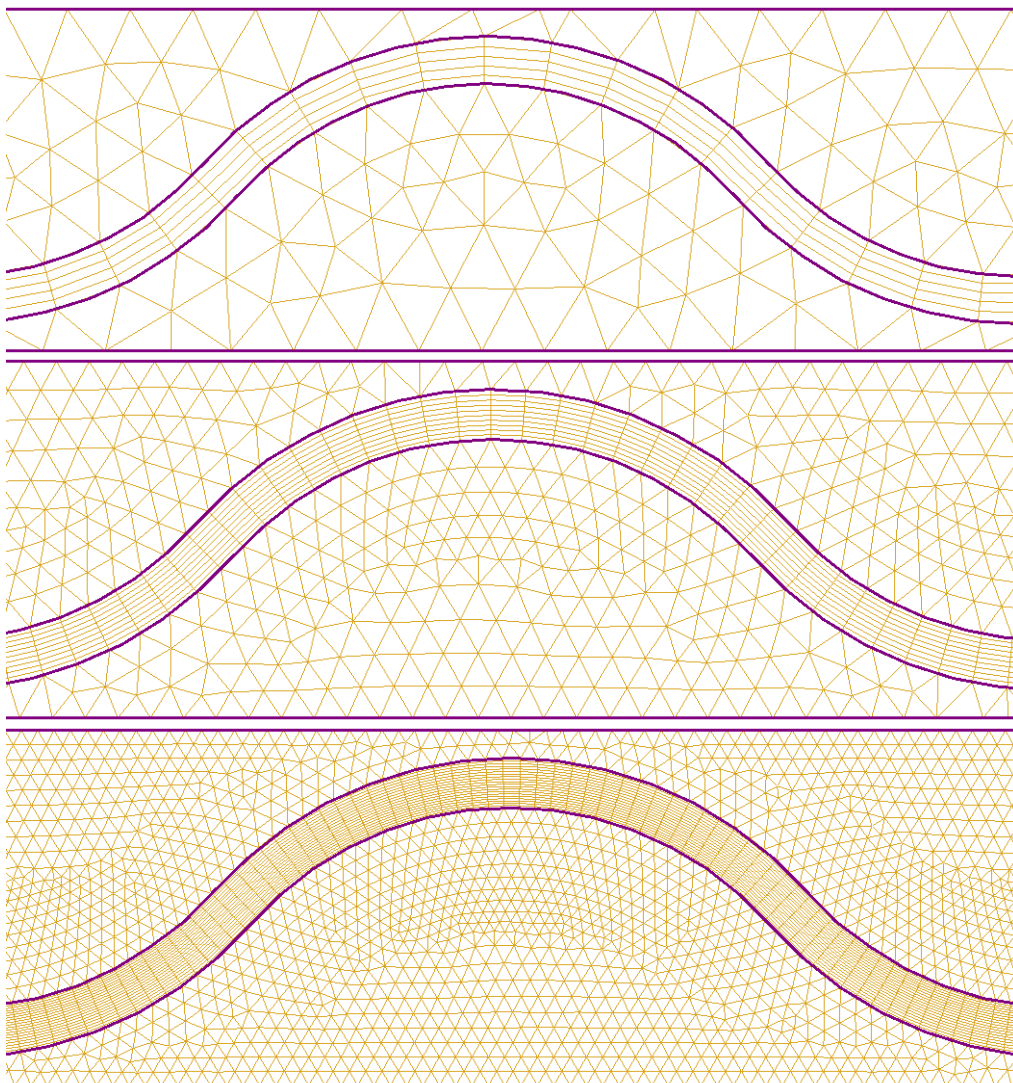


Figure 4-9: Grid used for analysis of influence of bathymetry discretization – 5, 10 and 20 curvilinear cells in cross sectional direction

¹² More on grid criteria can be found in Appendix C.

4.1.3 Simulation properties

In this paragraph an overview of all simulations will be given. Furthermore, the boundary conditions and observation methods will be discussed.

Overview of simulations

A total of 12 different profiles are schematized. With the use of Baseline this information can be converted into input files for D-Flow FM. Baseline is an ArcGIS application with which spatial model schematizations for SIMONA WAQUA, Delft3D, SWAN and SOBEK can be made. Baseline stores spatial data in such a way that it can be converted into the relevant model schematizations, cross sections and roughness sections. It is a suitable tool for projects where a structured storage of river data and a coupling of flow models with a GIS environment is desirable (Helpdesk Water, 2018). Besides performing the Baseline activities, a calculation grid must always be manually generated in the D-HYDRO Suite using the application RGFGRID.

With each of these profiles, simulations are carried out, where several combinations of scale, meandering and roughness are varied. Furthermore, besides the stationary simulations also flood waves will be simulated. Lastly, the number of grid cells will be varied in the simulations. The total list of simulations is shown in the table below.

Table 4-2: Simulations overview (see Table 4-1 for more information) – HW = high water (cf. Figure 4-7)

| Simulation | Scale | Discharge | Meandering | Roughness summer bed | Number of grid cells, time step |
|------------|-------|-----------------|--------------|----------------------|---------------------------------|
| 1D | | | | | |
| 1-18 | 5 | Summer / Winter | Variable (3) | Variable (3) | 1000, 1h |
| 19-36 | 50 | Summer / Winter | Variable (3) | Variable (3) | 1000, 1h |
| 37-54 | 500 | Summer / Winter | Variable (3) | Variable (3) | 1000, 1h |
| 65-72 | 5000 | Summer / Winter | Variable (3) | Variable (3) | 1000, 1h |
| 73-75 | 5 | 3 types HW | None | 0.03 | 1000, 1h |
| 76-78 | 50 | 3 types HW | None | 0.03 | 1000, 1h |
| 79-81 | 500 | 3 types HW | None | 0.03 | 1000, 1h |
| 82-84 | 5000 | 3 types HW | None | 0.03 | 1000, 1h |
| 2D | | | | | |
| 85-102 | 5 | Summer / Winter | Variable (3) | Variable (3) | 1000x10, 1h |
| 103-120 | 50 | Summer / Winter | Variable (3) | Variable (3) | 1000x10, 1h |
| 121-138 | 500 | Summer / Winter | Variable (3) | Variable (3) | 1000x10, 1h |
| 139-156 | 5000 | Summer / Winter | Variable (3) | Variable (3) | 1000x10, 1h |
| 157-159 | 5 | 3 types HW | None | 0.03 | 1000x10, 1h |
| 160-162 | 50 | 3 types HW | None | 0.03 | 1000x10, 1h |
| 163-165 | 500 | 3 types HW | None | 0.03 | 1000x10, 1h |
| 166-168 | 5000 | 3 types HW | None | 0.03 | 1000x10, 1h |
| 169,170 | 5 | Summer / Winter | Extensive | 0.03 | 2000x20, 1h |
| 171,172 | 50 | Summer / Winter | Extensive | 0.03 | 2000x20, 1h |
| 173,174 | 500 | Summer / Winter | Extensive | 0.03 | 2000x20, 1h |
| 175,176 | 5000 | Summer / Winter | Extensive | 0.03 | 2000x20, 1h |
| 177,178 | 5 | Summer / Winter | Extensive | 0.03 | 500x5, 1h |
| 179,180 | 50 | Summer / Winter | Extensive | 0.03 | 500x5, 1h |
| 181,182 | 500 | Summer / Winter | Extensive | 0.03 | 500x5, 1h |
| 183,184 | 5000 | Summer / Winter | Extensive | 0.03 | 500x5, 1h |

Boundary and initial conditions

The goal of this research is to find out what physical processes influence the model performance and in what quantity. Therefore, it is important to choose boundary conditions that do not influence the water level upstream. In other words, the boundary conditions have to be chosen in such a way that no backwater curves occur at the boundaries.

In this case, the upstream boundary is determined by the simulation type (see table above). The upstream boundary condition will therefore always be a discharge in m^3/s . The downstream boundary condition is influenced by the discharge and roughness. The degree of meandering does not influence the downstream boundary condition, because the flow is subcritical. Therefore, the meandering does not influence the flow downstream, only the upstream flow is influenced. The downstream boundary condition is in meters above the reference level.

To obtain a value for this boundary condition, a preliminary simulation has been run for all combinations of discharges and roughness coefficients. The (temporary) boundary conditions for these preliminary simulations has been calculated with the manning formula (eq. 4.1). This deviates from the actual model water level, so it induces still a small backwater curve. However, the water depth close to the upstream boundary is no longer influenced by this backwater curve, and is therefore suitable to be used as the water depth of the downstream boundary condition. The 1D model has different output compared to the 2D model, therefore the boundary conditions that are implemented in the models are not the same.

No initial conditions have been specified. Instead of this, the models are run sufficiently long to make sure the simulated situation is stationary. Then, the results are analyzed. The same applies to the flood wave simulations; the flood wave is built up slowly to minimize spin-up effects.

Observation points

The last step in the modelling process is to add observation points, of which the output will be compared. It is very important that these observation points are located on the exact same location for both models. This has been done by creating points containing XY-data in ArcMap and implementing them to both the SOBEK Suite and the D-HYDRO Suite.

In the SOBEK Suite, one can only choose to use observation points as output locations. In the D-HYDRO Suite, there is also an option to add observation cross sections. Observation points in SOBEK have as output, among others, the water level, water depth and velocity, all average values of the whole cross section at that location. D-HYDRO is modelling in 2D, which means that observation points have as output, among others, the water level, water depth and velocity (x- and y- vectors) at their exact locations. Observation cross sections are measuring values over the whole cross section, and have as output, among others, the average velocity, discharge and flow area. The observation cross sections are not able to generate water level output. Therefore, both observation points and cross sections are implemented in the D-HYDRO models. The observation points are located exactly in the middle of the summer bed, in order to be able to compare the values of water level or depth with the 1D model output. The velocity will be taken from the observation cross sections, because these are average values over the whole cross section, which is the same as SOBEK. The choice has been made to implement observation points over the reach of one single meander. On the next page, the locations will be shown in detail.

Regarding the flood wave simulations, other observation locations are used. In these models, a total number of 10 observation points are located, spread out over the entire model reach, with equal mutual distance. The output analysis will be on the time-discharge relation, which gives insight in the effects of storage, the expected causes of differences in output between 1D and 2D.

In the simulations, summer bed or floodplain flow will be distinguished. This is important for the orientation of the observation cross sections. Therefore, on all locations two different types of cross sections are created. The cross section for summer bed discharge is located perpendicular to the flow direction in the summer bed. The cross section for floodplain discharge is located perpendicular to the flow direction of floodplain, or vertically. Examples are given in Figure 4-10 and Figure 4-11. Regarding the flood wave simulations, the observation locations are given in Figure 4-12. Note that the flow direction is from left to right in all simulations.

Visualization models

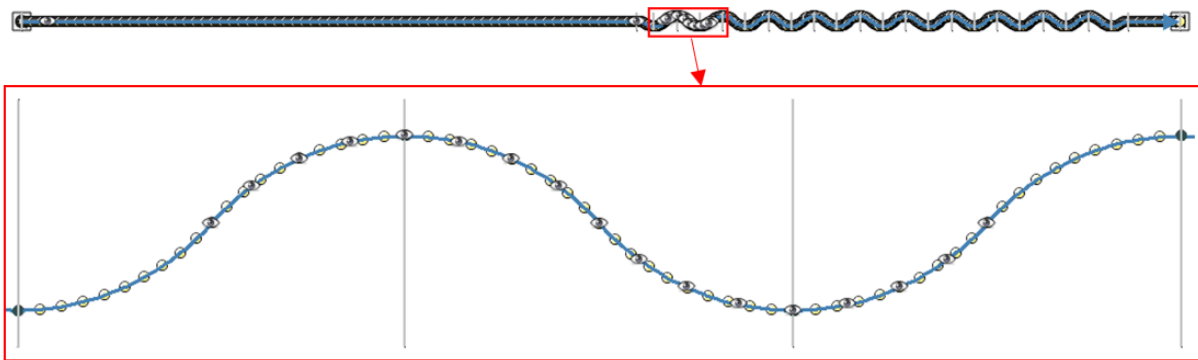


Figure 4-10: SOBEK D-Flow 1D (Q5000, extensive meandering) – upper figure is total model, bottom figure is zoom on single meander in red square – the eye icons represent the observation point locations

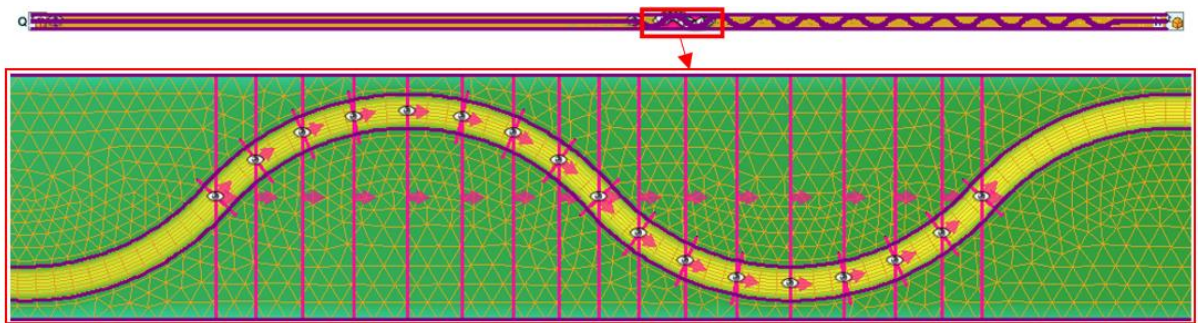


Figure 4-11: D-HYDRO D-Flow FM (Q5000, extensive meandering) – upper figure is total model, bottom figure is zoom on single meander in red square – the eye icons represent the observation point locations - the pink lines represent the observation cross section locations



Figure 4-12: Location and numbering of observation locations of flood wave models - top figure is 1D, bottom figure is 2D

4.1.4 Output

In this paragraph, the output generation method is described. This includes an overview of output parameters, calculation methods of parameters that are not directly computed by the models and some remarks on the way the observations are presented in the next paragraph.

Table 4-3: Output parameters

| Output | 1D | 2D |
|-----------------|----------------------------------|----------------------------------|
| Water level | Observation point | Observation point |
| Water depth | Observation point | Observation point |
| Velocity | Observation point | Observation cross section |
| Reynolds number | Model output and regression tool | Model output and regression tool |
| Froude number | Model output and regression tool | Model output and regression tool |
| Simulation time | Model output | Model output |

To be able to analyze the type of flow in the different simulations, the Reynolds and Froude number are calculated. A brief derivation of these numbers can be found in appendix B. The Reynolds number compares flow inertia, or turbulent forces, with the viscous forces (Chevion & Moussa, 2016; Anees et al, 2016). Usually, the Reynolds number is used to determine whether a flow is laminar or turbulent. A flow is laminar when $Re < 500$ and fully turbulent when $Re > 2000$. In between, there is a transition zone where both types occur simultaneously. Rivers and streams are typically very turbulent, with values of the Reynolds number in the order of $10^5 - 10^6$ (Birbir, 2008). In this research the Reynolds number will be calculated and analyzed whether there is relation between the system characteristics and the 1D-2D differences.

The Froude number denotes the influence of gravity on the fluid motion (Chevion & Moussa, 2016). In other words, it quantifies inertia versus gravity. Of the Froude number, the denominator is also denoted as c , the wave celerity. Therefore, the Froude number can be seen as a ratio between two velocities, the flow velocity and the wave celerity. The quantity tells something about whether disturbances in the flow can overcome the flow velocity and travel upstream (Birbir, 2008). Besides that, the Froude number can also be used to classify the shape of back water curves (Battjes & Labeur, 2017). The following Froude numbers are often distinguished (Anees, et al., 2016):

- $Fr < 1, c > u$, *subcritical*
- $Fr = 1, c = u$, *critical*
- $Fr > 1, c < u$, *supercritical*

In general, for rivers and streams the Froude number is very small, in the order of $10^{-1} - 10^{-2}$. In this chapter the Froude number will be calculated and analyzed whether there is a significant difference.

Both modelling suites are not able to generate these numbers as output on observation points or cross sections. Therefore, these numbers are calculated using the model output. The Reynolds number is calculated using the velocity and the hydraulic radius, the Froude numbers using the velocity and the hydraulic depth. The velocity is directly given by the model output, the hydraulic radius and depth have to be calculated in another way.

The SOBEK Suite offers an option to generate detailed information about the implemented cross sections. An example is given in the figure below.

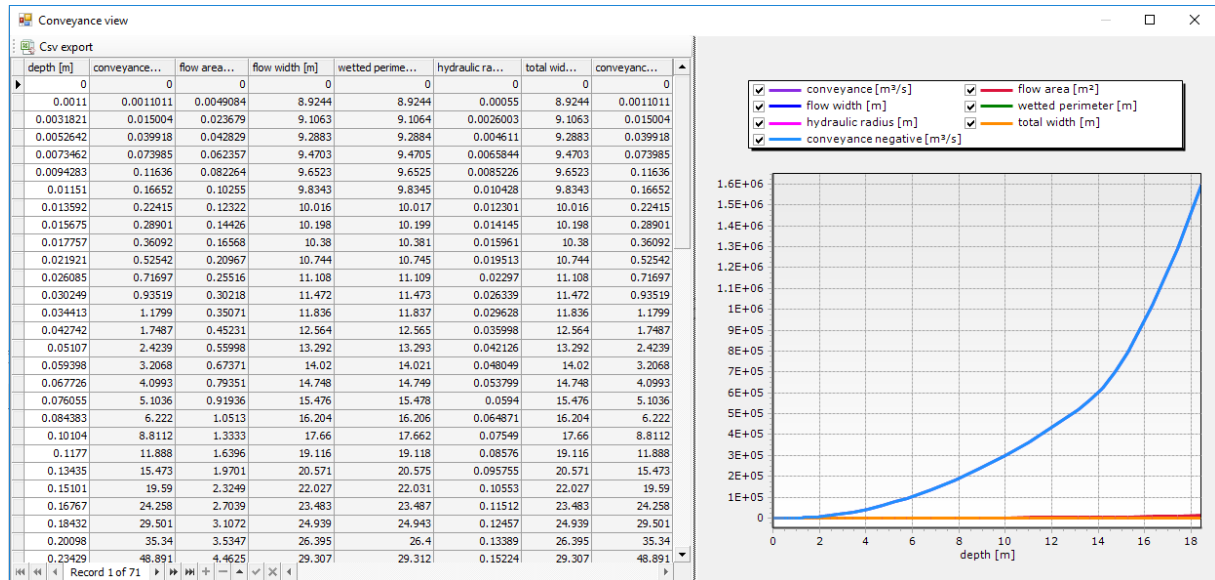


Figure 4-13: Conveyance view SOBEK Suite

This pre-processing tool gives values for several parameters like the conveyance, flow area, flow width and hydraulic radius for certain values of the water depth within the cross section. Interesting parameters are the hydraulic radius and hydraulic depth. The hydraulic depth is not a direct output, but can be calculated by dividing the flow area by the top flow width. By importing this data in a polynomial regression tool, a relation can be determined that relates a depth to a certain value of the hydraulic depth and hydraulic radius. Because the hydraulic radius decreases significantly when the floodplain is flooded, two separate relations have been made, one for summer bed flow and the other for floodplain flow. An example is shown in Figure 4-14. For other scales, and the hydraulic depth, which has a similar pattern as the hydraulic radius, the same method applies.

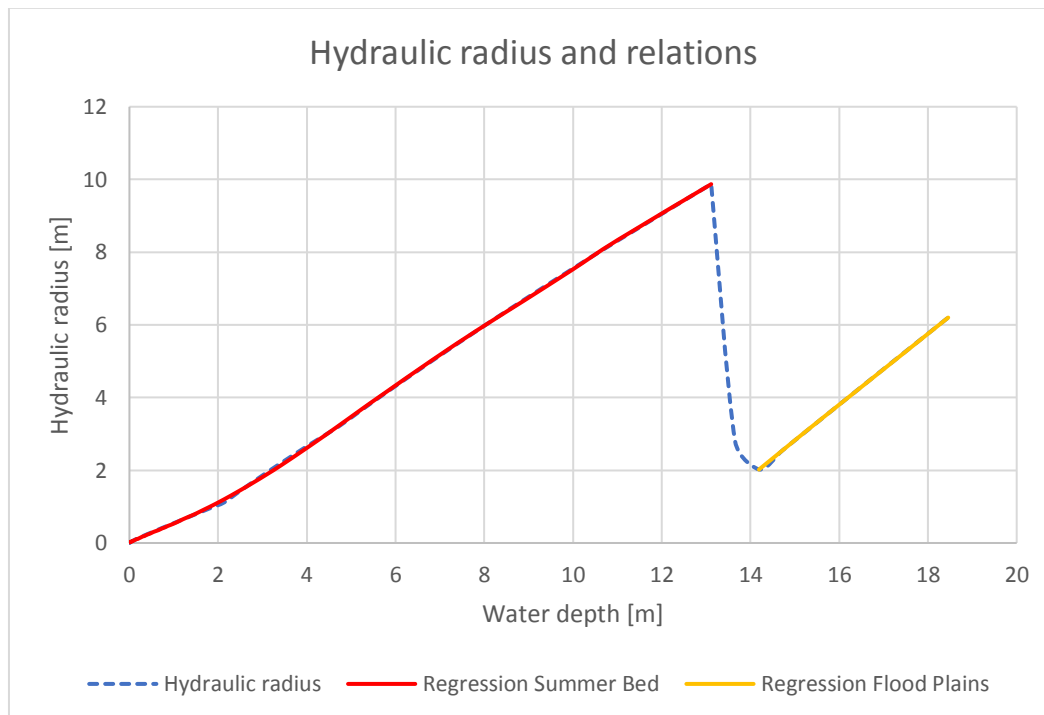


Figure 4-14: Hydraulic radius and polynomial regression relations for scale $Q = 5000 \text{ m}^3/\text{s}$

Based on the output, answers can be given to sub questions 1 and 2 and the differences can be quantified. The model output can be presented and compared in a lot of different ways. A lot of variables can be changed and compared with each other. Because not every comparison has direct value for the research, below some remarks are given on the way the model output will be compared.

First of all, regarding the water level, it is useful to compare the relative difference between 1D and 2D modelling. This relative comparison is useful here, because the water depth increases with increasing scale. It is therefore a logical consequence that the absolute difference will increase. The relative difference tells more about the importance of processes on different scales. It is however also interesting to analyze the absolute differences, to see how they vary over the scales.

Secondly, for the overall model performance, it has no use to compare every observation point separately with each other. Therefore, if a situation is compared for 1D and 2D, the average value of all observation points is taken and the standard deviation is added. In this way, large overall differences can be extracted from the simulations. Furthermore, using the standard deviation, large differences between the separate observation points can also be identified. When the overall differences are large, a detailed analysis will be carried out to see what processes are going on.

Thirdly, due to the number of variables it is not possible to compare all variables in one analysis. Furthermore, not all output can be shown. The basic goal of this research is to compare scale effects with each other, so this will be the starting point of all analyses. Therefore, several analyses are made, for instance one where the results of differences in the meandering intensity are compared for all scales.

Lastly, often the distinction between summer bed flow and floodplain flow is made. Summer bed flow means that the summer discharge is simulated, so there is only flow in the summer bed. Floodplain flow means that the winter discharge is simulated, so there is flow in both the summer bed as the floodplains.

As a remark it has to be said that no prior assumptions were made about whether 1D or 2D may be more accurate. However, when assuming 2D models are more accurate compared to 1D models, the following has to be kept in mind. If variations in meandering intensity or in roughness influence the 1D-2D difference, this only means that the 2D effects vary for different situations. It should not be the goal to implement changes in the model schematizations to bring the model output of the 2D model as close as possible to the 1D model. This analysis is made to show what changes in schematization have the largest influence on the 1D-2D difference, to see what parameters are important in the modelling choice between 1D and 2D.

4.2 Simulation results and observations

The graphs that will be discussed in this paragraph show the relative difference in water level. A relative difference of e.g. 10% means that the 2D model simulates a higher water level compared to the 1D model. Also a graph on the standard deviation between the observation points and the absolute differences are shown.

To obtain a general idea about the magnitudes of water depths and flow velocities on varying scales, an overview of typical values has been given. These are averages of all simulations, so both 1D and 2D. The water depth of the floodplain flow is the total water depth, observed in the summer bed (cf. Figure 4-4). This also applies for the flow velocity.

Typical water depths

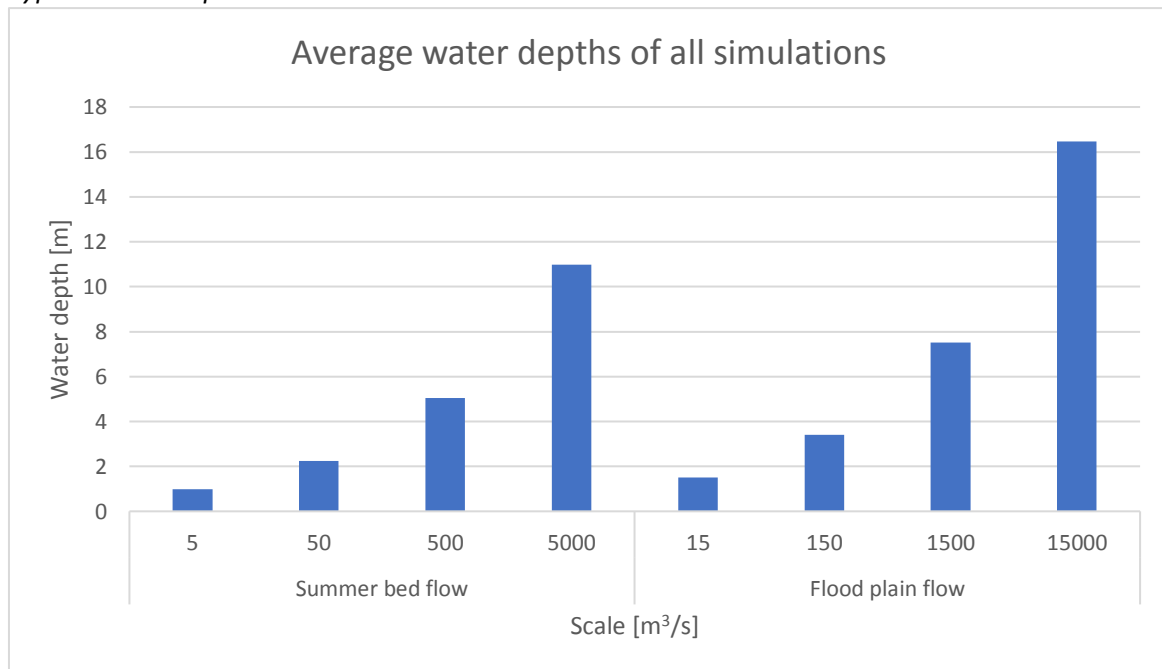


Figure 4-15: Average water depths of all simulations

The graph above shows the typical water depths of the systems that have been used for this research. This is shown to give a general idea about the orders of magnitude of the results on the next pages. Generally speaking, two conclusions can be drawn from the graph:

1. When the scale increases with one order of magnitude, the water depth increases with approximately a factor of 2.2.
2. The difference in water depth (measured in the summer bed) between summer bed and floodplain flow is approximately a factor of 1.5.

Typical flow velocities

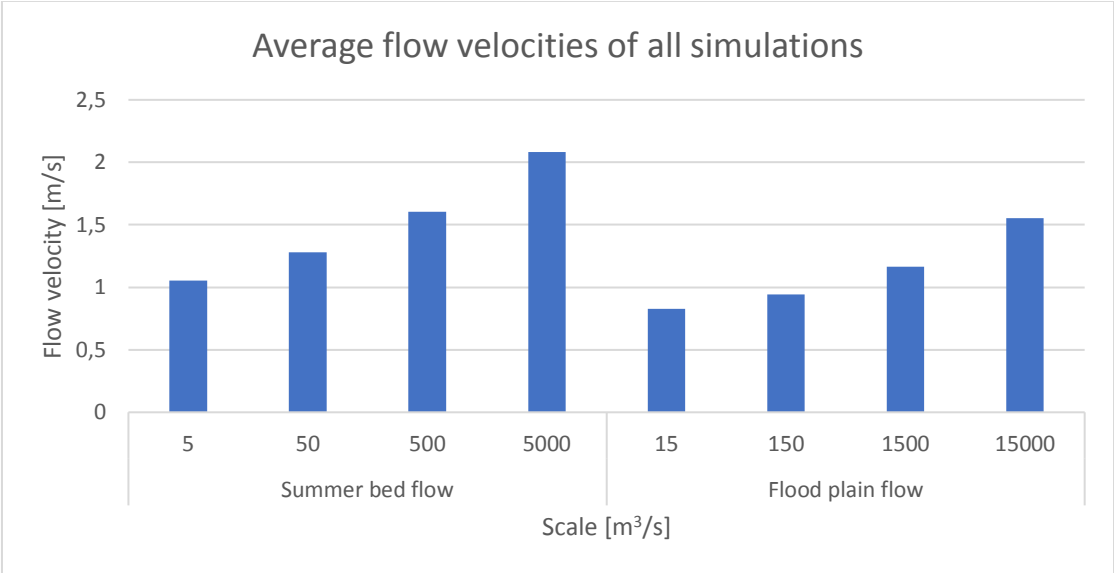


Figure 4-16: Average flow velocities of all simulations

1. When the scale increases with one order of magnitude, the flow velocity increases with approximately a factor of 1.25
2. The difference in flow velocity between summer bed and floodplain flow is approximately a factor of 0.75.

Relative difference 1D vs. 2D, averaged over roughness

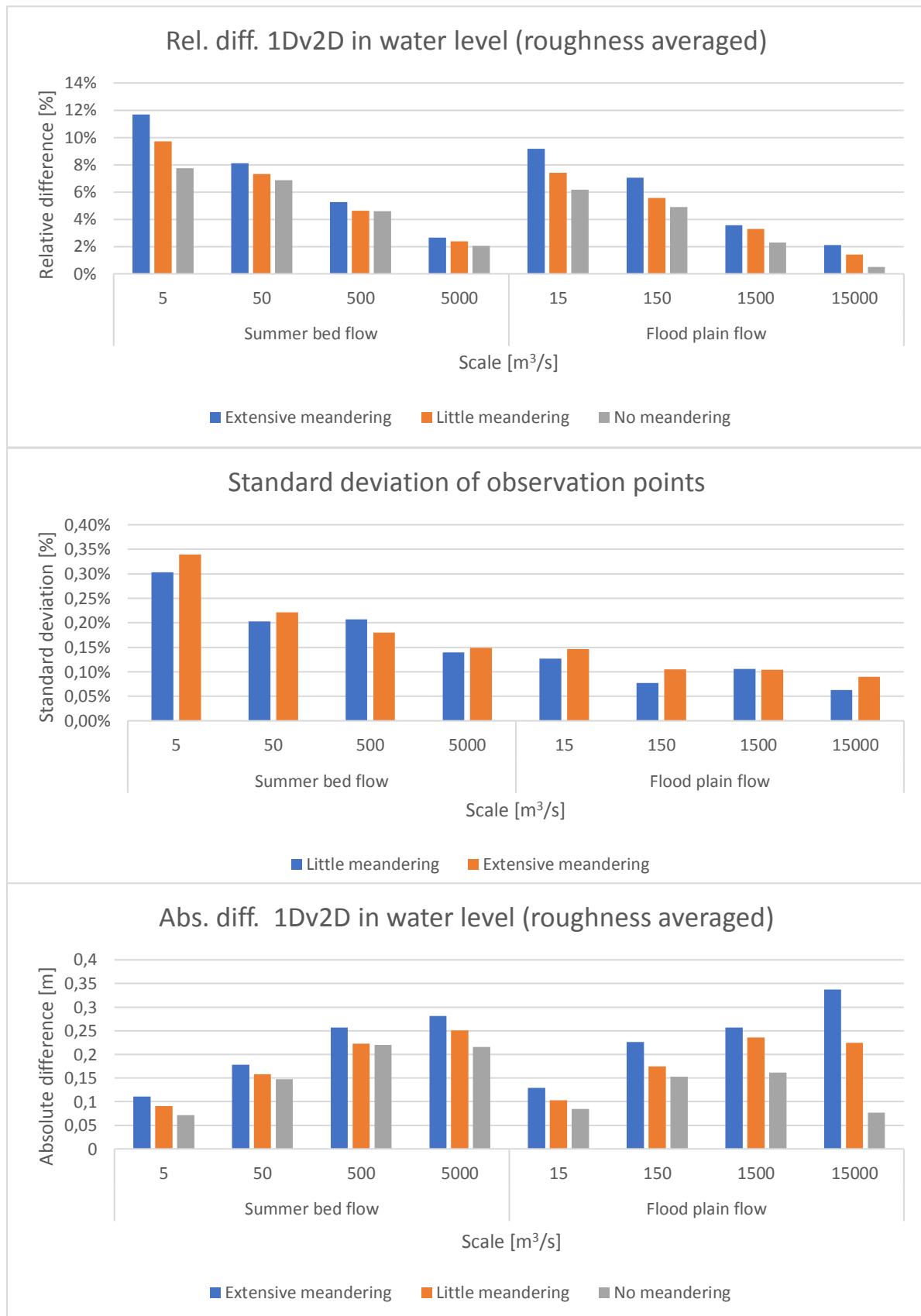


Figure 4-17: Differences in water level for varying meandering intensities

The upper graph shows the relative difference of the water level when the 1D simulation is compared to the 2D simulation. The differences in water level are made relative by dividing them by the water depth. The values are averaged over the roughness coefficients, so the influence of scale and meandering on the relative differences can be seen in the graph. The second graph shows the standard deviation between the relative differences of the observation points. Because the situation without meandering has a constant water depth over the entire model reach, there is no standard deviation in that case. The bottom graph shows the absolute differences.

First of all, it is obvious that the 2D simulation simulates higher water levels in all situations, as the differences are always positive. Secondly, differences decrease when the degree of meandering decreases. Also the absolute differences indicate that the highest differences are caused by extensive meandering. Thirdly, the smaller the scale, the larger the differences.

Lastly, if the standard deviations are observed, peaks are observed at small scales. This means that the differences among the observation points are high, which gives an indication that in these situations more cross-sectional processes are of influence compared to large scales. There are no significant differences observed between the several meandering intensities.

Relative difference 1D vs. 2D, averaged over meandering intensity

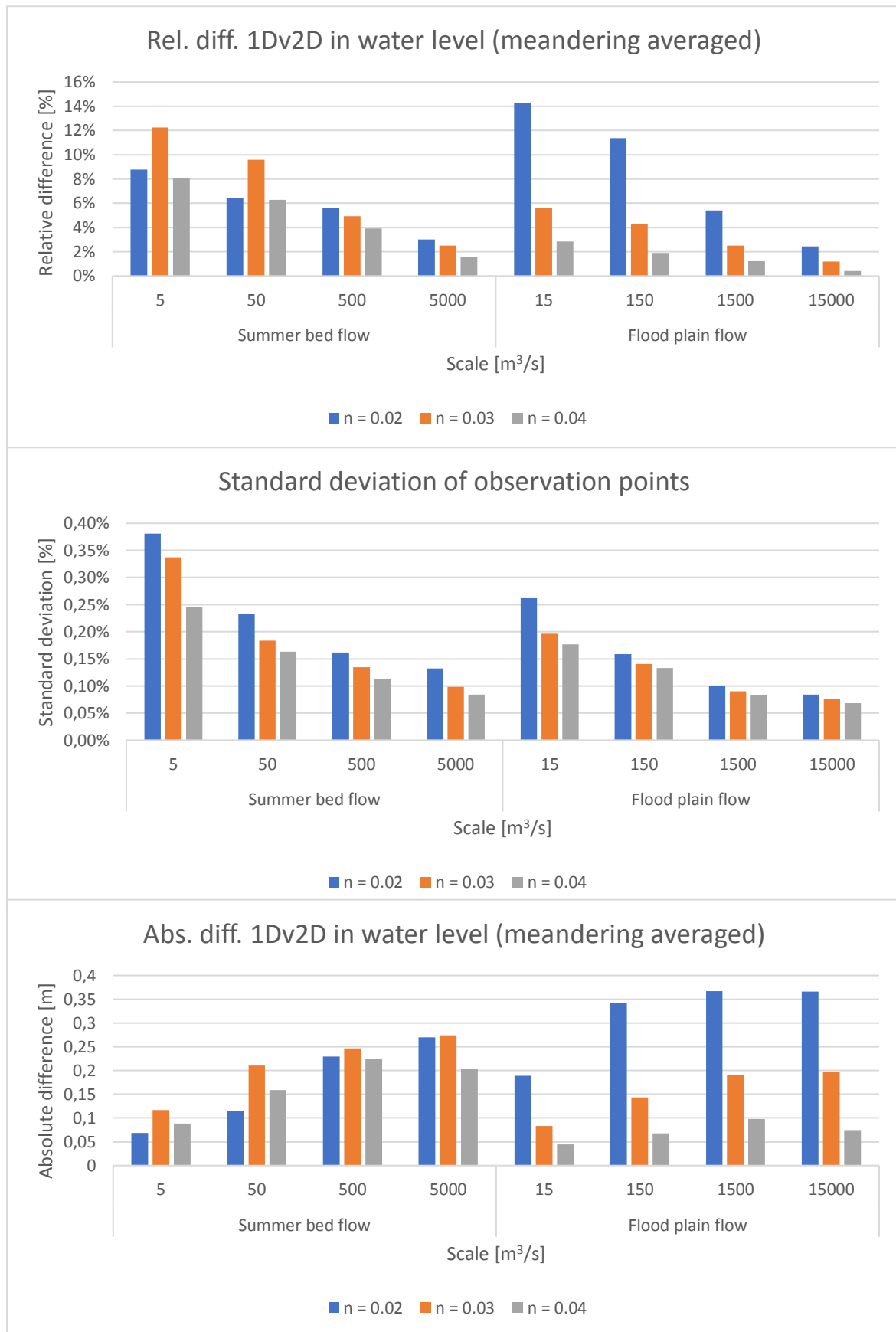


Figure 4-18: Differences in water level for varying roughness coefficients

The upper graph shows the relative difference of the water level when the 1D simulation is compared to the 2D simulation. The values are averaged over the meandering intensity, so the influence of scale and roughness on the relative differences can be seen in the graph. The second graph shows the standard deviation between the relative differences of all observation points. The bottom graph shows the absolute differences.

First of all, it is obvious that the 2D simulation simulates higher water levels in all situations. Secondly, it is observed that the relative differences increase with decreasing scale. Thirdly, for summer bed flow, the differences are largest for $n = 0.03$, see also absolute differences. For floodplain flow the differences are decreasing when the roughness is increasing. Especially a roughness of $n = 0.02$ gives relatively extremely large differences in water level.

Lastly, if the standard deviations are observed, peaks are observed at small scales in combination with low roughness coefficients. This means that the differences among the observation points are high, which gives an indication that in these situations more cross-sectional processes are of influence compared to large scales.

Grid size (bathymetry discretization)

Here, the results will be presented of the simulations that were performed with refined or coarsened grids. The upper graph shows the relative difference of the water level when the 1D simulation is compared to the 2D simulation. The differences in water level are made relative by dividing them by the water depth. The bottom graph shows the absolute differences. As discussed in the methodology paragraph, simulations with a summer bed roughness of $n = 0.03$ are performed for this section.

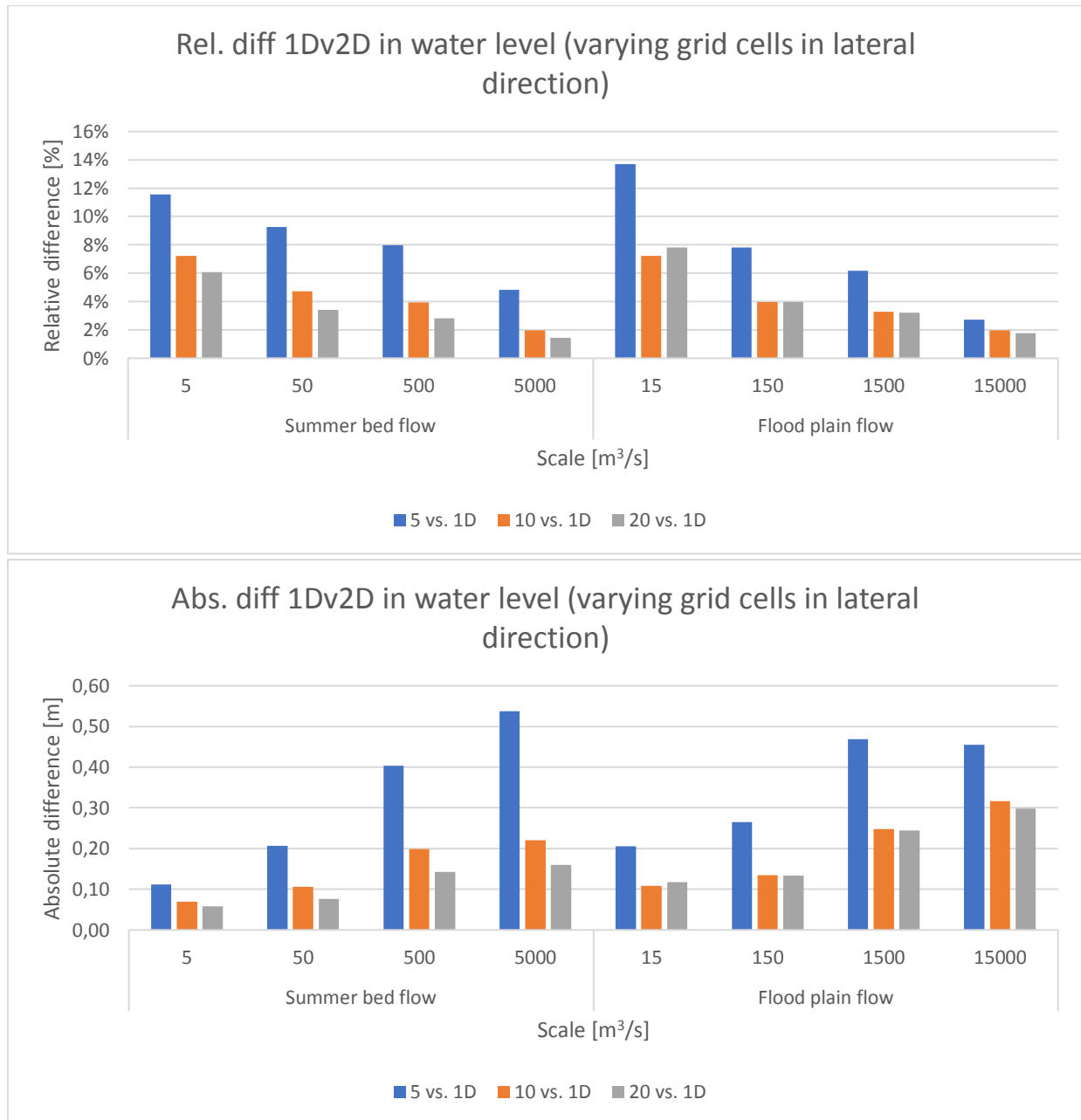


Figure 4-19: Results of grid size analysis (5 vs. 1D means: difference between 2D simulation with 5 grid cells in lateral direction and 1D simulation)

What appears from the graphs is that apparently a larger grid size introduces a larger difference between 1D and 2D. When increasing the grid cells to 20 in cross-sectional direction, a lower water level is simulated, which decreases the difference between 1D and 2D. For floodplain flow, there are not much differences between 10 and 20 grid cells.

Flood waves

As discussed in the methodology paragraph, three different types of flood waves have been simulated. The differences between these three wave lengths, 1, 3 and 12 days, and the differences between the different scales will be discussed below. Two analyses will be made, one to see what the overall differences of the whole flood wave are, and secondly, how the peak of the wave is simulated in time and magnitude.

The locations of the several observation points are given in Figure 4-20. For the analysis, not all observation points can be shown as this would be too much data for all scales and flood wave lengths. Instead, the root mean square error (RMSE) has been calculated for the last observation point, number 10, where the difference are the best visible. The RMSE is calculated as follows:

$$RMSE = \sqrt{\frac{\sum_{i=1}^N (Q_i^{2D} - Q_i^{1D})^2}{N}} \tag{4.3}$$

where

N = total number of observations

This value gives a good indication of the overall differences between 1D and 2D, as the differences of the whole time series are taken into account. The RMSE for all scales and flood wave lengths are given in Figure 4-21.

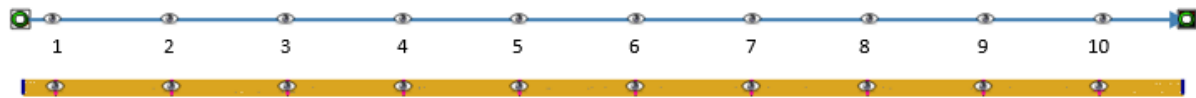


Figure 4-20: Numbering of observation points (left side is upstream) – top figure is 1D, bottom figure 2D

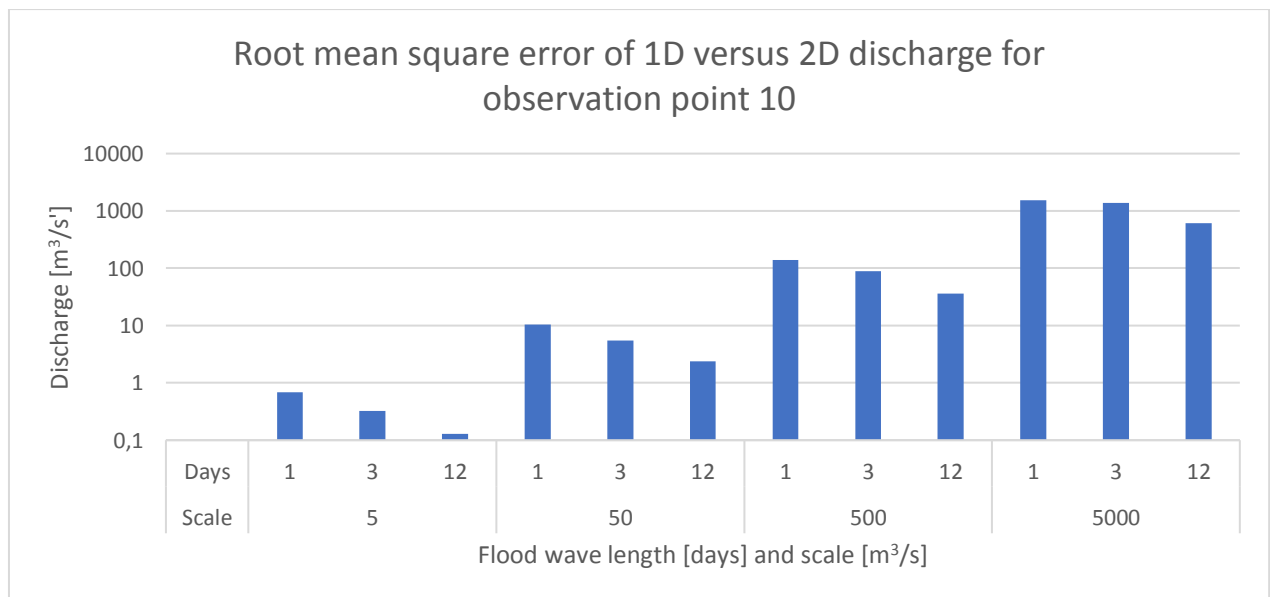


Figure 4-21: Root mean square error of discharge differences of flood wave over entire flood wave period, at observation point #10 (logarithmic y-axis)

From the figure appears that the RMSE is decreasing for increasing wave length. To be able to indicate what the scale effect is, the relative difference will be taken into account. The next figure

will show the relative 1D-2D difference of the peak discharge divided by the peak discharge of the flood wave (e.g. 15000 m³/s for the Q = 5000 scale).

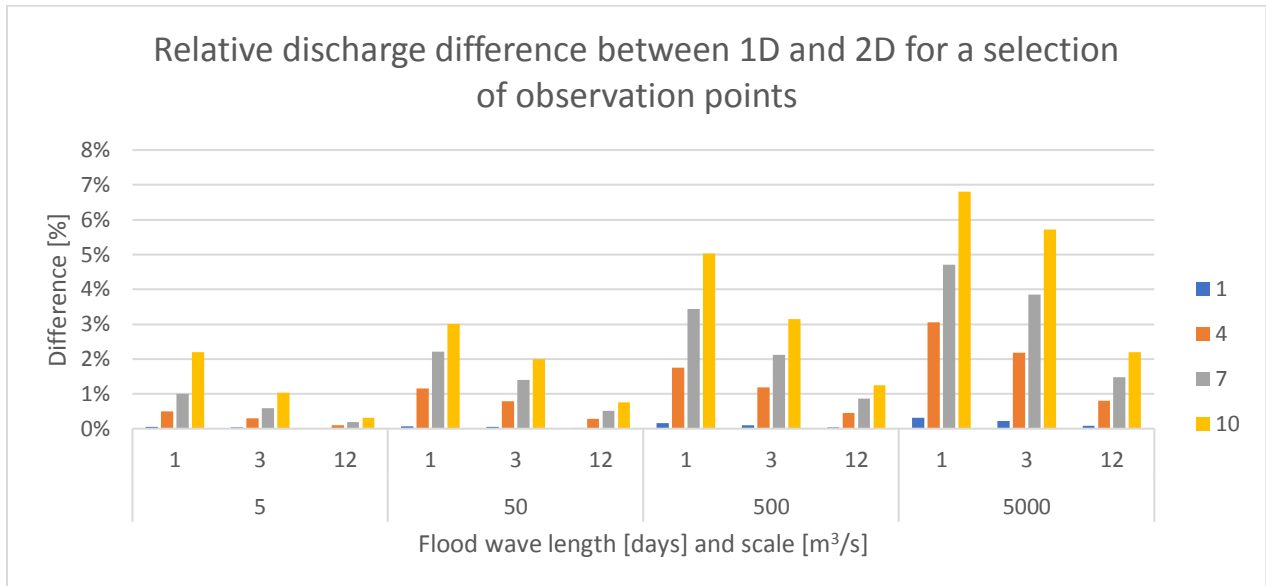


Figure 4-22: Relative (absolute differences divided by peak discharge of flood wave) difference flood wave (cf. Figure 4-20 for the observation locations)

The graphs show some general patterns:

1. The further away from the boundary, the larger the differences are
2. The longer the flood wave length, the smaller the differences are
3. The larger the scale, the larger the differences are

These patterns will be illustrated with some time-discharge graphs.

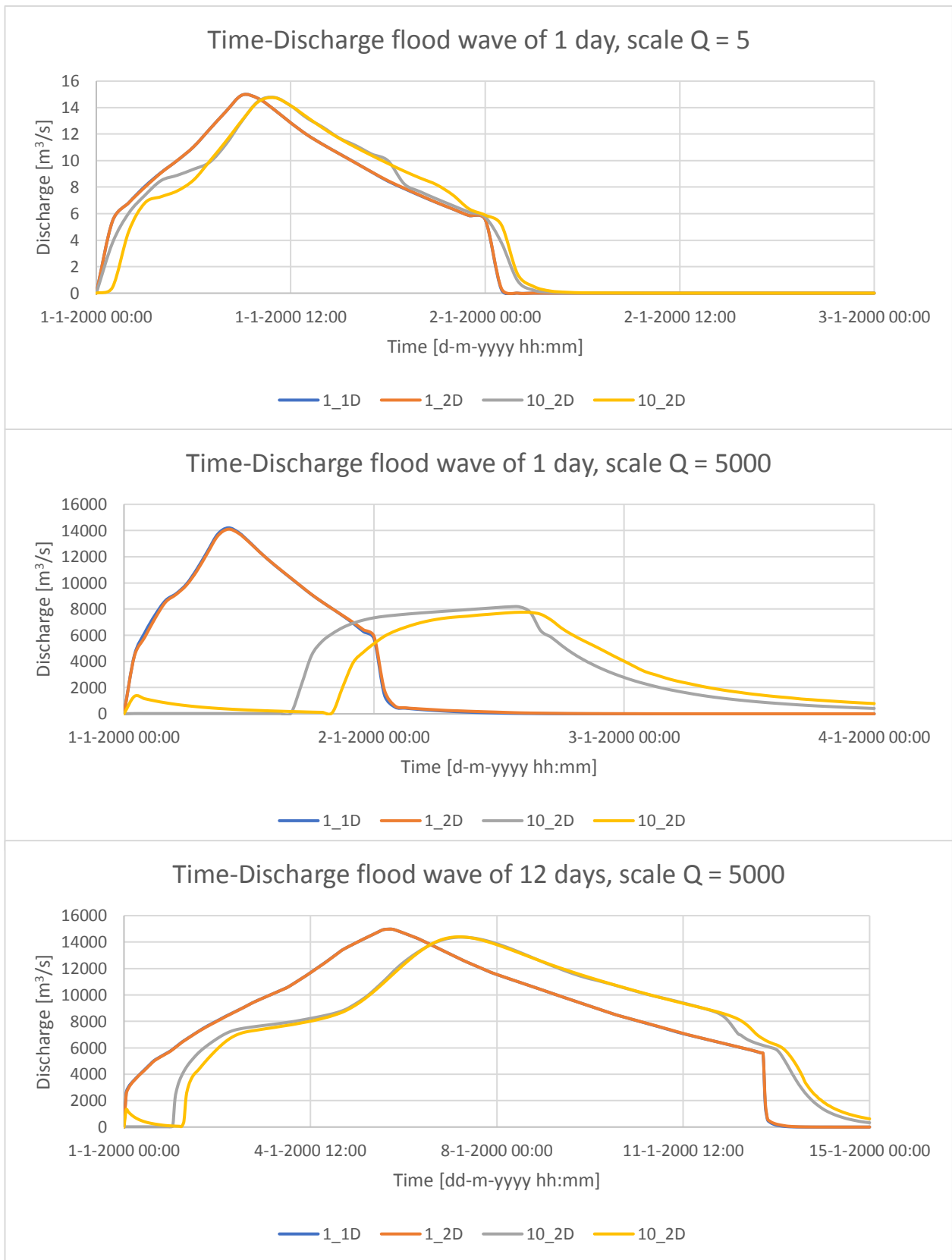


Figure 4-23: Q-t graphs flood waves (1_1D means first observation point, 1D model output, cf. Figure 4-20)

The graphs above show all three patterns. When comparing graph 1 to 2, pattern 3 is visible. The larger the scale, the larger the difference. Comparing graph 2 to 3 shows the effect of the flood wave

length, which is pattern 2. Pattern 1 is visible in all graphs, observation point 10 shows always more differences compared to point 1.

Generally speaking, a short flood wave on large scale shows much more storage compared to a long flood wave on small scale. More storage means more difference between 1D and 2D, which is clearly visible in graph 2, where the yellow and grey line are deviating significantly from each other. This process will be elaborated further in the next paragraph.

Analyzing the flood peaks gives the same observations. The smaller the scale and the larger the flood wave length, the smaller the differences are. The situation with the largest (relative) difference in peak time and discharge is given in graph 2. The time difference between the flood peak of 1D and 2D is approximately one hour and the discharge difference is about 400 m³/s.

Another phenomenon that appears from the graphs is that the largest differences are created at the moment the floodplains are flooded. With the roughness coefficient that is used in this simulation this is around a discharge of 6-8 m³/s (for scale Q = 5). The reason for this will be discussed in the next paragraph.

Lastly, an observation can be made on the duration of the peak to travel from the upstream boundary towards the downstream boundary. The longer this takes, the more storage plays a role. When comparing the scales with each other, a clear difference in flood wave celerity is found. The flood wave duration itself did not create large differences, whether the duration is one or 12 days; the wave celerity is in the same order of magnitude. This makes sense, because the wave celerity mainly depends on the water depth, which is equal for all wave durations. In the table below the average travel time, the distance and the resulting wave celerity has been given.

Table 4-4: Wave celerities on varying scales

| Scale [m ³ /s] | 5 | 50 | 500 | 5000 |
|--------------------------------|--------|---------|---------|--------|
| Average travel time [h] | 1.67 | 4.33 | 12 | 33 |
| Travel distance [m] | 3626.7 | 12868.1 | 45657.8 | 162000 |
| Wave celerity [m/s] | 0.60 | 0.82 | 1.06 | 1.36 |

As appears from the table; the increase in wave celerity is quite significant. Besides, the travel time is also increasing significantly for increasing scale. This has as a consequence that the larger the scale, the more possibility for storage effects to have influence.

Summary and conclusions

In the results that were shown on the previous pages, some remarkable observations were made. The most significant are listed below:

1. The smaller the simulated spatial scale, the larger the 1D-2D differences are
2. The higher the meandering intensity, the larger the 1D-2D differences are
3. The lower the roughness, the larger the 1D-2D differences are
4. The larger the 2D grid cell size, the larger the 1D-2D differences are
5. The smaller the flood wave duration, the larger the 1D-2D differences are

The most striking of them will be analyzed in further detail in the next paragraph, by discussing some theories that may explain the differences. Besides these theories, some basic processes could be playing a role here, such as:

1. The larger the scale, the smaller the flow velocity over water depth ratio becomes. Higher flow velocities normally cause more turbulence and other 2D effects, but as the water depth increases more, these effects are damped. Frictional effects, as these are non-linear, are also affected by the same scale effects.
2. The same applies to the flow width, the effects are spread out over a larger area. Applies both to increasing scale as to the comparison of summer bed flow to floodplain flow.
3. For flood waves, the following applies: the larger the scale, the larger the 1D-2D differences. This is initially caused by the wave celerity difference. The travel time on larger scale is, due to lower flow velocities, a lot longer compared to smaller scale. More travel time indicates that the storage effect can have influence for a longer time period.

To be able to explain in more detail the observed differences, some possible causes are discussed and analyzed below. These are the following:

1. The effects of grid size and bathymetry discretization
2. The water level and velocity gradients in cross-sectional direction for varying roughness
3. The water level and velocity gradients in cross-sectional direction for varying meandering intensities
4. The interaction between summer bed and floodplains
5. The Boussinesq approach¹³ and consequences for the summer bed – floodplain flow area ratio
6. Further effects of storage

One could argue that also secondary flow¹⁴ is playing a role here, but D-Flow FM only calculates spiral flow and streamline curvature post-process. This means that there is no direct coupling to the momentum balance. This results in the fact that this physical process is not included in the way the water levels or velocities are simulated. Therefore, this process cannot be used to explain differences in model output.

Another process that might seem important is the used time step for flood wave simulations. As discussed in the previous paragraph, a quick scan pointed out that the time step is not important for stationary simulations, which makes sense. However, for flood wave simulations, the conditions are

¹³ This name was given in the D-Flow 1D User Manual to the addition of the Boussinesq coefficient. This coefficient is added to perceive a better fit to real case scenarios, or 2D simulations, of flood plain flow simulations. It accounts for the non-uniform velocity distribution in a cross-section (Deltares, 2017c). It is not to be confused with the Boussinesq hypothesis, approximation or wave modelling.

¹⁴ See Appendix A for more on this subject

constantly changing, so the expectation is that this would have some effect. A second quick scan pointed out that this is not the case. The reason for this is the fact that the grid size is sufficiently small, so the CFL criterion already decreases the time step to a certain value at which a sufficient level of accuracy is reached.

Note that the observed differences for grid size are probably independent of the numerical scheme that is used. It is therefore not purely a numerical process that causes the 1D-2D differences. Issues like the truncation error¹⁵ are not the main issue here. Besides, the effect of grid size is very dependent on the case that is used, complicated bathymetries will be poorly represented compared to simple ones, when using the same grid size. However, the general pattern will be the same, which will be showed in the next section.

¹⁵ The truncation error is the 'error in approximating the differential equations or differential operators by discrete representations such as numerical schemes' (Zijlema, 2015). In other words, it measures the error between the numerical scheme and the original equation.

4.3 Explaining theories

This paragraph will discuss some theories that may explain the difference that were observed between the model output of the 1D model and the 2D model.

4.3.1 Grid size (bathymetry discretization)

The main direct effect of adjusting the grid size is the way the bathymetry is discretized. As explained before, the number of grid cells in cross-sectional direction is the most important here. The more grid cells, the more accurate the original bathymetry will be schematized in the model. To illustrate this, for a number of grid sizes the actual bathymetry as used in the simulations will be shown in the graphs below (Figure 4-24 and Figure 4-25). The graphs show the summer bed, together with a small part of the floodplains. This is where the differences in elevation are the largest, so the differences between the grid refinements are visible the most clearly.

Note that this theory only applies if the bathymetry is measured on a number of locations, for instance by means of a gauge rod. If on ten locations the depth is measured, one can derive ten data points as input for a cross section bathymetry. The other option is when the total bathymetry is measured, for instance by means of laser equipment. In this case, both the 1D as the 2D approach cause loss of accuracy, because in 1D one has to define certain data points (which cannot be infinite, so one has discretize manually), and in 2D due to the process as explained in this paragraph. Another issue is the resolution of the available bathymetry data. If one has for instance a DEM of 5x5m available, it makes no sense to use grid cells of 0.5x0.5m, because this does not increase the accuracy of the used bathymetry. Lastly, it also depends on the complexity of the bathymetry. A 2D elevation model is always better in capturing the complex geometries. Otherwise, when using a 1D model, an infinite amount of cross sections would have to be measured and implemented.

As systems of small scale, on which this research focuses, are often not measured with high accuracy, the issue is of importance. The assumption therefore is that 1D cross sections are the actual measured profiles, so 1D is in that respect the most accurate approach.

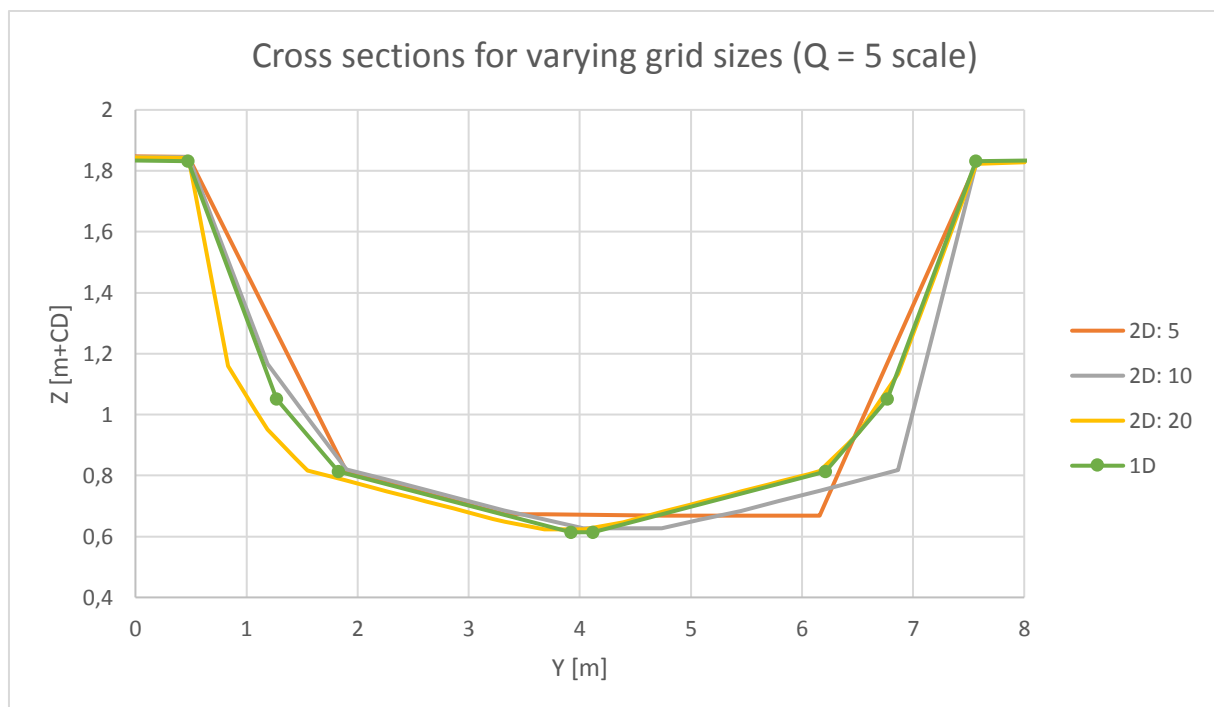


Figure 4-24: Cross sections for varying grid sizes (Q=5 scale) - the green dots indicate the data points on which the bathymetry is based

From the figures appears that a higher number of grid cells increases the accuracy of the cross section bathymetry. Especially when there are only five cells in cross-sectional direction, the bathymetry is represented poorly by the grid. One can observe that the smaller the grid size (which means more grid cells in cross-sectional direction), the more accurate the bathymetry becomes.

As shown in the graph, the cross section influences in the potential flow area. If these areas are calculated, they can be compared to the model output results and see whether they show the same pattern.

Table 4-5: Flow areas, for scale $Q = 5$ and varying schematizations (cf. Figure 4-19)

| Schematization | Flow area summer bed [m ²] | Relative diff. to 1D output |
|----------------|--|-----------------------------|
| 2D: 5 | 6.509 | 11.6% |
| 2D: 10 | 6.880 | 7.2% |
| 2D: 20 | 6.877 | 6.1% |
| 1D | 6.550 | - |

Two conclusions can be drawn from the table when comparing the flow area to the relative difference in water level output.

1. With 5 cells in lateral direction, the flow area matches the 1D flow area the most. This does not mean that the relative difference is small. On the contrary, it is the largest. The cross section shape is however very different, which may explain the large relative differences. There are obviously more processes playing a role, which will be dealt with in the next paragraphs.
2. 10 or 20 cells in lateral direction have a similar flow area, but the shape still differs. This might explain the small gap in relative difference that still exists between these two schematizations.

The same analysis has been done for the largest scale ($Q = 5000$). Here, it has been tried to create more convergence of the cross sections by creating 40 grid cells in lateral direction. But even in that case, there are still differences, although very small.

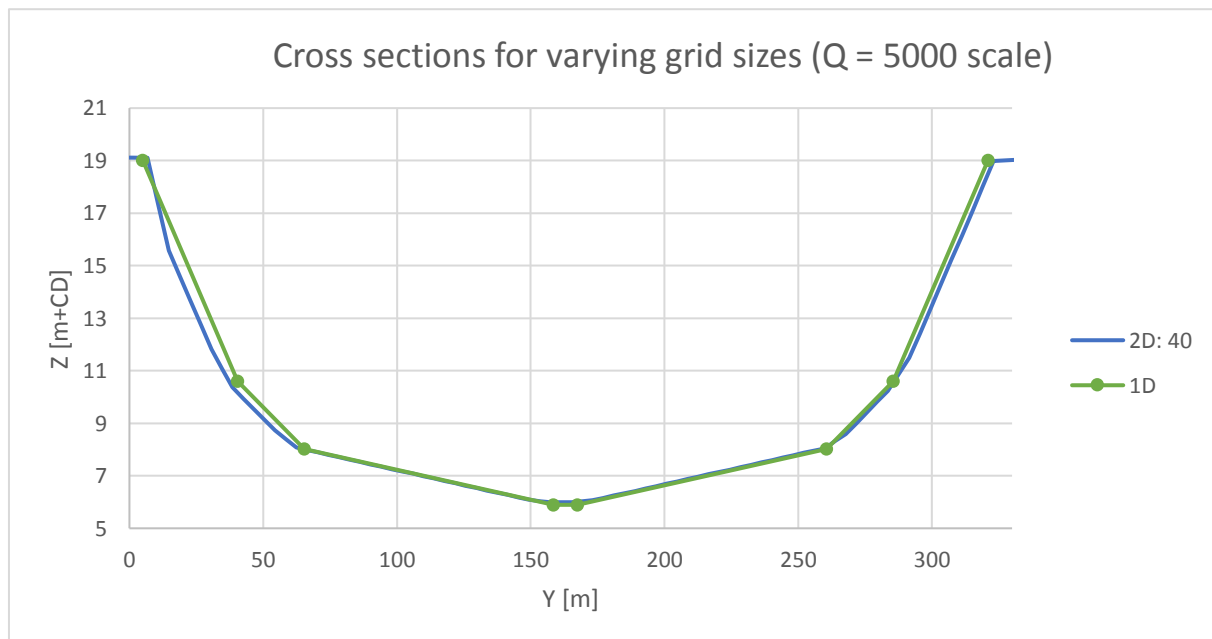


Figure 4-25: Cross sections for varying grid sizes ($Q = 5000$)

Another observation that is explained from grid size variation is that a roughness coefficient of 0.03 creates the largest (relative) difference. By refining the grid and rerunning the simulations of $Q = 5$, summer bed flow, no meandering and all roughness coefficients, it appeared that the differences between 1D and 2D changed into the following values:

Table 4-6: Grid size variation for no meandering situations

| | n = 0.02 | n = 0.03 | n = 0.04 |
|--------------------------|-----------------|-----------------|-----------------|
| Finer grid size | 3.96% | 2.72% | 2.30% |
| Default grid size | 7.34% | 9.24% | 6.68% |

This shows that, as initially expected, the effects of roughness increase for decreasing roughness. The reason for the sudden change is as following. Generally speaking, the water level rises due to increasing roughness. This causes more grid cells to flood at the edges of the summer bed. The schematizations as shown in Figure 4-24 and Figure 4-25 already showed that the largest difference in bathymetry is located at the edges of the summer bed. Apparently, the cell that is (partially) flooded when increasing the roughness from $n = 0.02$ to $n = 0.03$ has a low accuracy, which causes large differences. When refining the grid with more grid cells, this difference decreased, which led to the results as shown in the table above. This phenomenon has been checked for other scales and meandering intensities, and it checked out.

The observations also point out that the bathymetry discretization effects are the largest in summer bed flow, when analyzing the relative differences. This can be explained by the fact that the bottom level varies much more in the summer bed cross section compared to the floodplain cross section. The floodplain has almost no transverse slope, so the averaging by discretization will not introduce large differences. Therefore, the discretization introduces more differences in the summer bed simulations. Generally speaking, it can be concluded that for floodplain flow, grid size does not have much effect, at least not when increasing the number of grid cells from 10 to 20 (cf. Figure 4-19).

4.3.2 Velocity and water level gradients over the cross-sectional direction for varying roughness coefficients

Velocity and water level gradients can cause differences in transport magnitudes. Constant water level gradients would not matter if the velocity would have a perfectly symmetric distribution, because on average the transport magnitudes would be equal to the 1D average. It is however the case that often they are not, so the magnitude of the water level gradient is of importance too. This section will give some examples of velocity and water level distribution over the cross sections, for varying roughness coefficients. The meandering intensity has influence on this process too, this will be dealt with in the next section.

The figure below shows three examples of varying roughness coefficients and the corresponding flow velocities. The white squares indicate the area that will be zoomed in to in the remainder of this section.

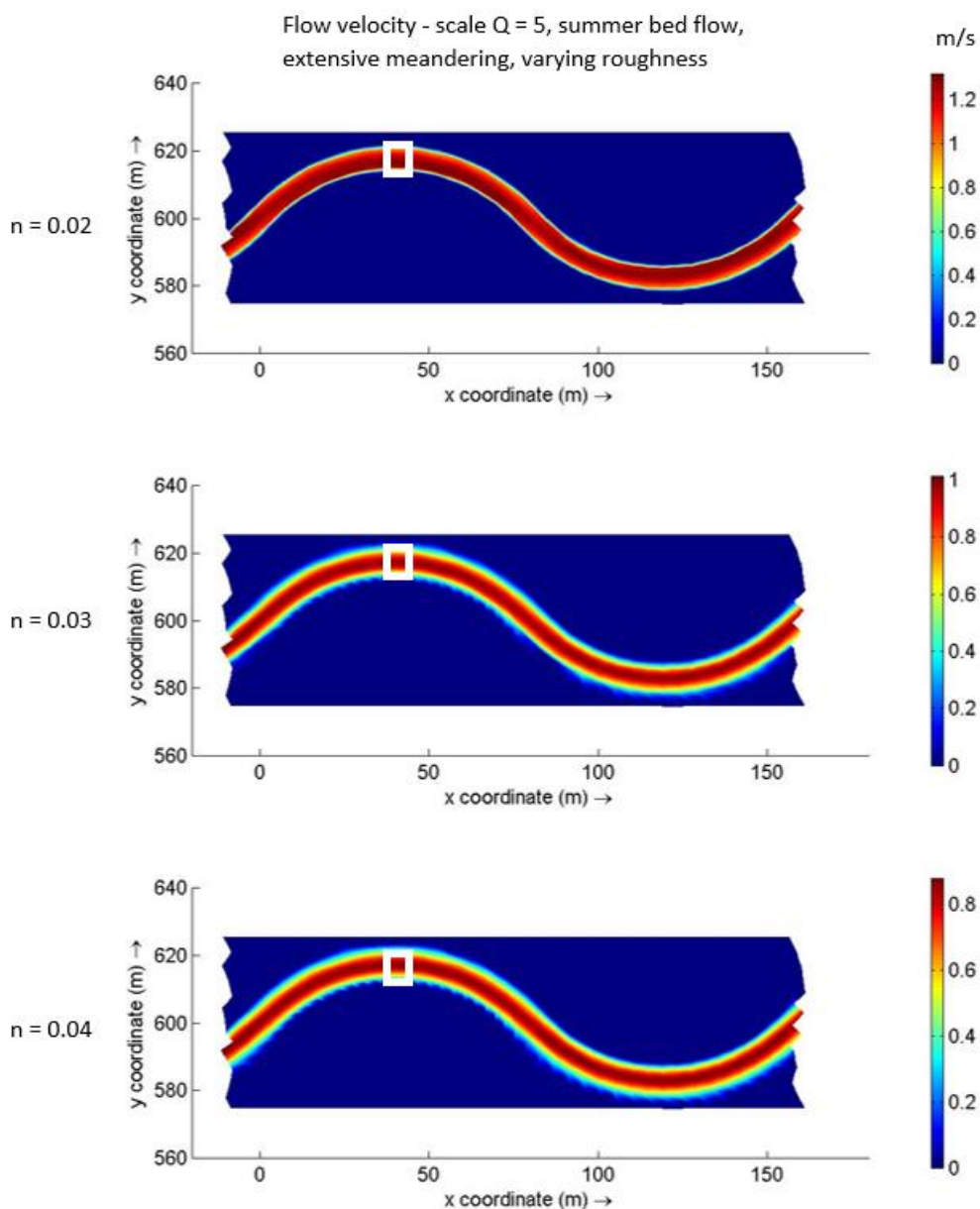


Figure 4-26: Flow velocity in cross-sectional direction in different situations

In the graph below, the flow velocity of the cross section in the white square is presented. The left hand side of the graph represents the most northern part of the channel as shown in Figure 4-26.

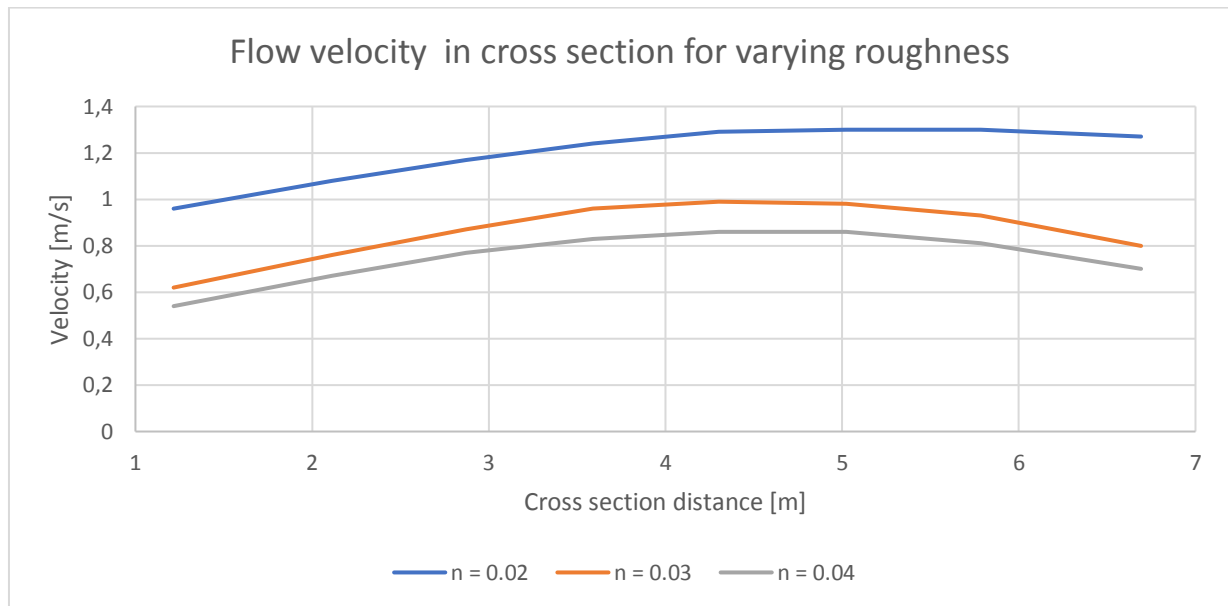


Figure 4-27: Flow velocity in cross section for varying roughness, derived from plots above ($n = 0.02$ causes lower water levels, therefore the outer two grid cells are not flooded, so no flow velocity is present there)

The velocity difference in cross-sectional direction is clearly visible in the plots above. The influence of roughness is the largest reason for these differences. With a roughness coefficient of $n = 0.02$, the bed of the summer bed is very smooth. This means that the flow has very little resistance of the bed close to the summer bed edges, therefore the flow can be close to the edges of the summer bed (at 1 and 7 meters in Figure 4-27). 1D-simulations simulate an average velocity which is based on the assumption that there is a uniform velocity distribution over the cross-sectional direction. As appears from the graph, in none of the three cases the velocity distribution is uniform. This may seem logical, but the distributions are not symmetric either. When the velocity distributions are combined with the water level distributions in cross-sectional direction, conclusions can be drawn about the discharge magnitude on the several locations in the cross section.

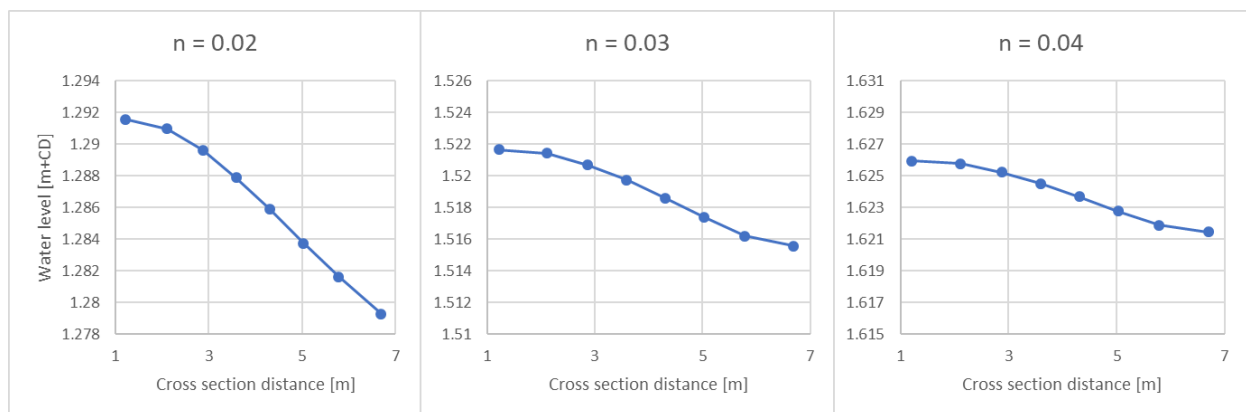


Figure 4-28: Water level gradients in cross section for varying roughness coefficients

The plots have the same domain magnitude of 0.016m on the y-axis, which allows to observe the difference in gradient. From the graphs appear that, due to centrifugal forces, the water level is highest at the outer bend. When combining this figure with Figure 4-27 it is clear that the transport magnitude of water will vary through the cross section. In the case of a perfectly symmetric

distribution and a constant water level gradient, the 1D approach would not cause much deviation, but with the velocity distributions as observed in this case, the differences are definitely present.

The last important issue that appears from these plots is the fact that the magnitude of the flow velocities is decreasing with increasing roughness. This is a logical process, which can also be derived from the Manning or Chézy formula (eq. 4.1). Higher flow velocities mean more turbulence and more water level differences in cross-sectional direction, see graphs of Figure 4-28. From the slope of the graph it can be derived that the higher the roughness, the lower the water level difference is in cross-sectional direction. This has everything to do with the velocity difference. The higher the velocity, the higher the forces that cause these water level gradients, the higher the water level differences. If the slopes are calculated, the following numbers are obtained:

Table 4-7: Water level gradients for varying roughness coefficients, scale $Q = 5$

| | Water level difference [m] | Water level gradient |
|-----------------|----------------------------|----------------------|
| n = 0.02 | 0.011 | 1.69E-03 |
| n = 0.03 | 0.006 | 9.23E-04 |
| n = 0.04 | 0.0045 | 6.92E-04 |

A higher cross-sectional water level slope means more deviations in transport magnitude. This explains why a lower roughness causes more differences.

We can do the same thing for scale $Q = 5000$. Then the following numbers are obtained:

Table 4-8: Water level gradients for varying roughness coefficients, scale $Q = 5000$

| | Water level difference [m] | Water level gradient |
|-----------------|----------------------------|----------------------|
| n = 0.02 | 0.058 | 1.16E-04 |
| n = 0.03 | 0.037 | 7.40E-05 |
| n = 0.04 | 0.026 | 5.20E-05 |

It is clear that the slopes of the water level in cross-sectional direction of higher scales is significantly lower compared to smaller scales. This has to do with the fact that the velocities are not increasing with the same order of magnitude as the scale itself, which decreases the effects of the centrifugal force that forces the water level gradient. Less steep slopes indicate relatively less difference in transport magnitude in the cross section for similar velocity distributions. This explains why the differences between 1D and 2D are decreasing for increasing scale.

4.3.3 Velocity and water level gradients over the cross-sectional direction for varying meandering intensities

The same analysis as discussed on the previous pages can be made for varying meandering intensities. Varying velocities and water levels in cross-sectional direction are not only influenced by the roughness of the bed, but also by the intensity of the meandering. The plots below show the effects on the scale of $Q = 5$ and 5000.

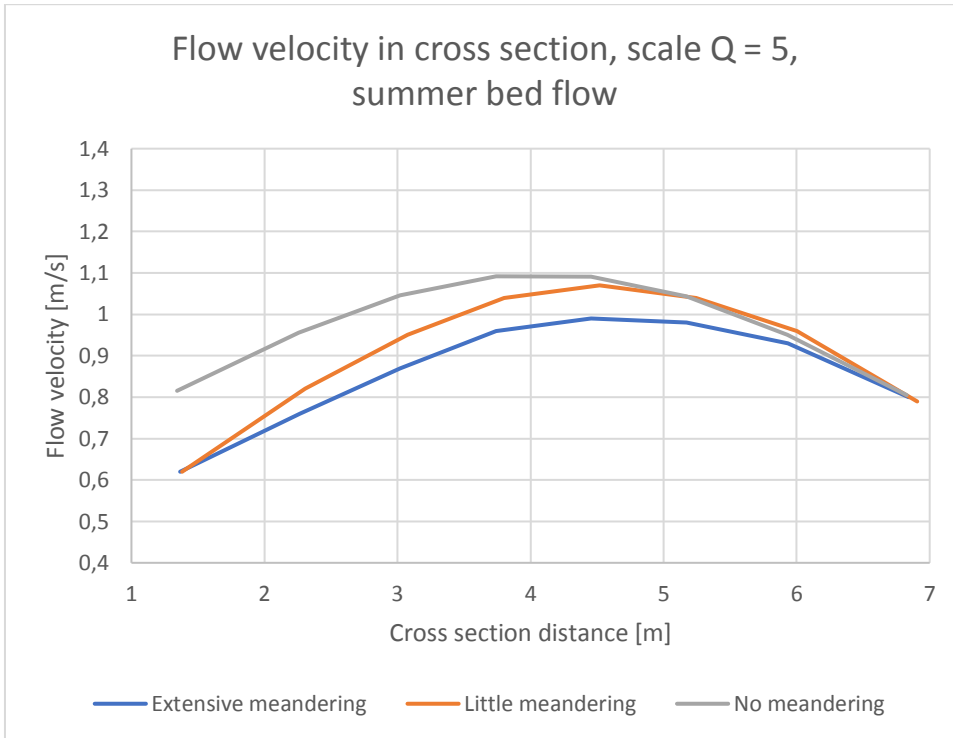


Figure 4-29: Flow velocity in cross-sectional direction for scale 5000 with varying meandering intensities

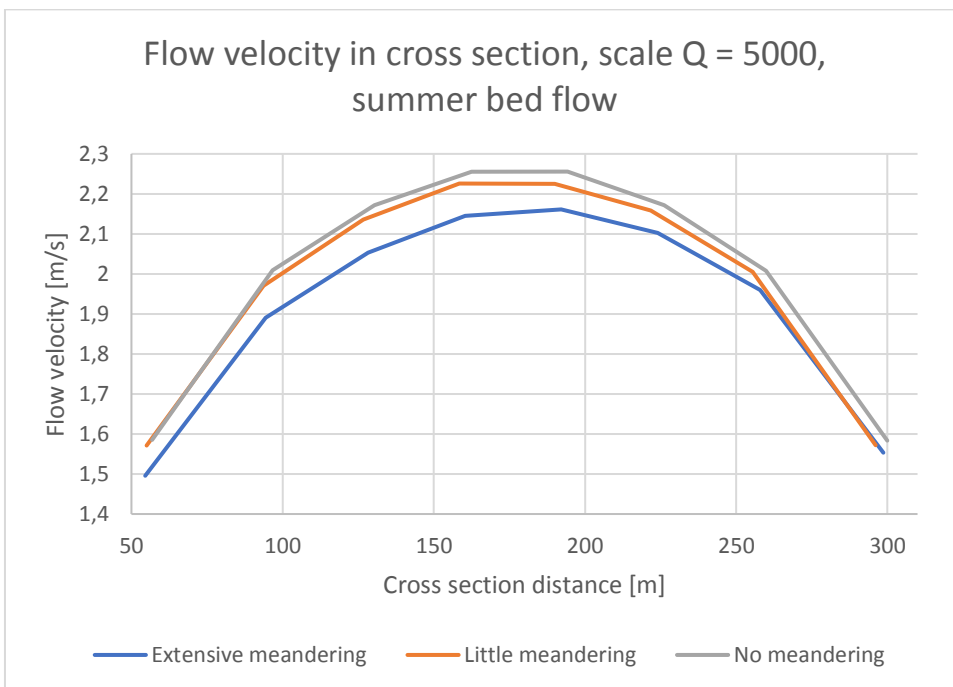


Figure 4-30: Flow velocity in cross-sectional direction for scale 5000 with varying meandering intensities

From the graph can be derived that the situations without meandering have a perfect symmetric distribution of the velocity cross-sectional direction. In the meandering situations this is changing. Again, the water level slopes have been determined and are given in the table below:

Table 4-9: Water level gradients for varying meandering intensities

| Meandering | Water level gradient Q = 5 | Water level gradient Q = 5000 |
|------------------|-------------------------------|----------------------------------|
| Extensive | 1.42E-03 | 1.24E-04 |
| Little | 5.69E-04 | 6.55E-05 |
| None | 0.00 | 0.00 |

A higher meandering intensity shows on both scales a higher water level slope in cross-sectional direction. Together with the asymmetric velocity distribution this implicates more difference compared to the 1D situation. Furthermore, the larger the scale, the closer the velocity distribution looks like a symmetric distribution in cross-sectional direction. Furthermore, the water level gradients are much smaller for larger scale. So again, this explains why larger scales are less influenced by meandering intensities.

The water level gradient can directly be linked to the centrifugal force. Both an increase of meandering intensity as a decrease in roughness cause the centrifugal forcing to be larger, as this depends on the velocity and the channel bend angle. The roughness has influence on the velocity – a higher roughness creates a lower velocity. The meandering intensity has influence on the bend angle – a higher intensity creates a higher angle. The consequence of this is difference in centrifugal forcing, which causes difference in the water level gradient.

4.3.4 Summer bed – floodplain interaction

The figure below shows the location of which the flow direction vectors will be analyzed.

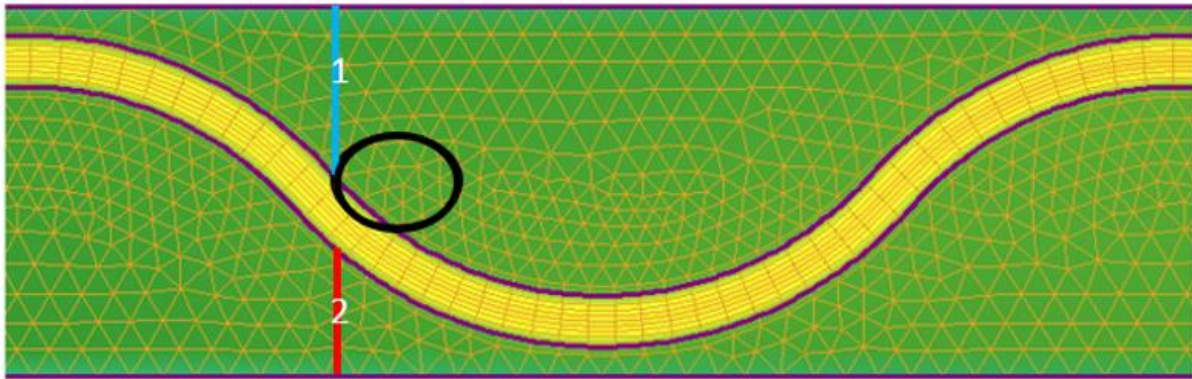


Figure 4-31: Location of the vector plot

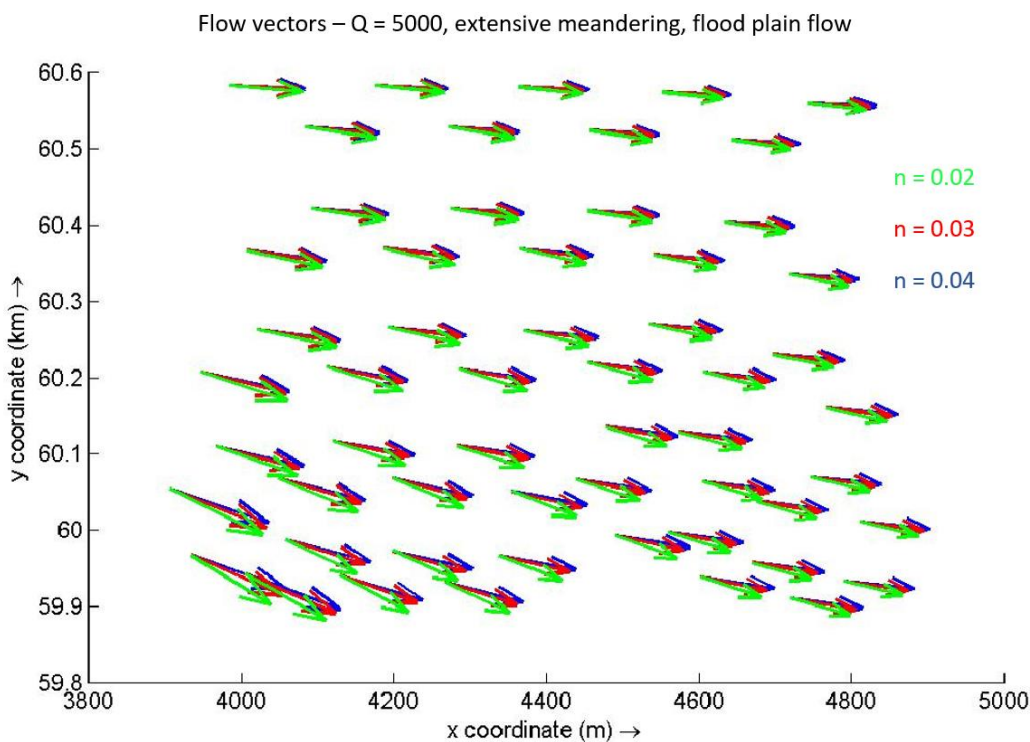


Figure 4-32: Flow vectors for varying roughness coefficients over floodplain, scale $Q = 5000$, floodplain flow

The vector plot shows the differences of flow velocity and patterns of the three roughness types. What is clearly visible is that the lowest roughness is flowing more in the direction of the summer bed compared to the other ones. This is caused by the fact that the floodplain has a constant roughness of $n = 0.045$. The summer bed has therefore a lower roughness, in all cases. The water will always flow in the direction of the least roughness, so will be flowing more or less in the direction of the summer bed. This effect is stronger when the roughness is deviating significantly from the floodplain roughness, as is the case for a summer bed roughness of $n = 0.02$. This is visible in the plot, the green arrows are the most in the summer bed direction. In the situation with high summer bed roughness of $n = 0.04$, the roughness of summer bed and floodplain is almost comparable, which causes the flow direction to be more in x-direction and less in summer bed direction. The total flow distance is shorter, the slope is therefore higher, which makes the flow velocity also higher. This causes lower water levels, so the difference with 1D decreases. When the flow velocities and

discharges over the floodplains (1 and 2 in Figure 4-31) are compared, the following ratios are observed:

Table 4-10: Discharges and flow velocities of floodplains 1 and 2 (Figure 4-31) - Q = discharge, U = velocity = FP1 = floodplain 1, SB = summer bed

| Roughness coefficient | Q FP1 | Q FP2 | U FP1 | U FP2 | U SB | % of total Q |
|-----------------------|---------|---------|-------|-------|------|--------------|
| n = 0.02 | 1696.80 | 650.02 | 0.66 | 0.36 | 2.90 | 15.6 |
| n = 0.03 | 3460.80 | 1726.00 | 0.83 | 0.58 | 1.99 | 34.6 |
| n = 0.04 | 4368.70 | 2398.90 | 0.87 | 0.67 | 1.58 | 45.1 |

The numbers in the table indicate that both the discharges as the flow velocities increase with increasing summer bed roughness. A higher summer bed roughness causes lower flow velocities, which makes sense. However, it also causes higher flow velocities in the floodplain, which does not make sense at first sight because the slope and bed roughness do not change. Together with the flow direction plots of Figure 4-32 it can however be concluded that the summer bed roughness influences the floodplain flow, so that there is a summer bed – floodplain interaction.

When modelling in 1D, the model assumes that the flow is always in summer bed direction. The flow vectors corresponding to a roughness coefficient of $n = 0.02$ are therefore closest to the 1D simulation. The higher the summer bed roughness, the less the flow pattern is in summer bed direction. As explained before, this causes lower water levels. Therefore, the 1D-2D difference is decreasing for higher roughness coefficients.

4.3.5 The Boussinesq approach and consequences for summer bed – floodplain flow area ratio

The Boussinesq coefficient is added in the D-Flow 1D module to perceive a better fit to real case scenarios, or 2D simulations, of floodplain flow simulations. It accounts for the non-uniform velocity distribution in a cross section (Deltares, 2017c).

The way the Boussinesq coefficient is calculated introduces deviations of its value for varying scales, which may explain the increase of 1D-2D difference for decreasing spatial scale. The coefficient is used in the discharge computation, in the form of a multiplier to the convective term in the momentum equation. It accounts for the non-uniform velocity distribution in a cross section (Deltares, 2017a). The general equation for this coefficient is as follows:

$$\alpha_B = \frac{1}{A_f R C^2} \int_0^{W_f} C^2(y) h(y) R(y) dy \quad 4.4$$

In the D-Flow 1D module it is possible to implement cross sections consisting of one, two or three parts with different roughness coefficients. The Boussinesq coefficient is formulated for these cases where the cross sections consist of more than one part. If the cross section is consisting of one part, the coefficient is equal to 1. For this research a summer bed and two floodplains were schematized. As the floodplains have the same characteristics, both the two or three part division can be used. For the single purpose of showing the calculation method, the two part division suffices. In this case, equation 4.4 can be rewritten as follows:

$$\alpha_B = \frac{C_0^2 A_{f0} R_0 + C_1^2 A_{f1} R_1}{C^2 R A_f} \quad 4.5$$

where the subscript 0 means summer bed parameters, 1 means floodplain parameters. In other words, the Boussinesq coefficient accounts for the weight of different roughness values, if present. The Boussinesq coefficient is, as visible from this equation, dependent on the Chézy coefficients and hydraulic radii of the summer bed and floodplain. The values in the denominator require that a single Chézy coefficient and hydraulic radius of the total cross section have to be computed.

The most accurate way to go would be to use equation 4.4 for every part, defined by the individual data points, of the cross section as defined by the user. When modelling in 2D, this is what actually happens, for every grid cell the hydraulic radius and Chézy coefficient is computed. In 1D this is not the case.

By means of an example will be shown how the deviation is introduced by this approach. The example will deal with the following situation:

- Scale: $Q = 5 \text{ m}^3/\text{s}$
- Summer bed roughness: $n = 0.02$
- Floodplain flow, so $Q = 15 \text{ m}^3/\text{s}$

This example is chosen because the effect is best visible in this situation. The model simulated a water depth of 1.3115m for this situation. Using the cross section data, the flow area and wetted perimeter can be calculated of the summer bed and floodplain. Using these parameters, the hydraulic radius can be calculated, which can then be used to calculate the Chézy parameter by using the relation

$$C = \frac{R_0^{\frac{1}{6}}}{n} \quad 4.6$$

The same is done for the whole cross section. Basically, the computation is using equation 4.5, where the subscript 0 represents the summer bed and the subscript 1 the floodplains. The denominator represents the total cross section. In the table below, the separate values of eq. 4.5 are given in the last column with the 'α_β part' title. This results in the following numbers:

Table 4-11: Alpha calculation method, default (the computation is written out below)

| | Wetted perimeter [m] | Flow area [m ²] | Hydraulic radius [m] | Chézy coefficient [m ^{1/2} /s] | α _β part |
|----------------------|----------------------|-----------------------------|----------------------|---|---------------------|
| Summer bed | 7.85 | 7.21 | 0.92 | 49.30 | 16121.14 |
| Floodplain | 40.02 | 1.87 | 0.05 | 13.33 | 15.47 |
| Total | 47.87 | 9.08 | 0.19 | 96.02 | 15882.00 |
| α_β | | | | | 1.02 |

$$\alpha_B = \frac{C_0^2 A_{f0} R_0 + C_1^2 A_{f1} R_1}{C^2 R A_f} = \frac{49.30^2 * 7.21 * 0.92 + 13.33^2 * 1.87 * 0.05}{96.02^2 * 9.08 * 0.19} = \frac{16121.14 + 15.47}{15882.00} = 1.02$$

It is obvious that the alpha value in this case is very low. When the alpha value approaches the value of 1, the less the momentum balance is adjusted. In this case, it practically means that the floodplain roughness is hardly taken into account. Now the calculation will be done using all segments of the cross section, using again equation 4.5, but now in the following shape:

$$\alpha_B = \frac{\sum C_i^2 A_{fi} R_i}{C^2 R A_f}$$

By using this formula, the coefficient is calculated using all available segments of the cross sections, instead of only the summer bed and floodplains. This results in the values as shown in the table below. It is immediately visible that this has a large impact on the final alpha value.

Table 4-12: Alpha calculation method, accurate method

| Segment <i>i</i> | Wetted perimeter [m] | Flow area [m ²] | Hydraulic radius [m] | Chézy coefficient [m ^{1/2} /s] | α _β part <i>i</i> |
|----------------------|----------------------|-----------------------------|----------------------|---|------------------------------|
| 1 | 20.01 | 0.93 | 0.05 | 13.33 | 7.73 |
| 2 | 1.12 | 0.39 | 0.35 | 41.88 | 233.62 |
| 3 | 0.61 | 0.55 | 0.91 | 49.25 | 1227.84 |
| 4 | 2.10 | 2.54 | 1.21 | 51.59 | 8150.14 |
| 5 | 0.20 | 0.26 | 1.31 | 52.31 | 937.92 |
| 6 | 2.10 | 2.54 | 1.21 | 51.59 | 8150.14 |
| 7 | 0.61 | 0.55 | 0.91 | 49.25 | 1227.84 |
| 8 | 1.12 | 0.39 | 0.35 | 41.88 | 233.62 |
| 9 | 20.01 | 0.93 | 0.05 | 13.33 | 7.73 |
| Total | 47.87 | 9.08 | 0.19 | 96.02 | 15882.00 |
| α_β | | | | | 1.27 |

If the scale is increased to 5000, the same calculations can be made. The alpha values for this situation are 1.117 and 1.255. It is clear that the alpha values when using the second calculation

method are more or less the same for the scales $Q = 5$ and 5000 . The alpha value using the original Boussinesq approximation is significantly higher than the scale of $Q = 5$. This is something that can directly be linked to the observations. It still is significantly lower, which explains the fact that there are still differences between 1D and 2D output.

This approach has also a direct link with the flow area ratio between the summer bed and floodplains. If these are compared between 1D and 2D, the effects of the alpha value are visible. The difference in alpha values have been projected in the graph as well.

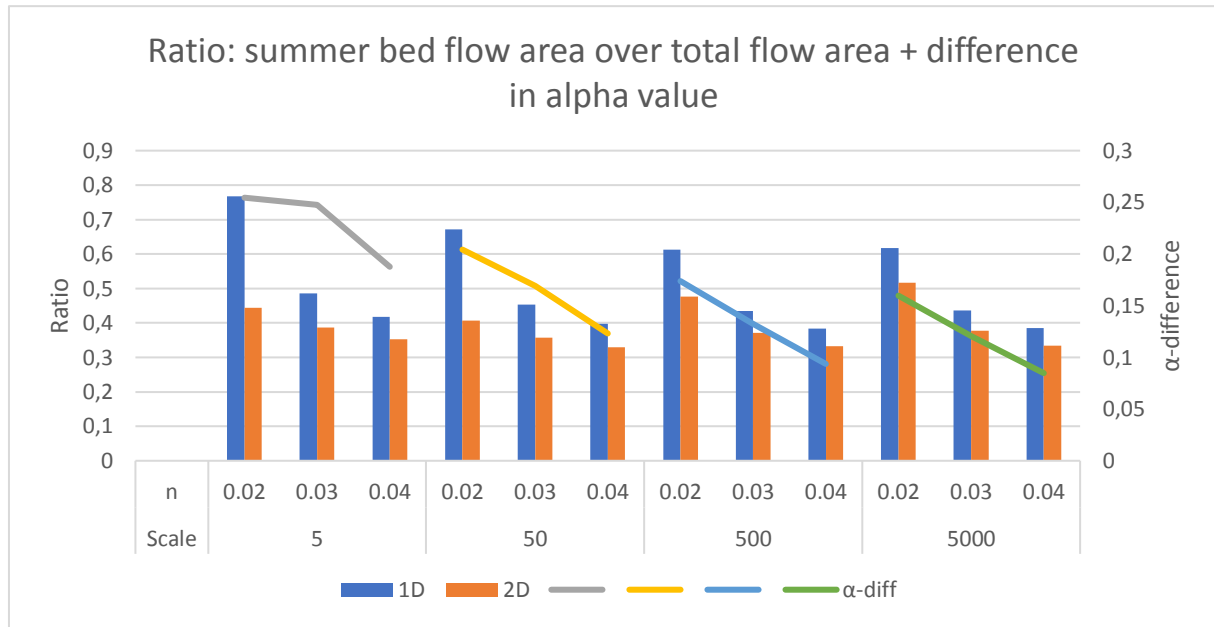


Figure 4-33: Ratio of summer bed flow area over total flow area

The difference in alpha value has a clear relation with the difference in area ratio. With increasing scale, as expected, the alpha value using the default D-Flow 1D method is close to the most accurate one. This explains why for increasing scale, the 1D-2D difference is very low (cf. Figure 4-18). In the table below the alpha values for all cases have been given, together with the difference in area ratio.

Table 4-13: Alpha values and difference in area ratio

| Scale | n | α -default | α -accurate | Ratio diff. |
|-------|------|-------------------|--------------------|-------------|
| 5 | 0.02 | 1.02 | 1.27 | 0.32 |
| | 0.03 | 1.25 | 1.50 | 0.10 |
| | 0.04 | 1.14 | 1.33 | 0.07 |
| 50 | 0.02 | 1.22 | 1.42 | 0.26 |
| | 0.03 | 1.32 | 1.49 | 0.10 |
| | 0.04 | 1.18 | 1.31 | 0.07 |
| 500 | 0.02 | 1.32 | 1.50 | 0.14 |
| | 0.03 | 1.35 | 1.48 | 0.06 |
| | 0.04 | 1.20 | 1.29 | 0.05 |
| 5000 | 0.02 | 1.33 | 1.49 | 0.10 |
| | 0.03 | 1.36 | 1.48 | 0.06 |
| | 0.04 | 1.21 | 1.29 | 0.05 |

From the table, another observation can be made. It appears that the 'accurate' alpha value is, at least for the smaller scales, the largest for a roughness of $n = 0.03$. As the scale increases, the alpha

value for $n = 0.02$ becomes the largest. This could mean, that on small scale, there is a balance between the flow area and the roughness. For instance, if the smallest scale with a summer bed roughness of $n = 0.02$ is considered, the floodplain flow area is very small, but the roughness coefficients are deviating a lot from each other. At a summer bed roughness of $n = 0.04$, the floodplain flow area is significant, but the roughness coefficients are not deviating a lot. Apparently, for that scale, the balance is in such a way that for a roughness of $n = 0.03$ the floodplain flow is of the most influence, considering the high alpha value. The same reasoning applies to all other scales.

The Froude number gives a good indication of whether the 1D water depths and flow velocities are approaching reality. For the situations with large difference, for example scale $Q = 5$, roughness $n = 0.02$, the Froude number is larger than 1. This has nothing to do with the fact that the flow is actually supercritical in that situation, but the combination of overestimated flow velocities and small water depths on floodplains causes the Froude number to be larger than 1.

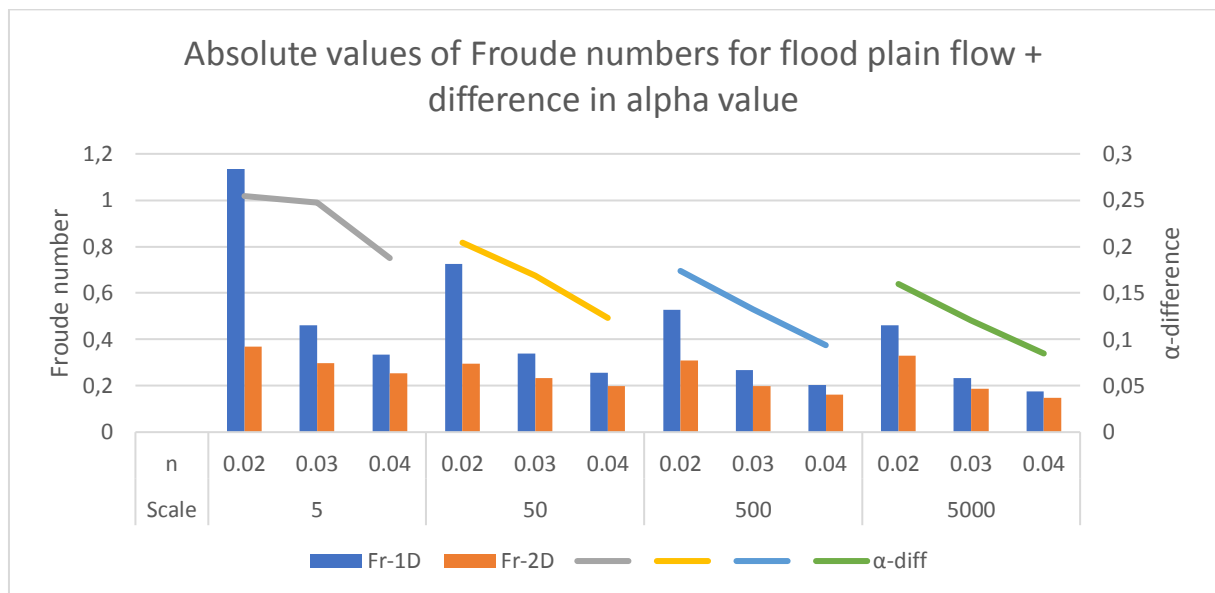


Figure 4-34: Froude numbers for floodplain flow, averaged over meandering intensity

It is obvious that, the less the difference between the Froude numbers, the more the Boussinesq approximation is correct.

4.3.6 Storage effects

The differences in time and discharge of the flood waves can be explained using flow velocity vector plots of several moments during the wave. In this example, the largest scale has been chosen and the flood wave of one day will be discussed. The plots show the flow patterns of a small part in the right floodplain, as shown in the figure below. This part is close to the upstream boundary condition, where no backwater effects of the downstream boundary are present.

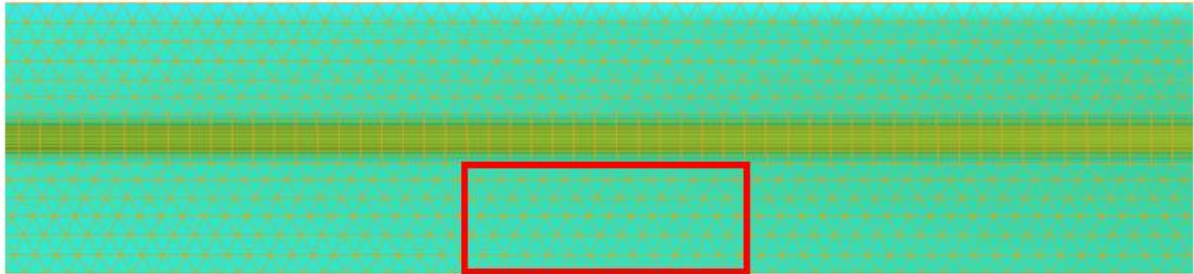


Figure 4-35: Location of vector plots

The plots are corresponding with the moments in time as represented by the orange dots in the graph below. They are chosen because the effects are clearly visible on these moments.

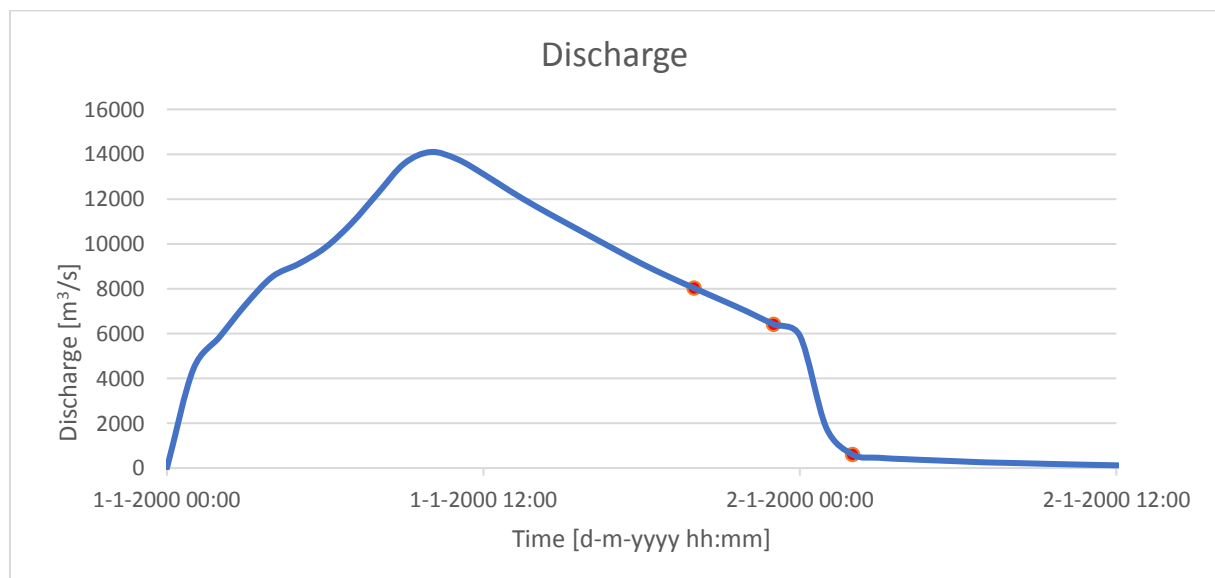


Figure 4-36: Q-t graph of analyzed situation

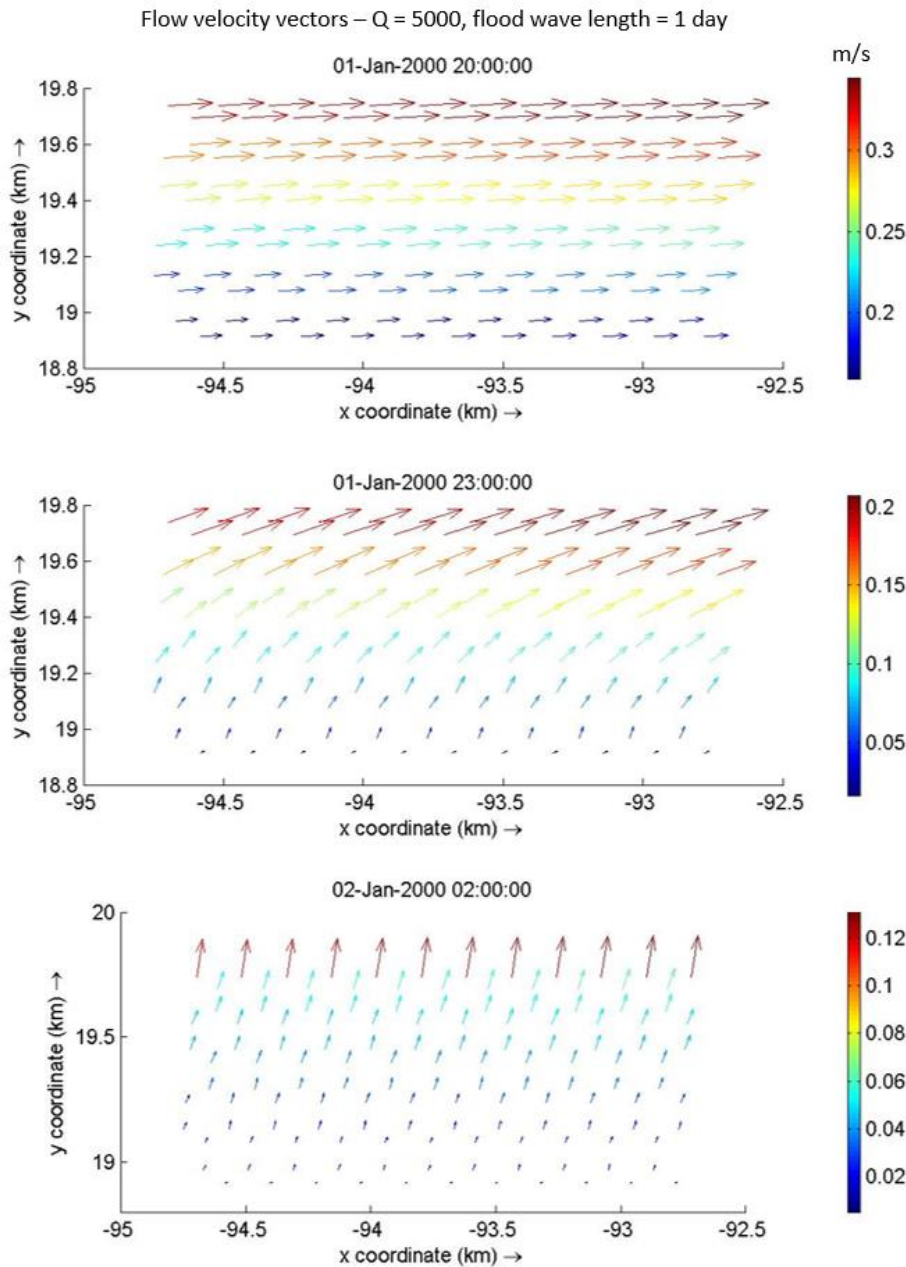


Figure 4-37: Flow velocity vectors on three moments in time

The plots show the direction and magnitude of the flow during three moments in time. The first plot shows the moment where the discharge is decreasing, but is still just enough to flood the floodplains. The flow is in the same direction as the summer bed, which means that no large 2D effects are of influence on the flow. Three hours later, the flow patterns of the second plot are observed, and six hours later, only flow in y-direction is left over. In these plots, the storage effect that occurs with flood waves is clearly visible. The 1D model assumes that a cross section part has a water depth equal to zero, immediately when the water level is below the bottom level of the floodplain. The 1D model just calculates the water depth using the discharge and flow velocity, no storage is taken into account. When modelling in 2D, the effect as visible in the plots above causes that the water depth of a cell decreases more slowly. In 2D, when a water particle is flowing on the floodplain, and when the discharge decreases, its velocity is decreased to a minimum. Then, it is drained in lateral direction towards the summer bed, because the cross-sectional slope of the floodplain is larger than the slope of the main flow direction. The latter process of cross-sectional flow is called storage, because the

water particles are not moving in downstream direction but only in lateral direction and are stored for a while at a certain location, before flooding back to the summer bed again. The process is depicted in Figure 4-38. This is a process that is not simulated by a 1D model. This process causes the flood wave to flatten out, mainly because the tail grows longer.

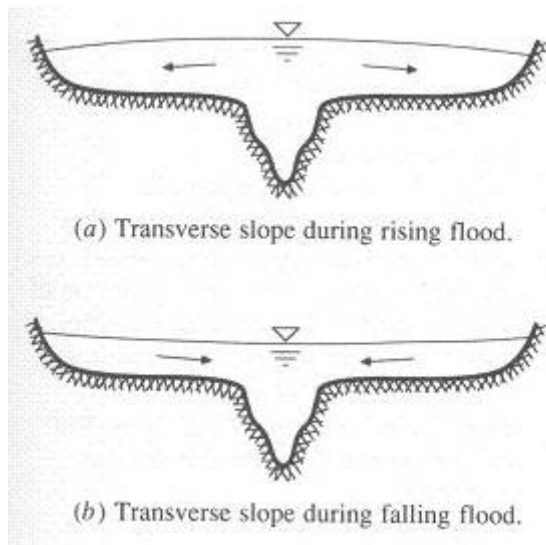


Figure 4-38: Water level slopes during rising and falling flood (Fox, 2015)

When comparing the flood wave of 1 day to the one of 12 days, it is observed that this storage effect has more influence on the one of 1 day. This is caused by the fact that the water level of the 12 day flood wave decreases much more gradually, which decreases the magnitude of the flow in y-direction. This is shown in the plot below. Because the water depth of a grid cell has more time to decrease, the storage effects are of less influence when the flood wave length is lower.

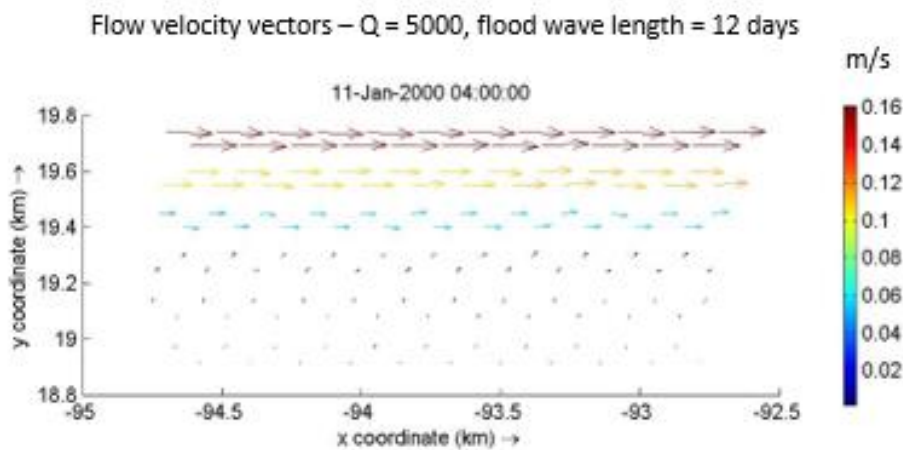


Figure 4-39: Flow velocity vectors, $Q = 5000$

The difference in storage effect is best visible when comparing the change in flood wave shape.

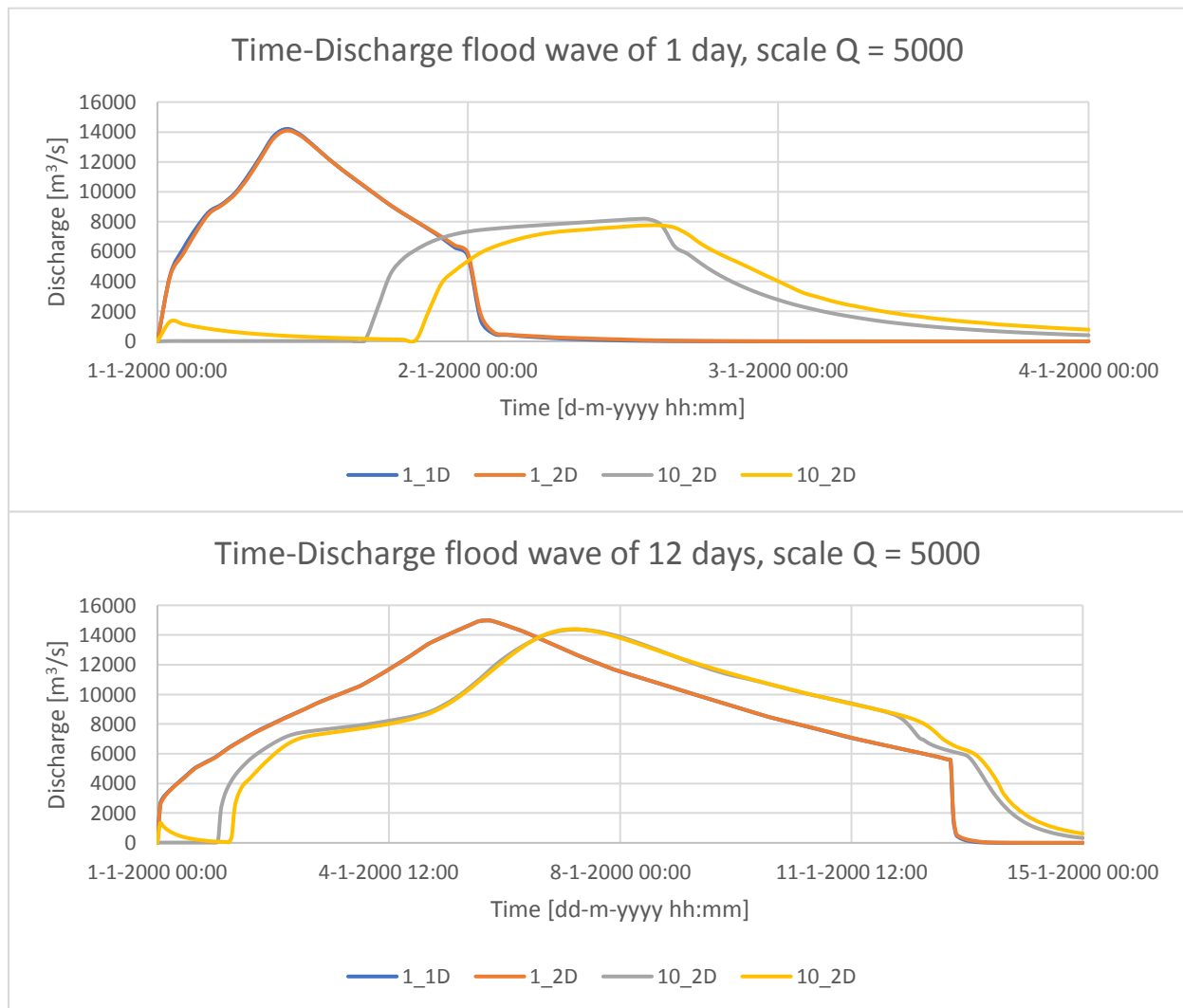


Figure 4-40: Q-t graphs of flood waves

The flood wave shape corresponding to the 12 day wave is much more comparable to the original shape than the one of the 1 day wave. This is caused by the storage effect, as discussed. This effect causes that the water is staying in the floodplains where the wave has already passed. The shape of the high water controls the amount of storage that is taking place. The shape is in this case determined by the wave duration. The wave of 1 day has a much steeper slope compared to longer flood waves. Because the water level drops much quicker in the 1 day wave, the storage effect is much larger. In the 12 day wave, this stored water has more time to flow towards the summer bed, but as the water level is still high in this case, the stored water ‘meets’ the flowing water, which reduces the tail of the flood wave.

The effect that causes difference between scales is for the largest part due to the changing flow velocity to scale ratio. The scale increases with a much larger factor than the flow velocity. This means that the total length of the water course is much longer for larger scales. This has as a consequence that flood waves travel relatively longer, because the wave celerity does not increase as much as the length. Therefore, the possibility and influence of storage or diffusion effects are larger.

4.4 Conclusions

Six different types of processes have been discussed in the previous paragraph. This last paragraph will try to use these processes as explanations for the observed water level differences. Firstly, a brief summary of the observations that are explained by the discussed processes will be given.

Stationary simulations:

- a) 2D simulates higher water levels compared to 1D in all situations
- b) Decreasing scale means increasing relative differences
- c) Less roughness gives more difference
- d) Less meandering gives less difference
- e) Roughness coefficient $n = 0.03$ creates largest differences for summer bed flow
- f) Roughness coefficient $n = 0.02$ creates large difference for floodplain flow

Flood wave simulations:

- g) The further away from the boundary, the larger the difference are
- h) The longer the flood wave length, the smaller the difference are
- i) The larger the scale, the larger the difference are
- j) Largest differences are created at the moment the floodplains are flooded

The processes that are discussed are the following:

1. The effects of grid size on bathymetry discretization
2. The water level and velocity difference in cross-sectional direction for varying roughness and meandering intensities
3. The interaction between summer bed and floodplains
4. The Boussinesq approach and consequences for the summer bed – floodplain flow area ratio
5. The effects of storage

In the table below the observations and process will be coupled. Below the table this will be elaborated.

Table 4-14: Concluding table of coupling between observations and processes

| | | Grid size | Gradients | Interaction | Boussinesq | Storage |
|----------|---|-----------|-----------|-------------|------------|---------|
| a | Water level 2D higher than 1D | X | | | X | |
| b | Decreasing scale: more differences | | X | | X | |
| c | Less roughness: more difference | | X | X | | |
| d | More meandering: more difference | | X | | | |
| e | Peak differences at $n = 0.03$, summer bed | X | | | | |
| f | Peak differences at $n = 0.02$, floodplain | | | | X | |
| g | Flood wave differences | | | | | X |

a) 2D modelling simulates higher water levels compared to 1D in all situations

For summer bed flow, the most important contribution to the 1D-2D difference is made by the bathymetry discretization. For floodplain flow, the scale effect of the Boussinesq approximation can be held accountable for the largest differences.

b) Decreasing scale means increasing relative differences

The water level and velocity gradients have a large part in this. The gradients caused by varying meandering or roughness intensities decrease when the scale increases. Furthermore, for 1D, the difference with 2D, introduced by the Boussinesq approximation, decreases for increasing scale. Also the effects of grid size and bathymetry discretization increase for decreasing scale.

c) Less roughness gives more difference

Less roughness means a steeper water level gradient in the cross-sectional direction, which means more difference in transport magnitude in that direction, initiated by the non-uniform and asymmetric distribution of flow velocities. This causes increasing water depths, so more difference with 1D. This is the cause for summer bed flow. The main cause for floodplain flow is the summer bed-floodplain interaction. There is more interaction for higher roughness, which means lower water levels in 2D, so less difference with 1D.

d) Less meandering gives less difference

Less meandering means also a less steep water level gradient in the cross-sectional direction, which means less difference in transport magnitude in that direction. This causes decreasing water depths, so less difference between 1D and 2D.

e) Roughness coefficient $n = 0.03$ creates largest differences for summer bed flow

The grid size refinement is used to explain this phenomenon.

f) Roughness coefficient $n = 0.02$ creates relatively extremely large difference for floodplain flow

The Boussinesq approach is the most important here.

g), h), i), j) Flood wave observations

All observations with flood wave can be explained with the effects of storage.

Conclusion on quantity of effects

Generally speaking, some statements can be made that summarize and conclude this chapter. The sub question that has been dealt with in this chapter is as follows: What are the differences in model output for varying physical properties of the systems and which processes are causing these differences? The answer to this question has been given, and it can be stated that the differences are influenced by a number of physical effects. To be able to quantify the effects, a final overview of the magnitude of the effects will be given. This includes the effects of the change of magnitude of:

- Scale
- Meandering intensity
- Roughness
- Grid size

The overview will contain relative differences, because of the fact that with increasing scale, the absolute differences logically increase too. Comparing those would make no sense at all.

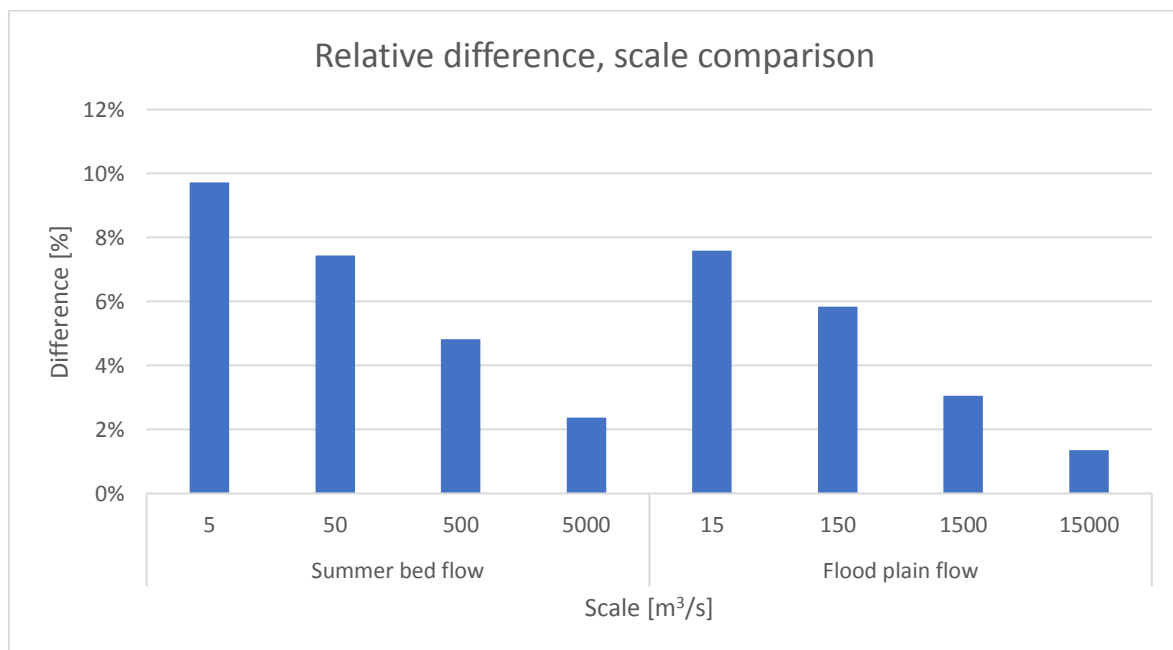


Figure 4-41: Relative difference, scale comparison

The figure above shows the average relative differences when comparing the analyzed scales with each other. The general conclusion that can be drawn from this, is that for small scale the differences are quite significant, up to almost 10%. On a water level of almost a meter (see Figure 4-15), this is a 10 centimeter difference, which could be very important during extreme rainfall events for the inundation of certain areas.

The figure below shows the effects of the other three processes, shown in one overview, for summer bed flow. The figure shows the change in difference for varying model schematizations. For instance, if at the extensive meandering intensity the average 1D-2D is 10%, but at the little intensity 8%, the change in difference for varying meandering intensity is 20%.

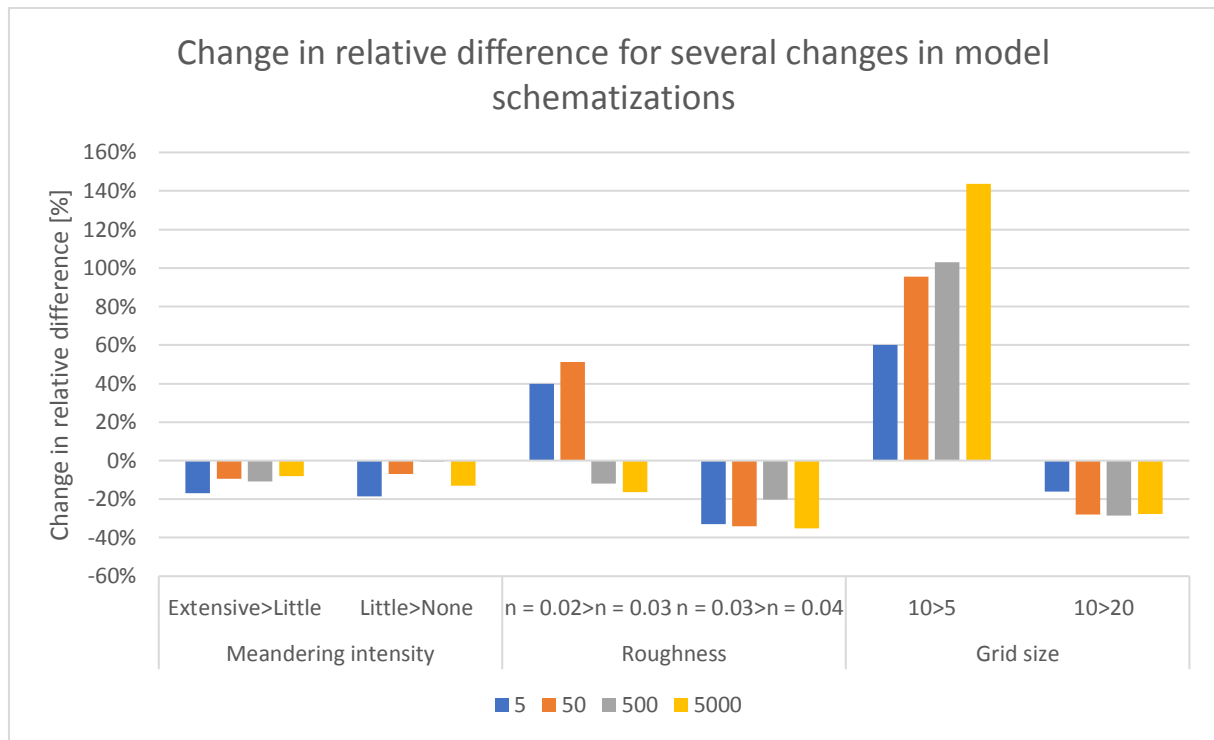


Figure 4-42: Change in relative difference for several changes in model schematizations, summer bed flow

The figure shows the three parameters that were varied in the model schematizations; the meandering intensity, the roughness and the grid size. The peak at the roughness section, when increasing the roughness from $n = 0.02$ to $n = 0.03$, is the deviation in the graph. Where almost all changes result in a decrease of the 1D-2D difference, the increase in roughness from $n = 0.02$ to $n = 0.03$ results in an increase. This is due to the phenomena explained in the beginning of this paragraph. Furthermore, the decrease of the number of grid cells also results in a large increase in 1D-2D difference.

When zooming even further out, the average values can be analyzed of the effects of the three parameters. These values are as follows:

Table 4-15: Average values of changes in relative difference, summer bed flow

| Scale | Meandering intensity | | Roughness | | Grid size | |
|-----------------|----------------------|-------------|-----------------------|-----------------------|-----------|-------|
| | Extensive>Little | Little>None | $n = 0.02 > n = 0.03$ | $n = 0.03 > n = 0.04$ | 10>5 | 10>20 |
| All | -11% | -10% | (16%) | -31% | 101% | -25% |
| 5/50 | -- | -- | 46% | -- | -- | -- |
| 500/5000 | -- | -- | -14% | -- | -- | -- |

A distinction between the two smaller and larger scale has been made in the situation with the change in roughness from $n = 0.02$ to $n = 0.03$, where the smaller scales deviate from larger scales. From the table it can be concluded that the roughness and grid size have the largest effect on the 1D-2D difference.

In the same way the floodplain flow can be analyzed. As variations in the grid size did not result in significant decreases in difference, this has been left out this conclusion. The figure below shows the values that resulted of changes in model schematizations:

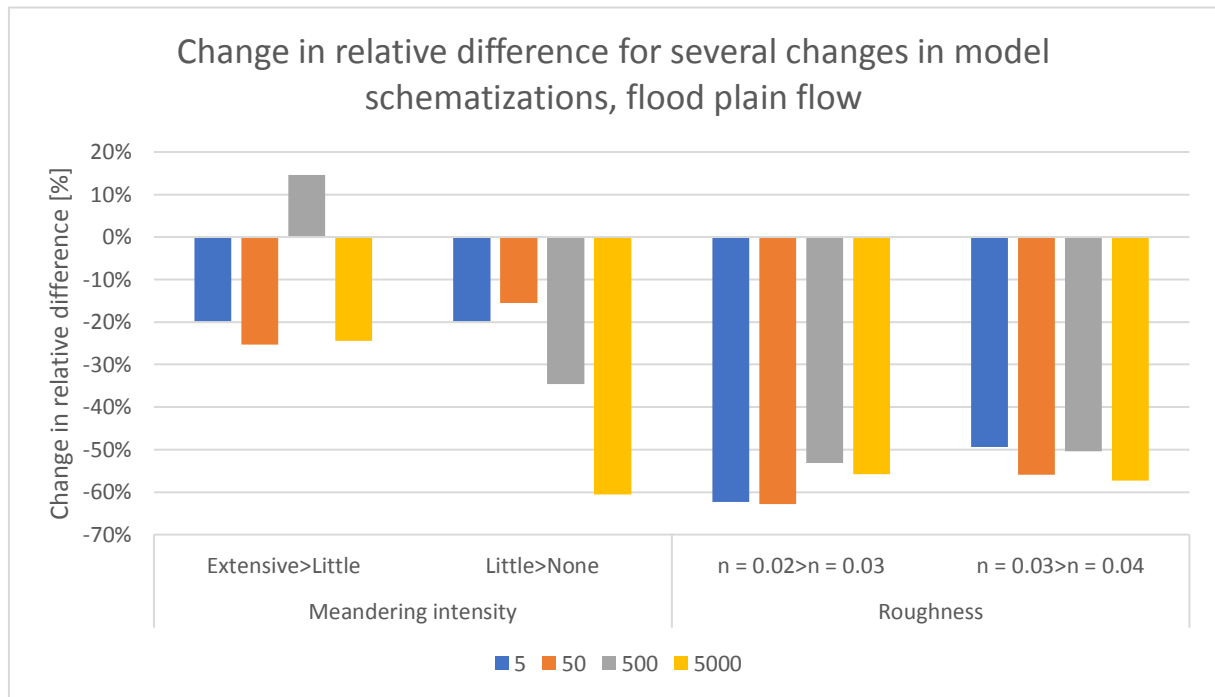


Figure 4-43: Change in relative difference for several changes in model schematizations, floodplain flow

Again, roughness has more effect on the model differences compared to the meandering intensity. When determining the average values, the following numbers are obtained:

Table 4-16: Average values of changes in relative difference, floodplain flow

| Scale | Meandering intensity | | Roughness | |
|------------|----------------------|-------------|-------------------|-------------------|
| | Extensive>Little | Little>None | n = 0.02>n = 0.03 | n = 0.03>n = 0.04 |
| All | -14% | -33% | -59% | -53% |

First of all, the effect of the roughness variations is significantly larger here compared to the summer bed flow. This can be explained by the interaction between summer bed and floodplains. Due to the presence of this interaction, variations in roughness have more effect.

Relation dimensionless numbers and 1D-2D difference

Lastly, an overview of the typical Reynolds and Froude numbers will be given for all scales, both for summer bed and floodplain flow. When taking a look at these numbers, a general relation between the 1D-2D difference and the system characteristics, in the form of these numbers, can be perceived. In this way, one can make a quick first estimation of the system characteristics and decide what the best modelling choice might be.

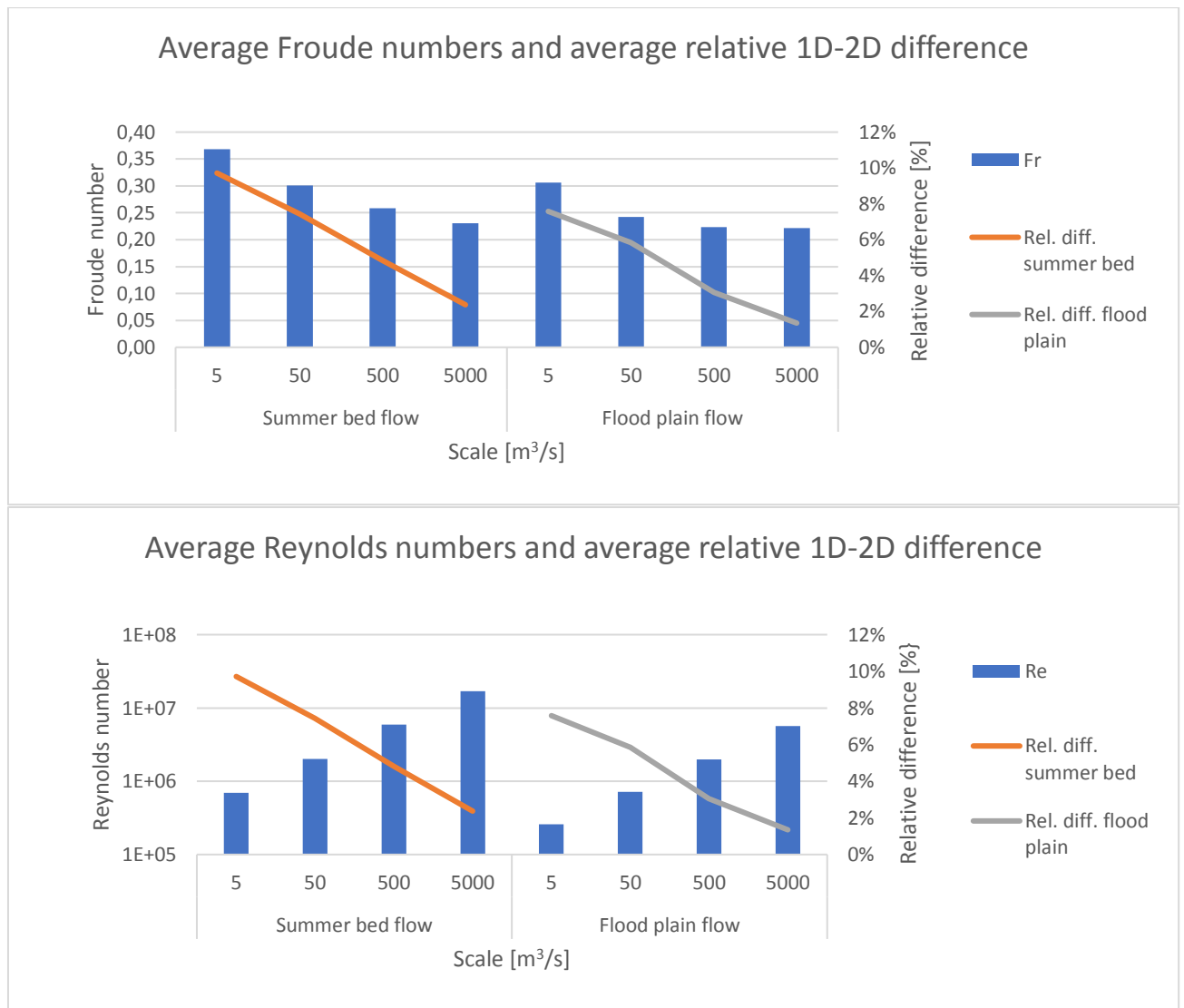


Figure 4-44: Average Reynolds and Froude number for all scales, averaged over all simulations

Chapter 4 elaborated briefly on the Reynolds number. It was stated that typical Reynolds numbers for streams and rivers are between 10^5 and 10^6 . This is confirmed by the simulations that were carried out in this research. Chapter 4 also indicated that typical Froude numbers are between 10^{-1} and 10^{-2} . This is a little underestimated, as the Froude numbers in this research are on average between 0.2 and 0.4. The figure above shows a few general patterns, which are listed below:

1. The larger the Reynolds number, the smaller the 1D-2D difference becomes.
2. The smaller the Froude number, the smaller the 1D-2D difference becomes. In the research, this has been related to the effects of the Boussinesq approach in the Flow 1D model.

These very general observations might help making a quick estimate of a modelling choice.

5. Practical application

In this chapter the catchment of the stream Molenbeek will be analyzed. Based on the discharge and dimensions, the case is somewhere in the spatial scale range of this research, discussed in the previous chapter. This chapter will find an answer to sub question 3 and find out whether theory is in these cases applicable on practical situations. This chapter is built up as follows: First of all, some background information of the case area will be given. Recently, a stream restoration project was performed on the Molenbeek part. This resulted for instance in changes of the water course, such as more meandering, which could influence the modelling choice. Therefore, the background description will also contain some information on this restoration project. Secondly, the methodology of answering the third sub question will be discussed. This contains among others things the modelling method, the data sources and the grid characteristics and boundary conditions. The third paragraph will show the simulation results and lastly some conclusions will be made and an answer will be given to the third sub question: What physical processes are particularly important in a practical case of a small-scale system?

5.1 Case area background

The location and the elevation data of the total catchment of the stream are given in the figures below.



Figure 5-1: Location of the case area

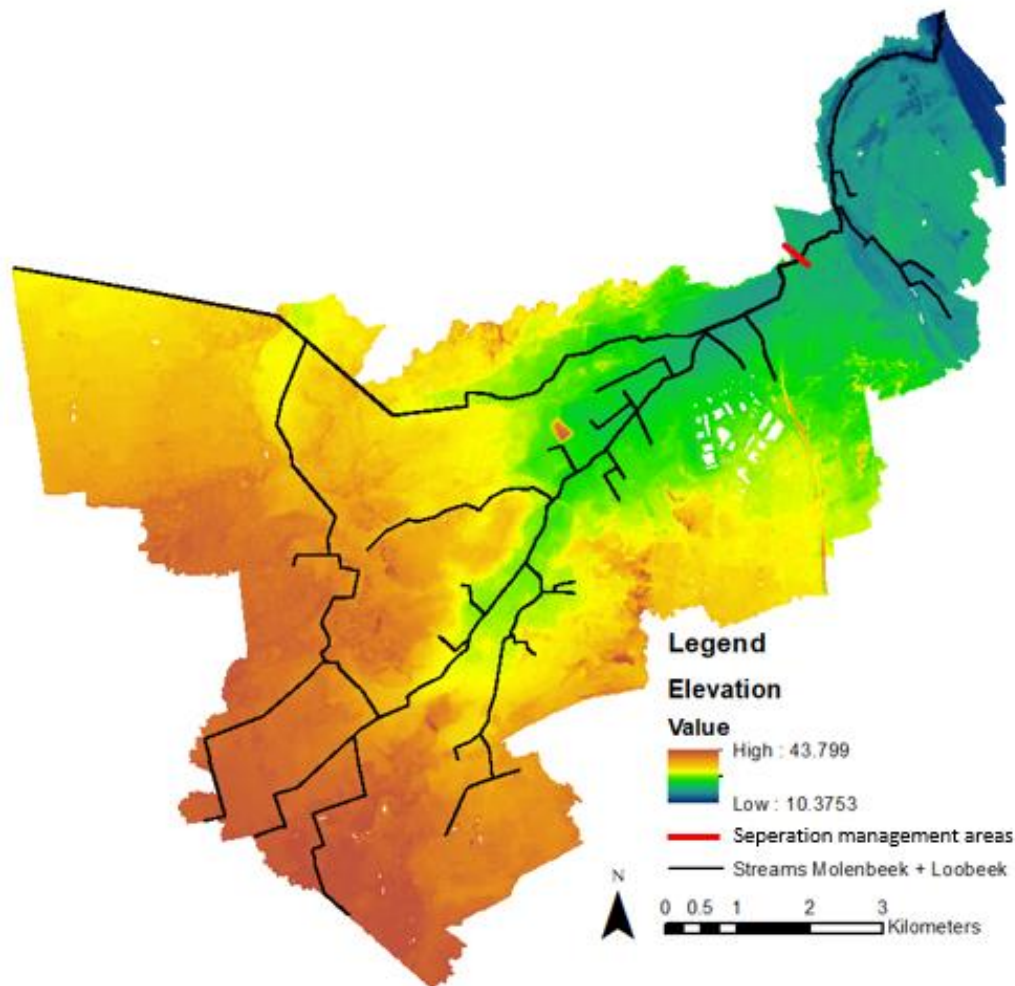


Figure 5-2: Elevation data of the Molenbeek catchment

The stream is a medium-sized lowland stream located in the municipality of Boxmeer in the northeastern part of the Dutch province of Noord-Brabant. The stream originates from various sources on the western side of the river Meuse in the province of Limburg. The *Aa en Maas* water board manages the lower reaches of this system from the border between the provinces of Limburg and North Brabant to the mouth in the Meuse. The other part of the catchment area, left of the red line, is located in the province of Limburg and is therefore managed by the *Limburg* water board. The main stream in the Limburg area is called Loobeek (Kurstjens ecologisch adviesbureau & Bureau Strooming, 2013). This research, and therefore this chapter will mainly focus on the part that is located in the province of Noord-Brabant, the stream Molenbeek, because more information, such as bathymetry, is available on this part.

The stream is for a large part located in a former meander of the river Meuse, which is clearly visible in elevation maps (see Figure 5-2). The so-called ‘terrace edges’ (in Dutch: terrasranden) function as the natural boundaries of the area. In the past decades, the stream has been modified by the local people. Examples of these modifications are canalization, deepening and widening of the stream and construction of weirs (Kurstjens ecologisch adviesbureau & Bureau Strooming, 2013). These modifications are nowadays considered to be unfavorable to the water quality and management.

A few years back, in 2013, a report was published by the water board. The report is about a project plan on stream restoration of the Molenbeek. The report provides a lot of information about the

area and the adjustments that were designed at the time, and have been performed in the past few years. The water board had to adjust several parts of the stream in order to be able to meet the targets set by European Water Framework Directive (WFD, in Dutch: Kaderrichtlijn Water (KRW)) (Kurstjens ecologisch adviesbureau & Bureau Strooming, 2013). The main targets of this directive are improvement of fish migration, water quality and natural morphology. Furthermore, water storage targets need to be met. Climate change causes peaks both in discharge as in drought periods. Water storage is therefore advantageous for the entire area.

To achieve these goals some measures have been designed. One can think of weir removal, shoaling and narrowing of the stream course and digging and stimulating a meandering stream course. The intended result is a meandering stream of on average 0.5 meter depth and a width of about 5 meters. Due to the meandering character, the banks are supposed to erode at some places and accrete at other places. Furthermore, the intention is that the stream valley floods more often, contributing to the storage function (Kurstjens ecologisch adviesbureau & Bureau Strooming, 2013).

Using the terminology of this research, one can describe the stream system using the average summer and winter discharge, bed roughness, dimensions, slope and meandering intensity. In the table below these parameters are shown.

Table 5-1: System characteristics of stream system Molenbeek

| System parameter | Value |
|--|---|
| Average summer discharge | 0.76 m ³ /s |
| Average winter discharge | 2.16 m ³ /s |
| Discharge with T = 1 | 4.9 m ³ /s |
| Maximum discharge in history (1998) | 16.26 m ³ /s |
| Bed roughness | k _n = 0.05 (White-Colebrook/Nikuradse) |
| Dimensions (width x depth) | 8 x 1.5 m |
| Slope | 1e-03 |
| Meandering intensity | On average little, some locations more than extensive |

The bed roughness, defined as a White-Colebrook/Nikuradse parameter, is comparable to a Manning roughness coefficient of $n = 0.025-0.03$ (depending on the local hydraulic radius).

Based on the parameters, the stream can be classified as a Q = 5 scale stream as defined in chapter 4, with varying grades of meandering. The bed roughness is also in the same range, as are the dimensions. The slope is a little steeper, which may be the case to compensate for the higher roughness due to the very discontinuous bathymetry, if compared to the very smooth bathymetry of the test models of chapter 4.

5.2 Methodology

The previous chapter indicated some processes that could be of influence on the model output. The question is whether these processes are in a practical case of importance. To examine this, some models have been constructed of the catchment of the stream Molenbeek.

The models of the case area has been constructed using the following data sources:

- 1D cross sections of the existing SOBEK models – the catchment is located in the management areas of two separate water boards, which use separate models for the part that is in their management area
- AHN (in Dutch: Algemeen Hoogtebestand Nederland), which is a Digital Elevation Model (DEM) of the Netherlands

- TOP10NL, which is a topographic database which contains land use, locations of trees, roads, hedges and other objects that are of importance

The AHN database does not contain the bathymetry of streams and rivers. Therefore, the 1D cross sections of the existing SOBEK-model of the area had to be used to adjust the elevation of the DEM in the channels. These cross sections are measured profiles, and are therefore suited to use for model construction. Of course, there is a limited amount of measured cross sections available, so the missing areas in between these cross sections have to be interpolated. The operations have all been done in ArcGIS. Using the application Baseline (see for explanation paragraph 4.1) all data has been stored in a database of the catchment area. RGFGRID has been used to construct the grids of the areas of interest. Baseline converts, using these grids, all the information that is in the database and within the grid area towards D-Flow FM input files.

Unfortunately, the D-HYDRO Suite does not yet support the modelling of culverts. This is a development which will be introduced in the near future, but at the moment of this research this was not possible yet. This does have influence on the model results, because especially the smaller streams upstream of the Molenbeek have a lot of these culverts resisting the flow. During high water waves, some of these culverts act like weirs, resulting in high water levels upstream the structure.

To minimize the effect of this, only the model output of the Molenbeek part, which has no culverts, is used for process analysis. The Loobeek part, with culverts, will only be used to estimate the travel time of a flood wave. This is, however, influenced by the absence of culverts. Here, another (temporary) disadvantage of 2D modelling comes forward, more on this will be discussed later on.

Grid specifications

There are a few options for the area that will be modelled. To be able to observe the processes described above, the grid has been constructed for a small region of the Molenbeek, small enough to restrict the simulation time to maximum three days. This grid exists of the stream itself, a small part of the banks and surrounding area and some low-lying areas which are vulnerable for flooding. The initial idea was to construct a grid for the total low-lying areas between the stream and the river Meuse. This however resulted in a simulation time of more than three weeks, which would cause problems for the research progress.

Another option is to only construct a grid for the streams. This has been done for both the Molenbeek as the Loobeek parts. This provides insight in the flood wave propagation in an area like this. A third option is the model only the areas of interest. Figure 5-3 shows the total catchment of the Molenbeek. The area inside the black square has been enlarged, because this is the most interesting part of the area. It contains the low-lying areas that may flood during high water in the Meuse or extreme rainfall events. In the end the red area has been simulated, the grid of the area inside the purple square is shown in Figure 5-4. This figure shows that the stream itself has a curvilinear grid, where the surrounding areas have a triangular grid. As discussed, the initial idea was to simulate the blue area, but this resulted in extremely high simulation times. In addition to the red area, also a model has been constructed of only the streams, which are represented by the black lines in Figure 5-3.

As discussed in the previous chapter, the number of grid cells in cross-sectional direction is the most important for the final accuracy of the model output. Therefore, a curvilinear grid with a minimum of six and a maximum of eight grid cells are used in lateral direction. As proven in the previous chapter, increasing this number adds a significant amount of accuracy to the model, however the simulation time increases with it. Therefore, this amount has been chosen, as a sort of compromise. The size in

flow direction has been dimensioned in such a way to keep the aspect ratio¹⁶ within normal range. The surrounding areas have been modelled used a triangular grid, which also applies to the grid criteria. An example is shown in Figure 5-4.

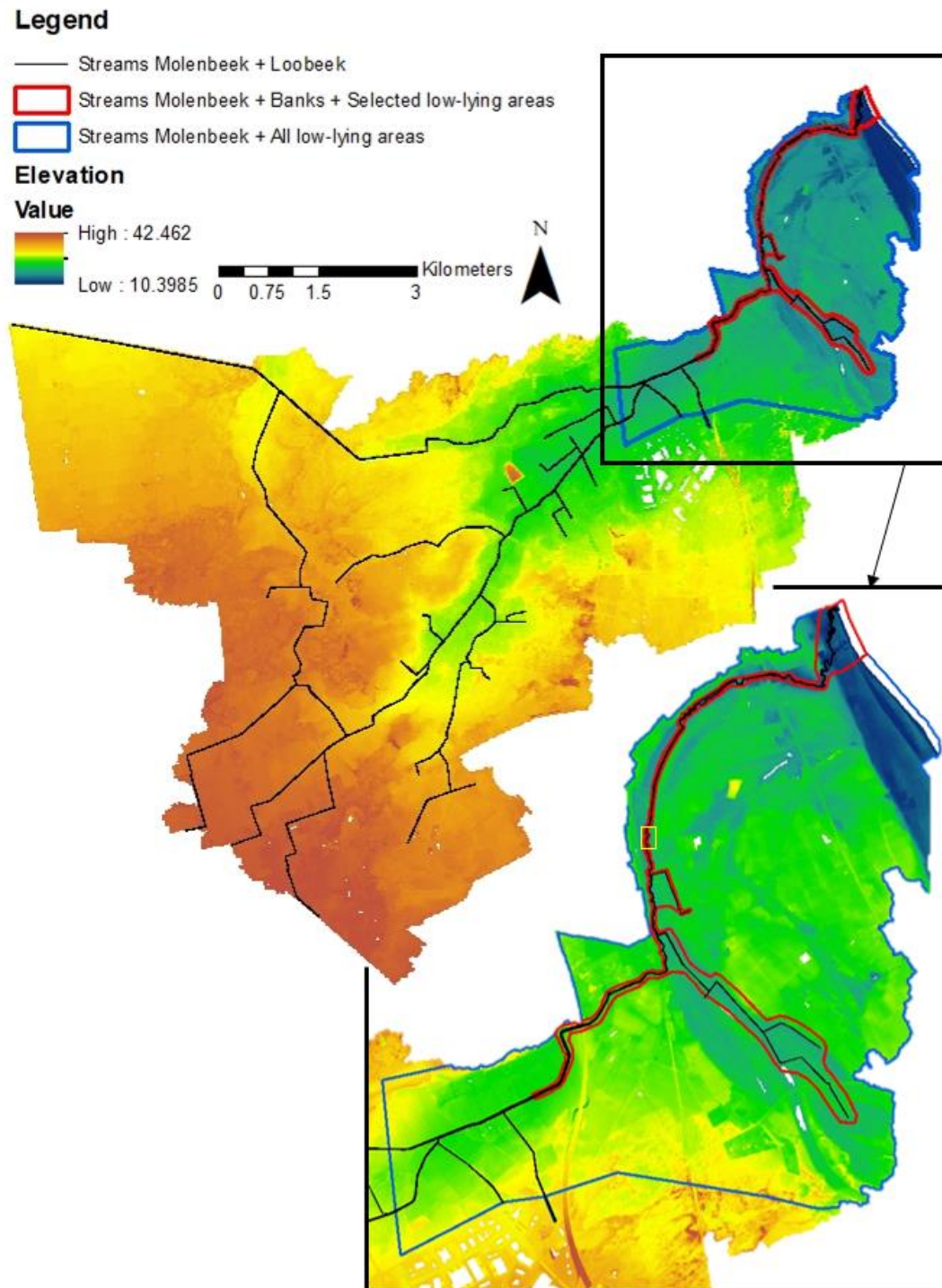


Figure 5-3: Modelled areas - the black square is an enlargement of the area of the most interest

¹⁶ The aspect ratio is a grid criteria which officially only applies to regular grids, but is still used for irregular grids as a guideline for curvilinear grid cell dimensions. It represents the ratio between the length and width of a grid cell.

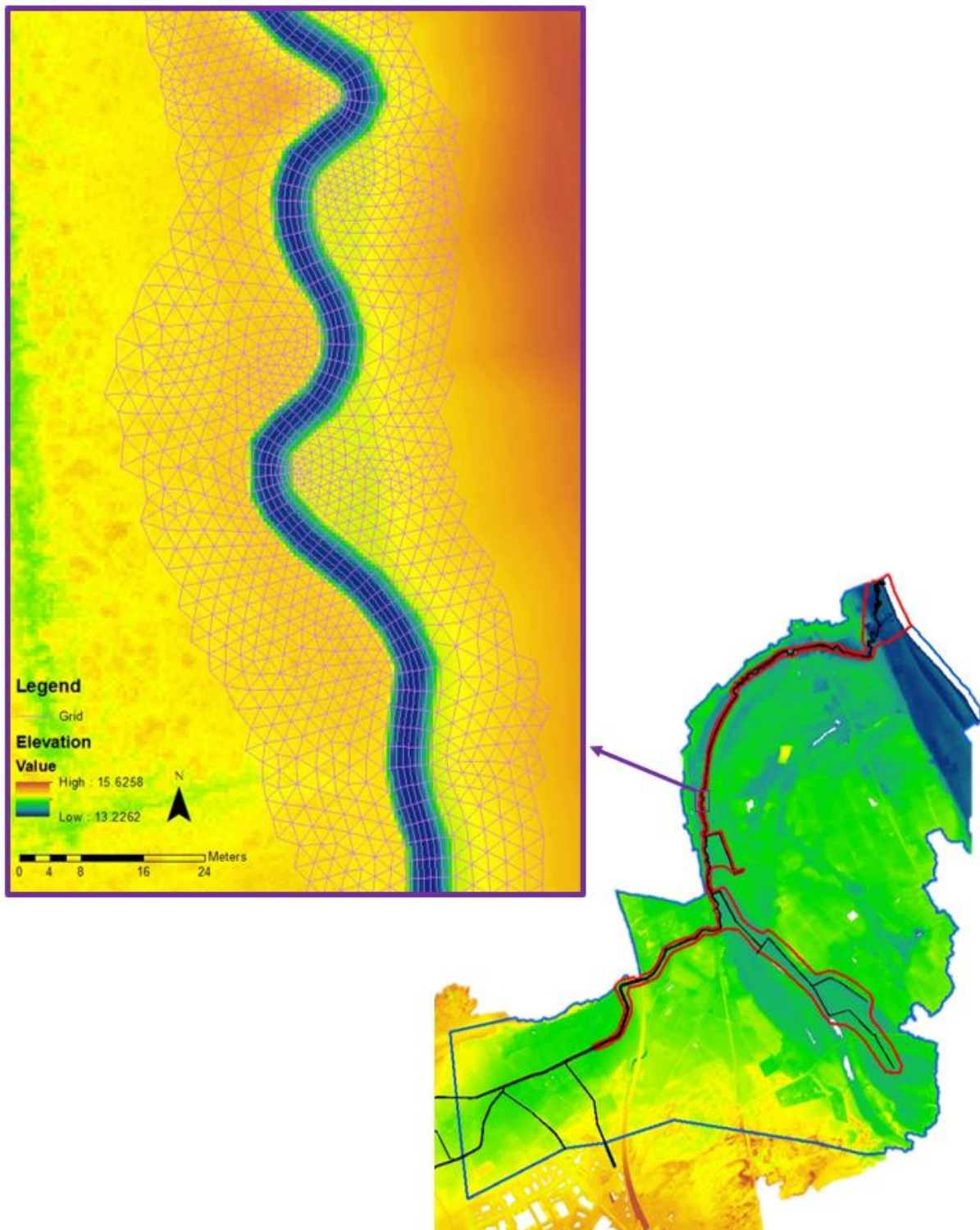


Figure 5-4: Example of the implemented grid structure – enlargement of the purple square

Boundary and initial conditions

The boundary condition is in this case the water level of the river Meuse. Initially, this will be copied from the SOBEK model, which is a water level of 11.1m. This creates a water depth of 0.7m at the stream mouth. For future simulations, this water level can be varied with for instance a high water wave of the river Meuse. This causes additional problems in the stream valley, which may be inundated from the river.

In the situation of the model of only the streams, no upstream boundary condition is specified. Instead, on some points lateral sources are located which have a discharge value attached.

In the situation of the model of only the Molenbeek and surrounding areas, a boundary condition is specified with a discharge. The maximum simulated boundary discharge is $6.5 \text{ m}^3/\text{s}$. This is also in practice the upper limit, because a weir is located in the stream that maximizes the discharge during extreme events.

Because, logically, 2D modelling does not allow to implement a water depth as initial condition, two options remain: running a stationary simulation and creating a restart file, which contains the water levels on all locations, which then are used as initial condition for the new simulation. The other option is to start with a stationary flow and after a while implement a flood wave. The latter has been chosen, because several initial conditions or stationary inflows are simulated. To restrict the total simulation time, the second option is the best one in this particular case. When running several slightly different simulations on the same model, creating a restart file would be a better option.

Observation points

At regular locations along the flow direction, observation points and cross sections have been specified. The locations are shown in the figure below.

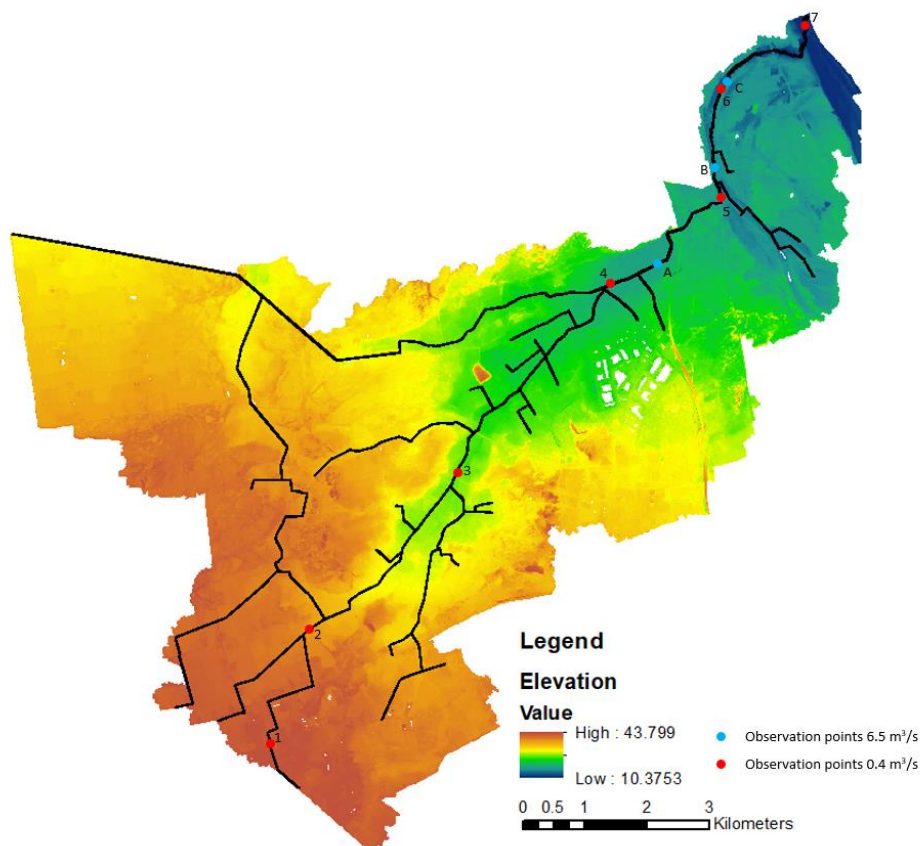


Figure 5-5: Observation locations

Observation of processes

In chapter 4, several processes were analyzed. The next step is to analyze the described case area and examine whether the same processes are playing a role here. Summarizing, the following processes will be searched for in the models:

1. Discretization of cross section depths, often more data points than grid cells in cross-sectional direction – this introduces differences in bed level
2. Water level gradients in meanders, which are even more extensive at some locations compared to the meanders of the theoretical models discussed in the previous chapter
3. Summer bed – floodplain (or main channel – bank) interaction
4. Small water depths on the banks, which will have similar characteristics as floodplain flow, which can be problematic when using 1D models due to the Boussinesq approximation
5. The amount of storage taking place when modelling flood waves

The expectation is that the processes will occur on several locations in the area, but especially on parts with an extensive meandering intensity. An example of a part like this is shown in the figure below. This may be an interesting location to generate model output of, for instance, water levels and velocities, to see whether they are varying across the cross-sectional direction.

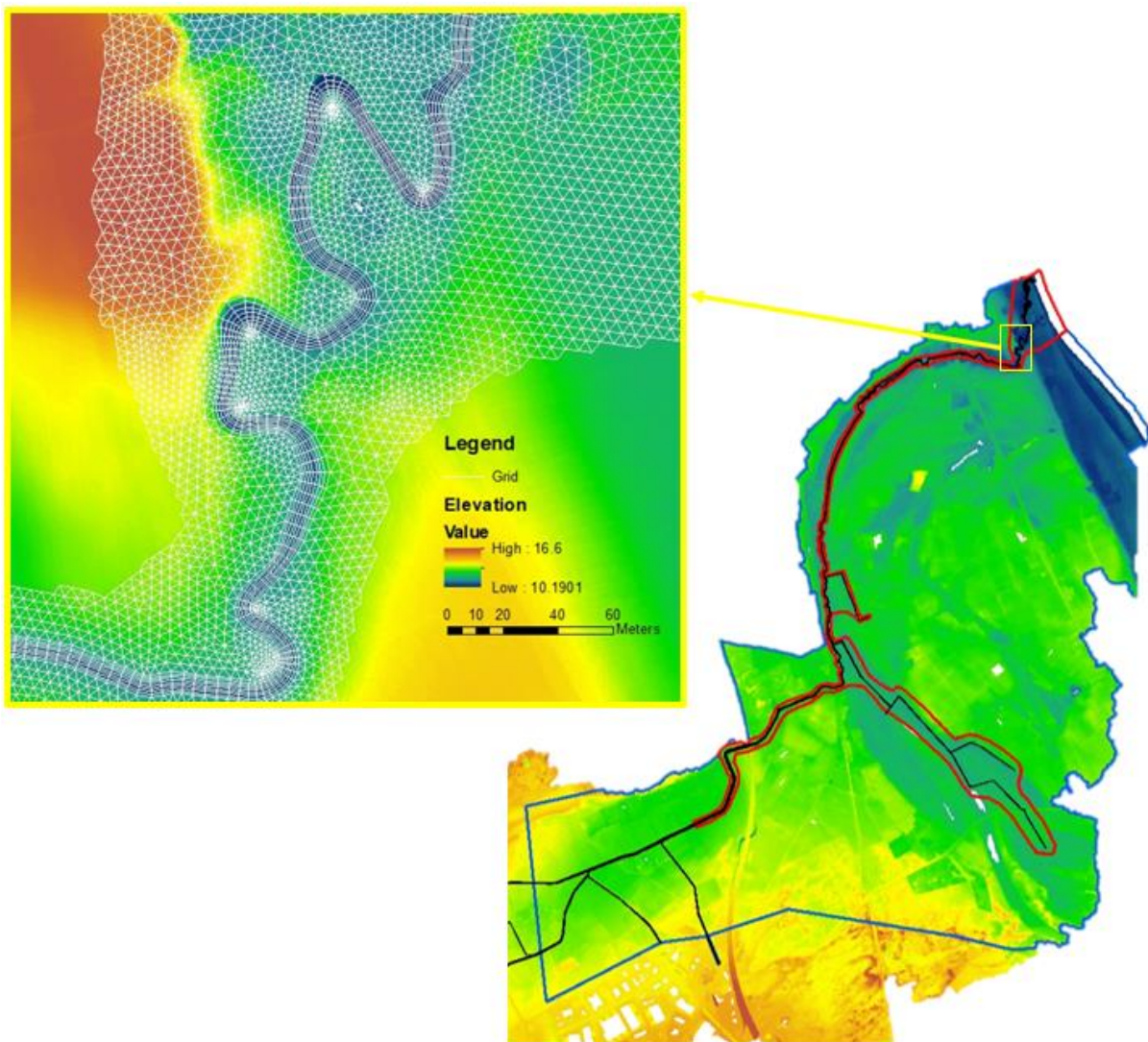


Figure 5-6: Area of interest for observation 1

The expectation is that processes 1 to 4 are best visible when simulating a constant discharge. The Molenbeek part of the catchment has the most meanders, so the model of the stream and surrounding areas will be used for this analysis.

Process number 5 will be simulated using two different models. An important difference between the case area and the test models, that is of influence on the observation of this process, is the changing channel shape. The channels become wider and deeper when propagating downstream. This makes a similar comparison as performed for the test models impossible, as the shape of the flood wave will be influenced by more processes than storage. Therefore, the following two models are used:

- The model of the streams Loobeek and Molenbeek: at a location far from the mouth, a boundary condition of a small flood wave with a peak discharge of $0.4 \text{ m}^3/\text{s}$ will be implemented, and observed how long it takes for this wave to reach the mouth.
- The model of the streams of the Molenbeek, banks and selected low-lying areas: at a location where the stream is sufficiently wide, a flood wave with a peak discharge of $6.5 \text{ m}^3/\text{s}$ will be released. Here, a flood wave shape analysis is possible, because the channel dimensions are not changing much anymore.

A flood wave of $0.4 \text{ m}^3/\text{s}$ will, especially when it has reached the wider channels, propagate with a very low celerity, as the wave celerity is directly dependent on the water depth. The expectation is that the flood wave of $6.5 \text{ m}^3/\text{s}$ will travel much faster.

In the table below, an overview of all performed simulations and corresponding observations of processes is shown.

Table 5-2: Simulation overview case area

| Simulation (#) | Model | Boundary condition | Observed processes |
|----------------|---|--|--|
| 1 | Stream Molenbeek + Banks + Selected low-lying areas | Stationary $6.5 \text{ m}^3/\text{s}$ | 1. Discretization 2. Gradients 3. Interaction 4. Water depth on banks |
| 2 | Streams Loobeek and Molenbeek | Stationary $0.2 \text{ m}^3/\text{s}$ + peak of $0.4 \text{ m}^3/\text{s}$ | 5. Storage |
| 3 | Stream Molenbeek + Banks + Selected low-lying areas | Stationary $3 \text{ m}^3/\text{s}$ + peak of $6.5 \text{ m}^3/\text{s}$ | 5. Storage |

5.3 Results

Discretization of cross sections

As discussed before, the 1D cross section on which the bathymetry is based, consists of more data

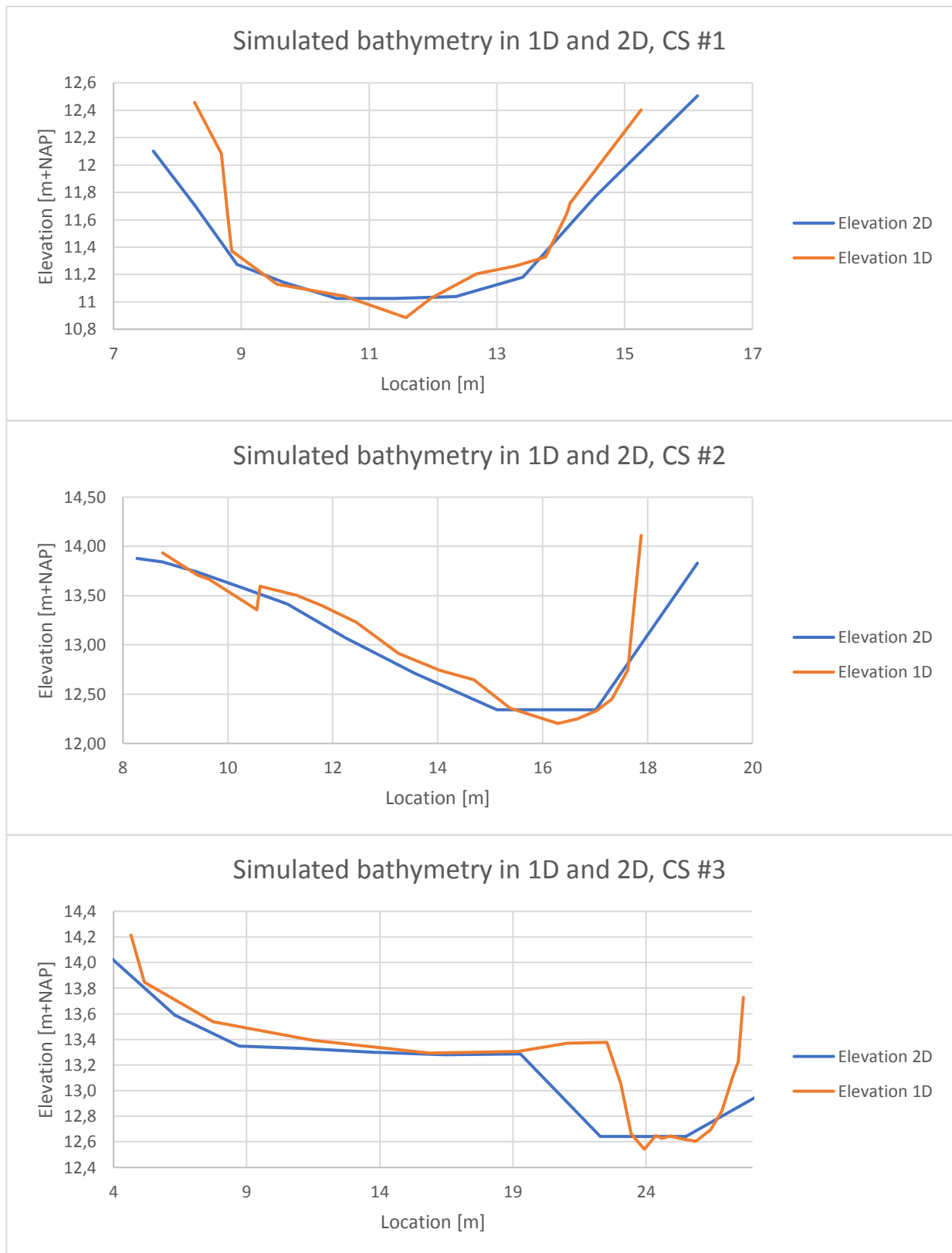


Figure 5-7: Three examples of simulated bathymetries in 1D and 2D

points than the 2D grid has grid cells. This introduces differences in the bed level. This section will compare a number of 1D cross sections to the bathymetry as implemented in the 2D model.

The graphs in the figure above point out that there are significant differences, although the general shape is still quite similar. This indicates that the fact that less grid cells can be used in 2D as data points in the 1D cross sections causes differences in the final bathymetry as used in the simulations. The effect of this is clear: the difference in potential flow area varies, which has significant effects on the simulated water levels.

Water level and velocity gradients in meanders

In the figures below the model output of the area shown in Figure 5-6 are given.

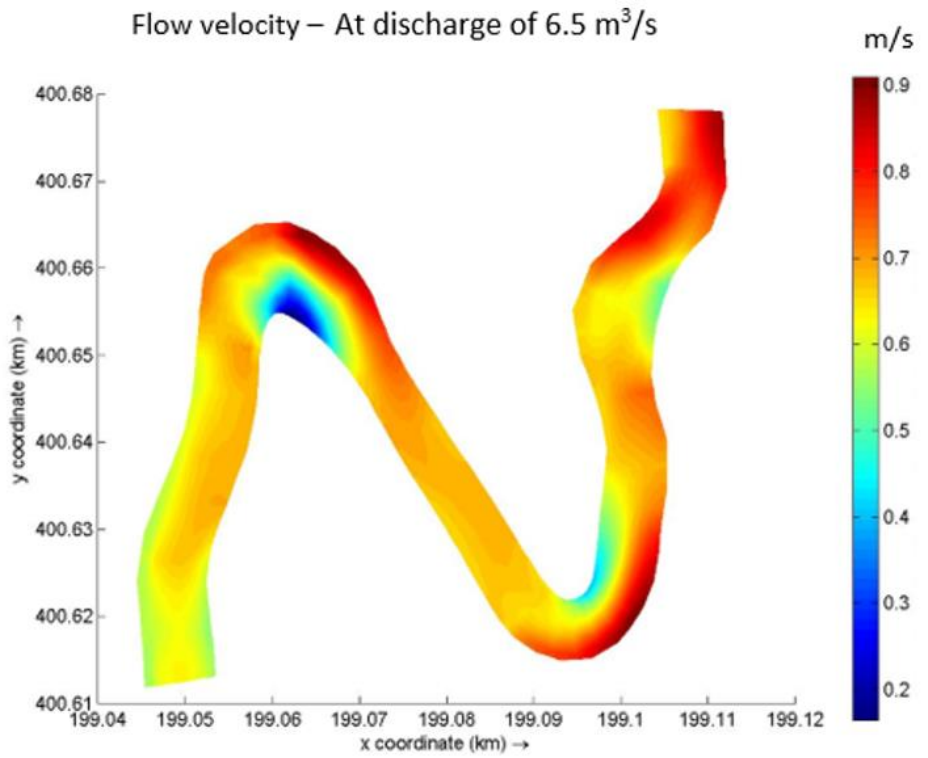


Figure 5-8: Flow velocity at discharge of 6.5 m³/s

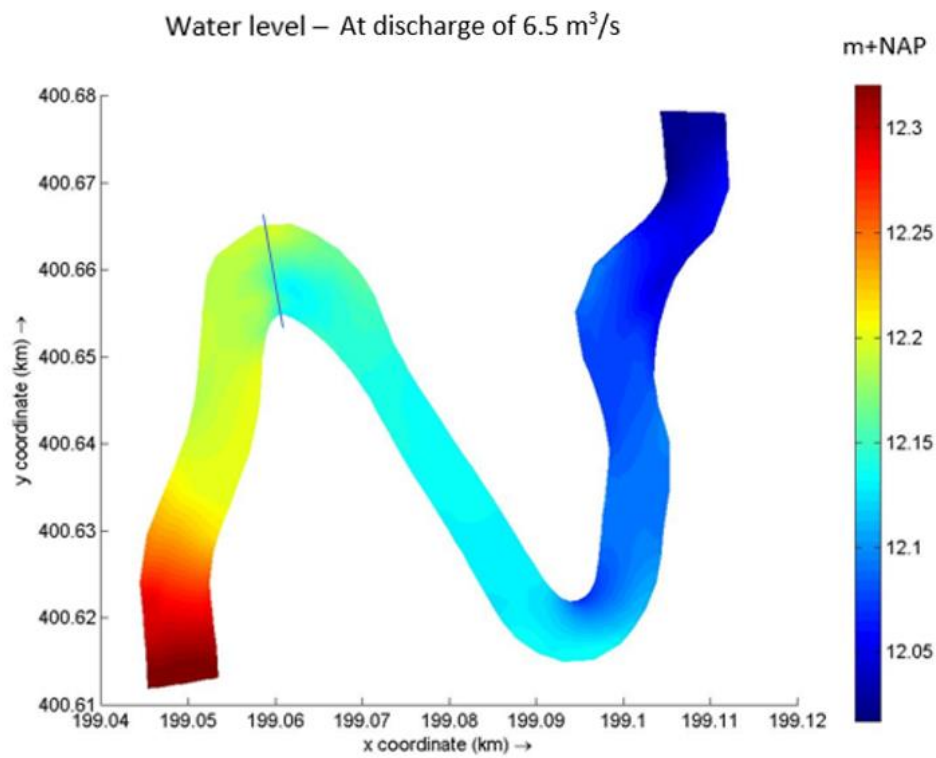


Figure 5-9: Water level at discharge of 6.5 m³/s

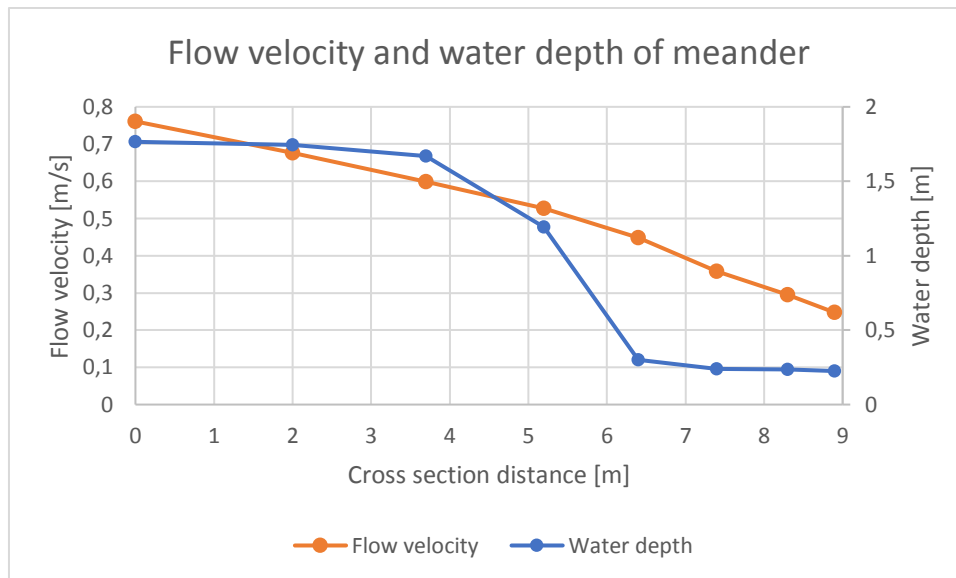


Figure 5-10: Flow velocity and water depth of indicated cross section in previous figure

A few observations can be made from the output presented in the figures above. First of all, the velocity differences are clearly visible. The outer bends always have a higher velocity compared to the inner bends. This is different from the output shown in the previous chapter. The difference is created by the fact that in the previous chapter symmetric cross sections are used. The natural process is erosion of the outer bend and sedimentation in the inner bend. This is also visible in the water depth figure, which shows large differences in depth in cross-sectional direction.

Whereas the water level gradient (not presented in the graph) on the same scale of the theoretical models (see table below) was approximately maximum 0.0015, in this case it is approximately 0.006. This is a large difference, mainly caused by the high intensity of the meandering.

Table 5-3: Comparison case area to theoretical models (Q = 5 scale)

| Meandering | Water level gradient |
|------------|----------------------|
| Extensive | 1.42E-03 |
| Little | 5.69E-04 |
| None | 0.00 |
| | |
| Case area | 6.00E-03 |

The expectation here is that the effects are significant, although this also depends on the velocity distribution in the lateral direction.

What is even more striking is the difference in water depth. Due to the extensive erosion of the outer bend, the water depth decreases significantly when moving from the outer towards the inner bend. The combination of water depth and velocity gradient causes significant differences compared to using an average water level and velocity. The highest velocity and highest water depth are at the same location, so when simulating an average velocity and an average water depth, the discharge will be underestimated significantly. It may be the case that this effect is decreased due to the opposite effect in the inner bend, although the asymmetric gradients will always cause differences compared to a 1D approach.

Main channel – bank interaction

It is important to analyze whether the bank flow is in the same direction as the main channel flow, because this is an important process which can influence the modelling choice. Figure 5-11 and Figure 5-12 show the flow vectors, which are colored using the flow magnitude.

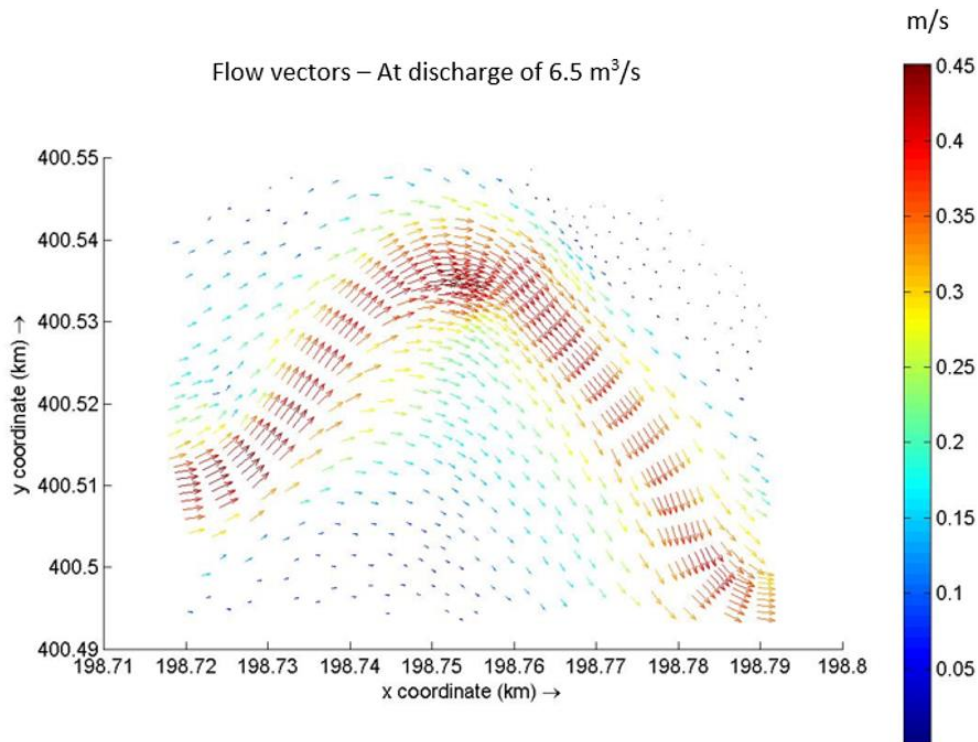


Figure 5-11: Flow vectors (colored by magnitude) in meander, at discharge of 6.5 m³/s, example 1

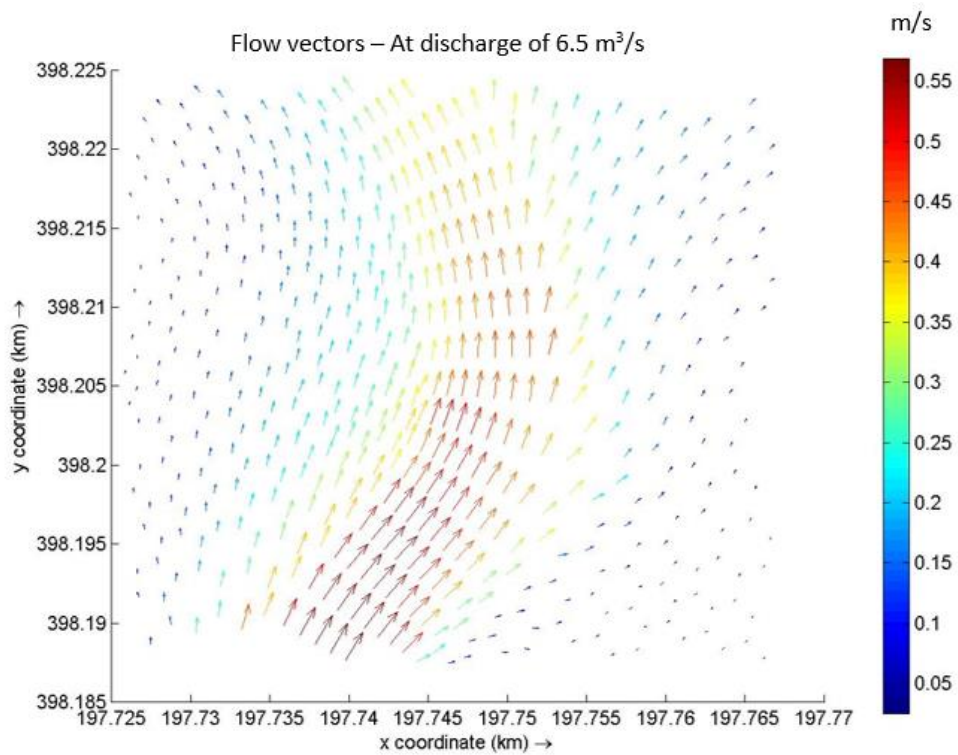


Figure 5-12: Flow vectors (colored by magnitude) in meander, at discharge of 6.5 m³/s, example 2

Both figures show the same pattern: the largest flow velocities on the banks occur in the inner bend. The flow takes a shorter route over the banks, which means the flow direction is also at another angle. As shown in chapter 4, a 1D model is not capable of simulating this effect, because it assumes that all flow is in the direction of the main channel. As shown in the figures, this is definitely not the case. When processes like these are often observed, it is necessary to keep this into account when choosing a modelling approach.

Small water depths on the banks

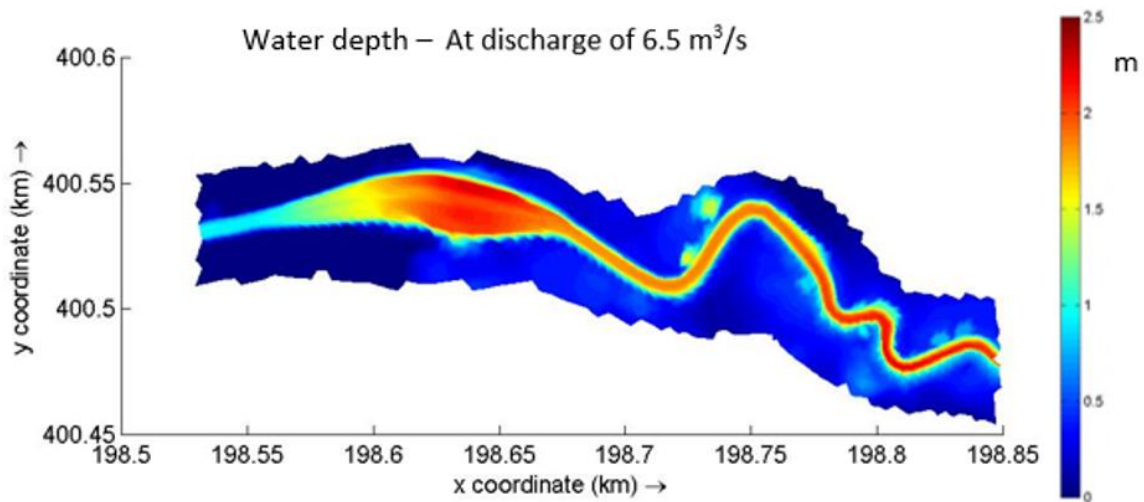


Figure 5-13: Water depth at discharge of 6.5 m³/s, part 1 – dark blue is not flooded

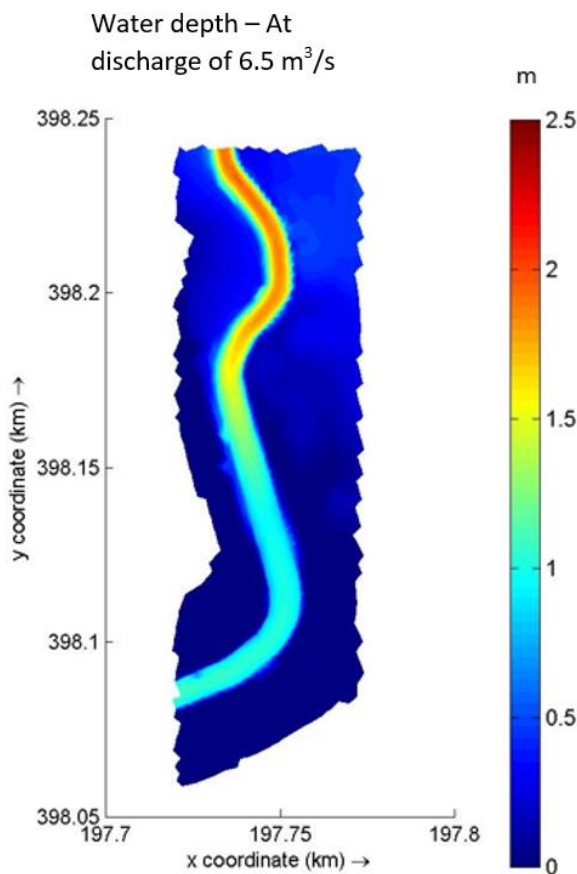


Figure 5-14: Water depth at discharge of 6.5 m³/s, part 2 – dark blue is not flooded

The figures above show that, during the maximum peak of 6.5 m³/s, the banks are flooded at some locations. Mainly the locations with meandering parts and just upstream of meanders. This is because meanders cause higher water levels, which cause backwater effects. Due to these higher water levels, the banks are flooded. Maximum water depth on the banks is a few decimeters, which corresponds with the situation of the theoretical models shown in the previous chapter.

Flood waves

Figure 5-15 shows the locations on which the discharge has been shown in the graph that will be the next figure. The red dot with number 1, on the left hand side of the figure, presents the location where a small flood wave is released. In the graph, the numbers represent the observation points, counted from the first one onwards.

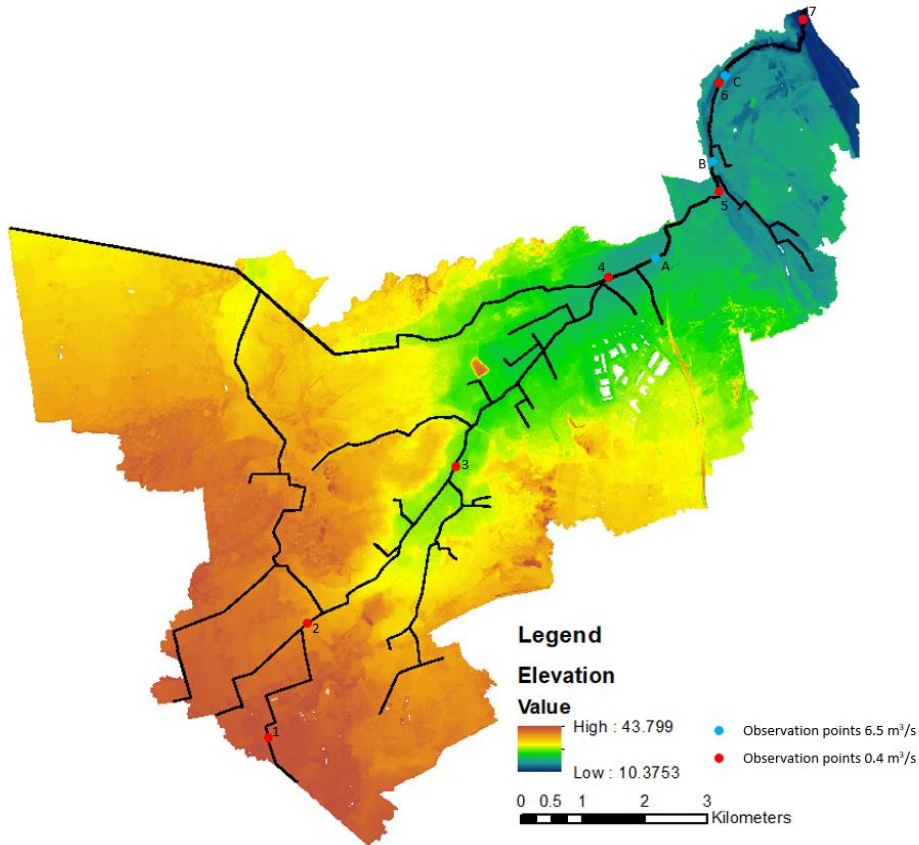


Figure 5-15: Locations of all observation points used for this section

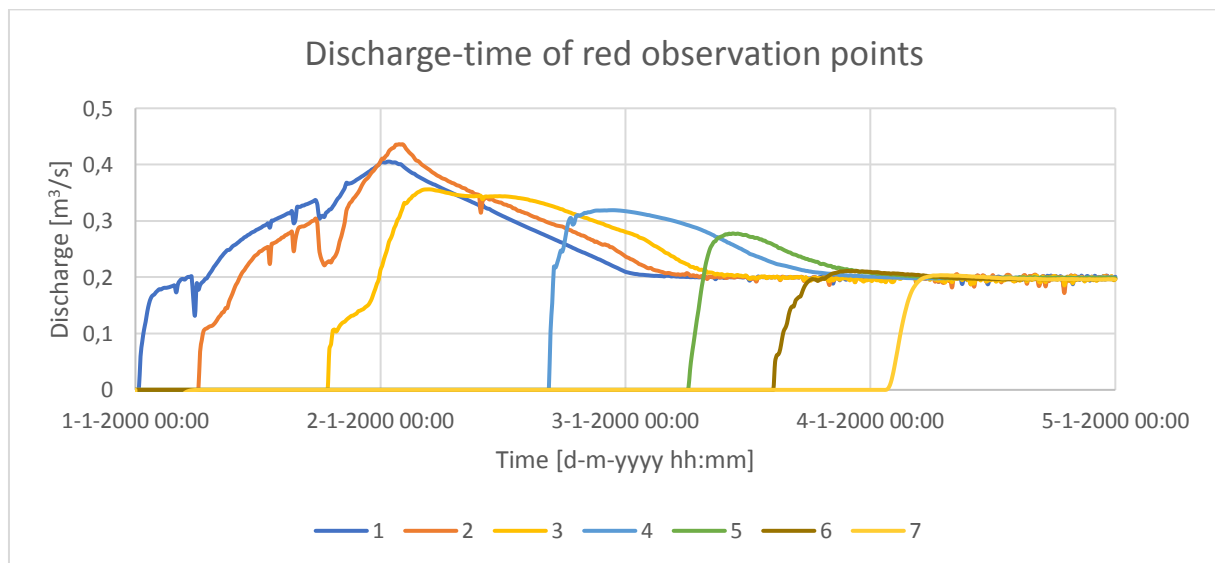


Figure 5-16: Discharge time of all observation points during small flood wave

The figure above shows the discharge-time graph of the observation points for the Loobeek/Molenbeek streams model (red observation points in Figure 5-15). The wave progress is clearly visible. The total duration of the water to travel from the most upstream point to the mouth is approximately 3 days. The decrease in peak discharge indicates a certain amount of storage. At observation points 6 and 7 the wave is almost completely damped out. It looks like this process is in practice an important one to take into account. The relatively large amount of time it takes for the wave to travel from upstream to the mouth indicates that there is a lot of storage taking place.

Furthermore, the ponding effect is clearly visible in this case. In the test models, a continuous surface was schematized, so this effect was not observed. In the case area, the surface is very discontinuous, and a lot of small open water bodies are present. These features cause the water to stay behind, i.e. pond. Therefore, the law of mass conservation is not visible in the discharge-time graph as shown in this paragraph.

The wave celerity is also very interesting to observe. The distances and travel times between the reaches are given in the table below. Mind the change in wave celerity over the total reach.

Table 5-4: Distances and travel times between observation points

| Reach | Distance [m] | Travel time [s] | Wave celerity [m/s] |
|-------|--------------|-----------------|---------------------|
| 1-2 | 2692 | 6000 | 0.45 |
| 2-3 | 3562 | 10200 | 0.35 |
| 3-4 | 4107 | 65400 | 0.06 |
| 4-5 | 2661 | 42000 | 0.06 |
| 5-6 | 2334 | 43800 | 0.05 |
| 6-7 | 3093 | 29400 | 0.11 |

The wave celerity decreases from the upstream boundary towards the downstream boundary. This has mainly to do with the channel dimensions that increase, which decreases the water depth of the flood wave. This means a lower wave celerity.

A second flood wave is released at the blue dot with the character A next to it. The result is shown below.

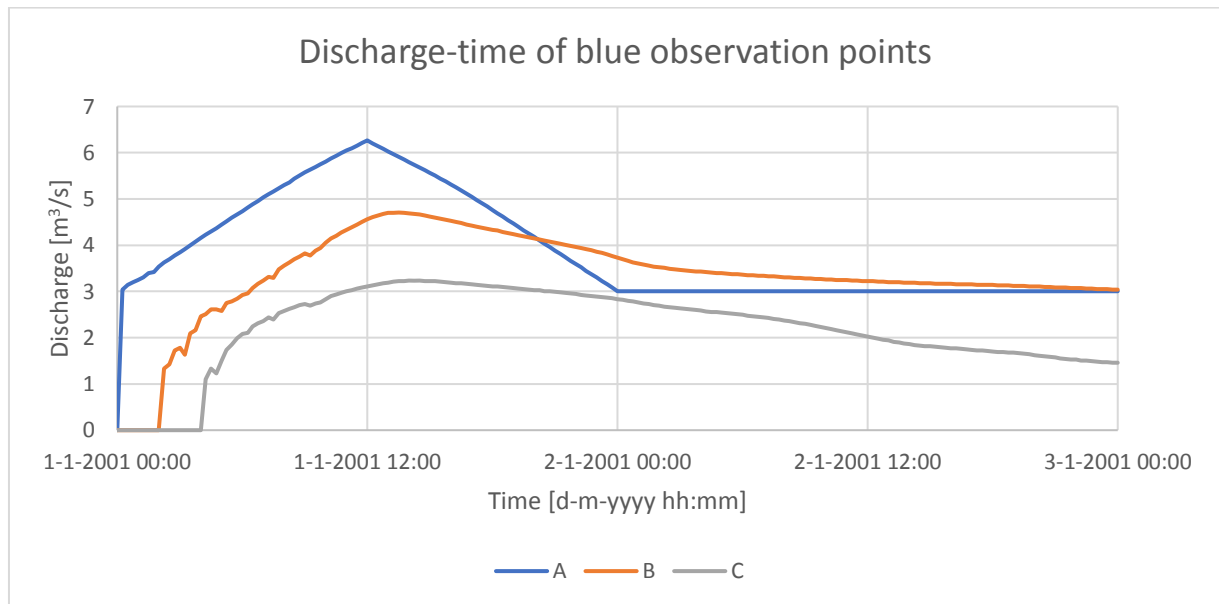


Figure 5-17: Discharge time of all observation points during large flood wave

The figure above shows the discharge-time graph of the observation points for the Molenbeek and surrounding areas model (blue observation points in Figure 5-15). The change in shape is clearly visible. This indicates a large amount of storage, as the peak discharge is halved over a distance of less than 4 km.

Again, the wave celerity is also very interesting to observe. The distance and travel time over the reach are given in the table below.

Table 5-5: Distance and travel time of flood wave

| Reach | Distance [m] | Travel time [s] | Wave celerity [m/s] |
|-------|--------------|-----------------|---------------------|
| A-C | 3854 | 8100 | 0.48 |

Note that in the Molenbeek part, the wave celerity of this large flood wave is almost 10 times larger compared to the small wave. The wave celerity of the large flood wave is however very comparable to the flood wave of 0.4 m³/s in the first reach. This means the amount of storage is more or less similar over the entire catchment, because the channel dimensions are equal when they are based on the local discharge magnitude.

5.4 Conclusions

This chapter has given an answer to the third sub question: What physical processes are particularly important in a practical case of a small-scale system? Several parts have been analyzed and the processes that were found to be important have been shown. Now, the observations will be summarized and an indication of the individual importance will be given. By means of a few samples the Reynolds and Froude numbers were calculated for this system. Of course, it varies along the system because of changing dimensions and discharges, but on average the Reynolds number is $4 \cdot 10^5$, the Froude number 0.1. In the figure below, these numbers are indicated in the overview of the range of results from chapter 4.

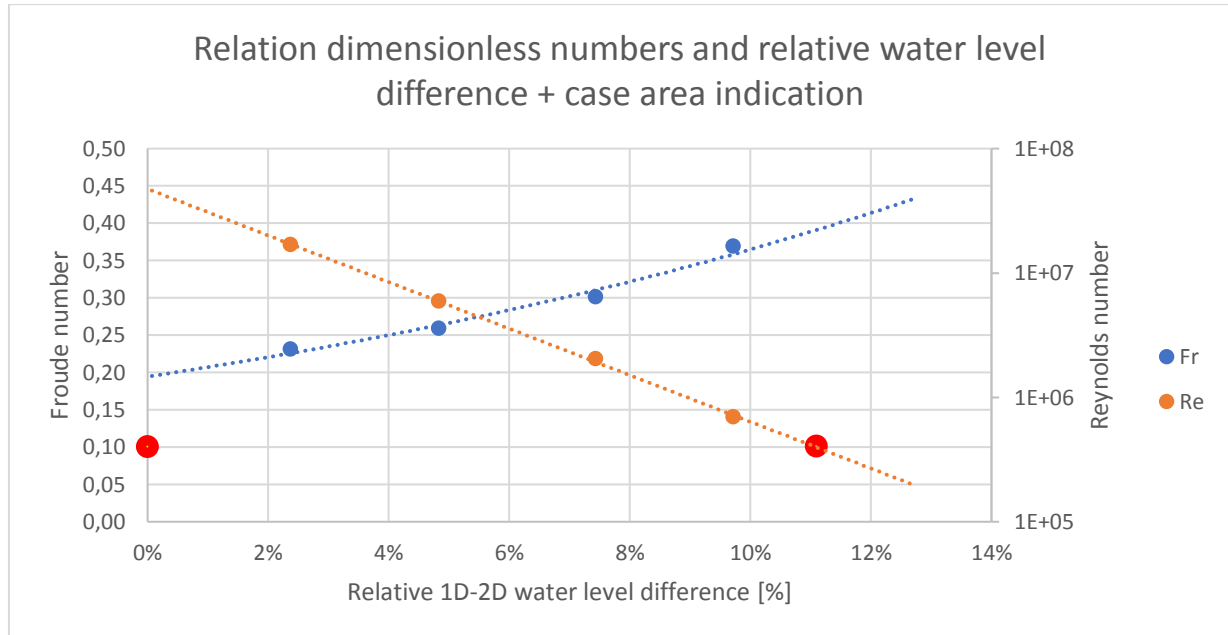


Figure 5-18: Relation dimensionless numbers and relative 1D-2D water level difference + case area indication (red dots)

As appears from the figure, based on the Reynolds number of the case area, the expected 1D-2D difference is significant, whereas the Froude number indicates that the differences will be small. As the Froude number for 1D simulations is heavily influenced by the Boussinesq approach, the expectation is that in practice the Boussinesq approach will work properly. This needs to be validated, however. Based on the Reynolds number, one should be critical towards the model output of the 1D model.

The processes that have been dealt with in the previous paragraph will be summarized below and the general conclusions will be drawn.

1. Discretization of cross sections

The observations were quite clear, differences are present between 1D and 2D bathymetry schematization. 1D modelling is the most accurate on the location of the cross section itself, but the locations are often very arbitrarily chosen. 2D modelling is less accurate on the measured cross sections due to the discretization of the grid, but is more accurate in between these cross sections, because the whole bathymetry can be adjusted according to reality or by using common sense. No direct conclusions can be drawn which of these is more accurate. To be able to test this, the model output should be compared with a 1D model and actual measurements, but this is out of the research scope.

2. Water level and velocity gradients in meanders

This topic turned out to be even more important in practice than in the theoretical models. The water level gradient in cross-sectional direction is a few times larger compared to the models from chapter 4. The question remains what the exact influence of this process is on the water level, but the significance of this process is too large to be neglected.

3. Main channel – bank interaction

The observations on this section showed a lot of interaction. This causes 1D modelling to be less accurate, because the water is flowing in multiple directions. The expectation is that this will have a large influence on the model output, especially because 1D cross sections are often not modelled including the banks. The model takes the first and last data point of the cross section as boundaries, where the water is flowing in the angle of the main channel.

4. Small water depths on the banks

The Boussinesq approach may be playing a role here. This is something to keep into account when modelling in 1D. One should always check whether the Froude number is not too large, because this might be indicating that the model output is not accurate. In this particular case, the Froude number was on average within normal range, so the expectation is that in this case area, the Boussinesq approach is working properly.

5. Flood waves

If the results of this section are compared to the test models, in particular the $Q = 5$ scale, it appears that in practice flood waves are even more damped out compared to the test models. This is caused by the fact that the possibilities for storage are larger in practice, due to more elevation differences and open water bodies. These features also cause the process of ponding to occur in the area, which causes storage for longer periods. Furthermore, it has been observed that the wave celerity is comparable over the entire catchment, indicating that the amount of storage is more or less similar.

Especially the bathymetry schematization, water level and velocity gradients, main channel – bank interaction and storage effects are expected to be of large importance in practical situations. The small water depths on the banks will probably, based on the Froude number, not have the same effect as it had on the Boussinesq approach, compared to the test models of chapter 4.

6. Practical usability

Analyzing the practical usefulness of 1D versus 2D modelling, two things are in particular interesting to discuss. First of all, the simulation time. Especially when several situations and varying boundary conditions have to be simulated, the simulation time may influence the modelling time. Secondly, whether all options that are possible in 1D can also be used in 2D, or vice versa, is very important in practical situations. In chapter 9, based on the answer to the main question combined with the issues discussed in this chapter, some recommendations will be given on the modelling choice in practice.

Simulation time

The simulation time depends on a few parameters. Among these are the grid size, time step, model size and computer characteristics. The latter has quite a lot of influence, as there is a large variety in computers available. The characteristics of the computer that were used in this research are given in the table below.

Table 6-1: Computer characteristics

| Parameter | |
|---------------------|---------------------|
| Name | HP Workstation Z230 |
| No. of cores | 8 |
| Processor | Intel I7, 3.60 GHz |
| RAM | 12 GB |

Occasionally, a 56-core desktop has been available. This one has been used for the simulation of the case area. In the table below the simulation times of the four modeled scales, both in 1D as 2D, are given. The schematization properties that are used here are: extensive meandering, $n = 0.03$, summer bed flow.

Table 6-2: Simulation times 1D versus 2D

| Scale | 1D | 2D | Simulated days ¹⁷ | Time step | Ratio |
|-------------|----------|----------|------------------------------|----------------|-------|
| 5 | 00:00:29 | 00:27:59 | 2 | 1h | 1.73% |
| 50 | 00:00:14 | 00:14:15 | 3 | 1h | 1.64% |
| 500 | 00:00:07 | 00:06:46 | 4 | 1h | 1.72% |
| 5000 | 00:00:04 | 00:03:37 | 5 | 1h | 1.84% |
| | | | | Average | 1.73% |

The values in the table indicate two things:

1. Increasing the scale with one magnitude results in a doubling of the simulation time, both in 1D as 2D. The number of simulated days is not even the same, then the difference would be more.
2. The simulation time in 1D in seconds is approximately the time it takes in 2D, in minutes. To be exact, the 2D simulation time is a factor 58 larger than 1D modelling.

This difference is quite significant. Where chapter 3 indicated that most recent studies showed more than an order of magnitude difference in simulation time, it is showed in this research that it is even

¹⁷ The number of days is not the same, because the smaller the scale, the less time it takes for the system to become stationary.

more. This effect is also visible when analyzing the simulation time of the case area of the stream Molenbeek.

Figure 5-3 indicates the several areas that have been simulated. From all areas the (expected) simulation time has been shown. D-Hydro provides an estimate of the simulation time when starting the simulation. The latter two parts in the table below have not been simulated, because of the large times, but there, the indicated estimated simulation times have been given.

Table 6-3: Simulation time of case area parts

| Part | Cores | Time | Simulated days | Time step |
|---|-------|------------|----------------|-----------|
| Streams Molenbeek + Banks + Selected low-lying area | 56 | ≈ 3.5 days | 4 days | 5 min |
| Streams Molenbeek + Loobeek | 8 | < 2 days | 4 days | 10 min |
| Streams Molenbeek + All low-lying area (not simulated) | 56 | ≈ 6 days | 4 days | 5 min |
| Streams Loobeek + Streams Molenbeek + All low-lying area (not simulated) | 56 | > 3 weeks | 4 days | 15 min |

For the larger areas in particular, the simulation time is even longer than the simulated period. The main reason for this is the small grid size. This small size is necessary to maintain a certain level of accuracy, especially in cross-sectional direction of the streams. The effect of this is that the time step, according to the CFL criterion (see eq. 3.6), becomes very low. If, for instance, the velocity is approximately 1 m/s, the grid size is 0.5m (cf. Figure 5-4), which is necessary on locations where the width is only a few meters, then the CFL criterion requires a time step of 0.5 seconds. On some locations the stream width is only 1 meter, so one can imagine that the total simulation time can grow significantly.

The reason that larger scale systems do not have these large simulation times, is due to the fact that the grid cells are larger. The flow velocities are of the same order of magnitude, see Figure 4-16, so with increasing grid size, the time step also increases.

Available modelling options

As mentioned before, the D-Flow FM module does not allow culverts to be schematized. This is a serious shortage of the module. Especially in rural areas a lot of culverts are present. Only the catchment of the stream Molenbeek already contains over a hundred culverts. Culverts cause during high discharges extra resistance and often have not enough capacity to discharge all the water. Culverts are therefore crucial in high water modelling. However, in the near future it should become available to model some parts of the system in 1D, with the option to implement culverts in these 1D parts. How this works and when it comes available is not known at this moment.

As 1D and 2D approaches both have their advantages, one may suggest to use a combination of both, a so-called 1D/2D coupled model. This option is available in the SOBEK Suite, but is not working properly. A lot of issues came up during a short trial. It would offer short simulation times and the possibility to implement culverts in the 1D part, and inundation in the 2D part. Deltares is also working on this implementation, so this should come available in the near future as well.

No other issues were encountered in this research when comparing the practical use of both modules. In the near future, dike breach modelling should also become available in the D-Flow FM module. This would enlarge the attractiveness of D-Flow FM usage.

7. Discussion

This chapter will analyze some of the uncertainties and restrictions of the research.

First of all, the distinction between numerical and physical processes is sometimes hard to be made. One has to keep in mind that this research has mainly been performed to find out what the effects are of varying physical parameters. For instance, a higher meandering intensity causes a larger 1D-2D difference. The assumption is that the additional difference, when comparing two intensities which each other, are purely caused by the higher meandering intensity. Of course, a lot more could be said about the causes of the total 1D-2D differences when numerical aspects were also taken into account. This might be interesting for a follow-up research.

Besides this, sometimes it is hard to indicate whether the discussed processes during this research are purely physical or numerical. For instance, chapter 4 elaborated on the Boussinesq approximation of the 1D modelling approach and its effects for varying spatial scales. One may classify this as a numerical issue, because it is a coefficient which is part of the 1D solver. Somebody else may classify this as a physical issue, because it very much depends on the shape of the river profile. The choice has been made to analyze its effects, because of the remarkable observations that were made for some situations.

Thirdly, a phenomenon that has not been dealt with in detail is turbulence. D-Flow 1D uses another method of including turbulent forces compared to the D-Flow FM module. These are complicated processes which are not even described in the documentation of both modules. Generally speaking, increasing velocities often cause increasing turbulence (cf. the Reynolds number). This may be another cause of changes in 1D-2D differences when varying the roughness, which also directly influences the flow velocity.

Another issue that is up for some discussion is the fact that the observation results are very much depending on the shape of the case area and profile schematizations. Because of the steep bottom slope near the edges of the summer bed of the test models, the bathymetry discretization by the 2D approach causes significant differences. If the test models consisted of a more gradual transition between summer bed and floodplain, the bathymetry would not have had such a large difference. Furthermore, the meanders have been schematized as symmetric profiles. In practice, meanders are created by erosion and sedimentation of the outer and inner bend, so will never have a symmetric shape. This difference in bed shape causes the water level and velocity gradients in lateral direction to have very different effects. In an eroded bend, as shown in chapter 5, the highest velocities and the highest water levels are both at the outer bend. In the test models, shown in chapter 4, the highest velocities were mainly on the inner bend, whereas, due to centrifugal forcing, the highest water levels are at the outer bend.

There are some other natural processes that have not been taken into account, but are of importance to the reliability of model output. An example of this is rainfall. Rainfall influences the potential storage of an area. After it has been raining, small open water bodies and other storage areas will be flooded and allow no more storage. When a flood wave passes, the effect of ponding will be of less importance. Therefore, the conservation of the initial mass of a flood wave will be significantly higher. As most of the flood waves are initiated by rainfall, this is a serious effect to keep into account.

Furthermore, chapter 6 discussed the significant simulation times a 2D model often has. It has been stated that these long computation times are caused by the combination of the CFL condition and small grid cells. However, one has to keep into account that the CFL condition is a consequence of

using this particular numerical scheme. This suggests that one of possibilities to decrease the simulation time of a 2D model, is to simulate flow with a model that uses other numerical schemes, where the time step is not restricted by a CFL condition.

Other ways to decrease simulation times are the implementation of sub-grids (see e.g. McMillan & Brasington, 2007). These sub-grids can represent the topographical data on a sufficiently detailed level. It is still able to capture the important features, while keeping the grid cells larger. This reduces the simulation times significantly.

8. Conclusions

This chapter will provide some general conclusions of this research and will formulate an answer to the main question:

Which physical processes are of influence to the choice of a modelling approach, one or two dimensional, for the modelling of stream systems in particular situations?

To come to an answer, three sub questions have been answered. The starting point has been the analysis of differences in model properties. The used flow equations, numerical methods, computational grids and bathymetry implementation are analyzed and the differences were discussed. Concluding, it can be stated that there are differences, which may be of influence to the model output. The main differences are the number of dimensions on which the flow equations are calculated and the way the bathymetry is schematized. From the performed analysis appears that there are a few physical parameters that could cause differences in model performance. These are mainly the properties that cause 2D effects, like meandering and varying roughness coefficients. These processes are seen as the cause of gradients in water level and velocity in cross-sectional direction and summer bed-floodplain interaction. The modelling of flood waves could also cause differences due to the fact that the 1D model is not able to model storage with the used default settings. Lastly, the way the bathymetry is used in the simulations is of great importance, due to the way the bathymetry is discretized in 2D models.

The differences in 1D and 2D model output for varying physical properties have been analyzed, and the processes that are causing these differences have been analyzed as well. By constructing a range of test models, various physical properties were varied and the effects were mapped. The most remarkable observations were further analyzed in detail to find out what processes are causing the differences between the parameters. In the introduction, chapter 1, it was already mentioned that 2D approaches are until this moment mainly used for larger scale systems. This research pointed out that the differences are indeed very small (<2%) for the largest scale that has been analyzed. The smaller the scale, the larger the differences between 1D and 2D. In total, six physical processes were found to be the cause of difference in model output, which are:

1. The effects of grid size on bathymetry discretization
2. The water level and velocity difference in cross-sectional direction for varying roughness
3. The water level and velocity difference in cross-sectional direction for varying meandering intensities
4. The interaction between summer bed and floodplains
5. The Boussinesq approach and consequences for the summer bed – floodplain flow area ratio
6. The effects of storage

It appeared that especially the first process is accountable for a large part of the observed differences between the 1D and 2D water levels, mainly for summer bed flow. The second, third and fourth process explain the differences between the various magnitudes of physical processes, for instance between a roughness coefficient of $n = 0.03$ and $n = 0.04$. The fifth process is the main cause of the water level differences in floodplain flow simulations. The last process is causing the differences in flood wave propagation.

Besides analyzing the differences between 1D and 2D model output, also the change in difference, when varying the model schematizations, can be discussed. For instance, if the number of grid cells of the summer bed is halved, the difference between 1D and 2D becomes on average two times higher compared to the original situation. When doubling the number of grid cells, the difference

decreases with 25% on average. The same can be done for the meandering intensity and the roughness. For summer bed flow only, one has to expect an increasing difference of 10% for every step of increasing meandering intensity. For floodplain flow this is even more. Regarding the roughness, the smoother the bed, the higher the differences will be. Especially for floodplain flow, every step of -0.01 in the Manning coefficient results in an increase of more than 50% in the 1D-2D difference.

Lastly, dimensionless numbers can be used to give a first impression about the reliability of 1D model output compared to 2D. Basically, the following conclusions can be drawn:

1. The larger the Reynolds number, the smaller the 1D-2D difference becomes.
2. The smaller the Froude number, the smaller the 1D-2D difference becomes.

To be sure the analyzed processes are in fact of importance in practice, a case area has been analyzed as well. Especially the bathymetry schematization, water level and velocity gradients, main channel – bank interaction and storage effects are expected to be of large importance in practical situations. The next chapter will make some further recommendations for modelling studies, based on some practical issues.

Now, an answer can be formulated to the main question:

Which physical processes are of influence to the choice of a modelling approach, one or two dimensional, for the modelling of stream systems in particular situations?

First of all, these particular situations have to be defined. A total of four major situations can be formulated, based on the results of this research:

1. Situations where the bathymetry is complex, and a lot of cross section measurements are available
2. Situations with a high meandering intensity
3. Situations with a very low roughness compared to the surrounding area
4. Situations with a lot of elevation changes and open water bodies

In all these situations, physical processes are influencing the choice of a modelling approach. Of course, also four situations could be formulated where the characteristics are exactly the opposite. The situations as formulated above are all situations in which a two dimensional approach is preferred. The physical processes that are of influence on these situations will be discussed below.

1. In situations with a complex bathymetry the process of grid discretization is having the most influence. When the bathymetry is very complex, one should always give preference to a 2D model, as these are much better in capturing the complex geometries. However, it is not always the case that a lot of measurements are available. In the case there are, a 2D model is preferred.
2. In situations with a high meandering intensity two physical processes are playing a role: high water level and velocity gradients in lateral direction, and a high summer bed – floodplain interaction. In both these cases, a lot of 2D processes are present, which makes a 2D modelling approach preferable.
3. In situations with a very low roughness compared to the surrounding area two physical processes are playing a role. First of all, high water level and velocity gradients, due to the high velocities, which are induced by the low roughness. Secondly, a high summer bed – floodplain interaction; due to the large roughness difference this processes is playing a larger

role. In both these cases, a lot of 2D processes are present, which makes a 2D modelling approach preferable.

4. In situations with a lot of elevation changes and open water bodies, a lot of storage is possible. When a lot of storage is present, a 2D modelling approach is capable of simulating this, where a 1D approach is not, at least not as accurate as the 2D approach.

Of course, in situations with a complex bathymetry, but not a lot of data is available: a 1D model may be more useful. In a 1D model the channel course can be implemented very accurately, which might offer more accuracy. With relatively simple bathymetries, a 1D model suffices. Situations with a low meandering intensity are also suited to be modelled in 1D. The same applies to situations where the roughness has an average value and no floodplains or flooding banks are present. For situations without a lot of elevation changes and open water bodies a 2D model does not add much value compared to a 1D model, when modelling flood waves. Still, in these situations, on the small scales as defined in this research, the 1D-2D difference is on average larger than on larger scale (>10%). This has to be considered when choosing a modelling approach.

Of course, there are also some more practical considerations to be made about the modelling choice. In the next chapter these will be discussed.

9. Recommendations

This chapter will discuss some recommendations for modelling studies of stream systems or follow-up researches.

In this research just hydrodynamical physical processes were analyzed. It would add a significant amount of value when incorporating morphodynamical physical processes. Parameters like suspended load or particle size could be varied to see what influence they have on the 1D and 2D model performance. Furthermore, especially the flow velocity distribution in cross-sectional direction is of importance for channel erosion and sedimentation. This is a process that a 1D model is not able to accurately simulate.

Other parameters that might be interesting for further research are the water density and turbulence. The water density depends on temperature, salinity and suspended particle matter (SPM). Especially in coastal regions this may be of great influence to the differences between 1D and 2D modelling performance. The consequences and importance of the turbulence part has been discussed already in the seventh chapter.

The third issue that may be up for follow-up research is the fact that the D-Flow 1D module offers the possibility to specify a part of the cross section as storage part. Using this option, the results will probably show much less difference between 1D and 2D, at least for flood wave simulations. The reason for not using it in this research is clear, but it may be interesting to see how the model output changes when this option is used.

Lastly, the suggestion is made to further explore the possibilities of a 1D/2D-coupled model. This research has pointed out that both approaches have their advantages and disadvantages. A 1D/2D coupling could decrease the disadvantages and make use of the advantages of both approaches, although a 1D/2D approach also has its own disadvantages (see chapter 2). A proper implementation of a 1D/2D coupling in the SOBEK or D-HYDRO Suite would enable further research into this, which might offer the optimal modelling approach for stream systems.

When performing a modelling study on a stream system, there are a number of issues one has to analyze before choosing a modelling approach. The situations that are influenced by physical processes are dealt with in chapter 8. Furthermore, some practical considerations can be made that may influence the choice of a modelling approach. They are listed below, a brief analysis will follow.

1. The goal of the research: only channel modelling or inundation modelling and required model output
2. The importance of schematization and amount of culverts in the system
3. The available time for running the simulations

First of all, the goal of the research may already influence the modelling choice. If one wants to model inundation, a 2D approach is inevitable. Using a 1D-2D coupled approach is also worth considering, especially when a lot of culverts are present in the study area. When the only goal is to analyze the water levels in the streams or the effects of roughness parameters, a 1D model suffices. Furthermore, the model output that is required may be of influence to the choice. If, for instance, the goal of the research is to map velocity differences in magnitude and direction, in lateral direction, to be able to make an estimate of the expected amount of erosion that will take place, a 2D model has the preference. To make the right choice, one should always analyze up front what the desired output is.

Secondly, if there are a lot of culverts present in the system and they are of influence to the flow, one might consider using a 1D approach, until the possibility to implement culverts in D-Flow FM comes available.

Thirdly, the simulation time may play a large role in the choice for a modelling approach. As shown in chapter 6, the differences between the simulation time of a 1D model compared to a 2D model is approximately a factor 60. Especially when the goal is to make a quick estimate and run a few scenarios, constructing and simulating a 2D model might be unfeasible. When the study area is of comparable size to the Molenbeek catchment, a simulation time of more than five times the number of simulated days is to be expected. Of course, the simulation time depends on the available computational resources. If sufficient computational power is available, the disadvantage of the large simulation times may decrease.

Bibliography

- Abdelhaleem, F. S., Amin, A. M., & Ibraheem, M. M. (2016). Updated regime equations for alluvial Egyptian canals. *Alexandria Engineering Journal*, *55*(1), 505-512.
- Anees, M. T., Abdullah, K., Nawawi, M. N., Ab Rahman, N. N., Piah, A. R., Zakaria, N. A., . . . Omar, A. M. (2016). Numerical modeling techniques for flood analysis. *Journal of African Earth Sciences*, *124*, 478-486.
- Battjes, J. A., & Labeur, R. J. (2017). *Unsteady flow in open channels*. Cambridge University Press.
- Birniir, B. (2008). Turbulent Rivers. *Quarterly of Applied Mathematics*, *66*(3), 565-594.
- Bladé, E., Gómez-Valentín, M., Dolz, J., Aragón-Hernández, J. L., Corestein, G., & Sánchez-Juny, M. (2012). Integration of 1D and 2D finite volume schemes for computations of water flow in natural channels. *Advances in Water Resources*, *42*, 17-29.
- Blanckaert, K., & De Vriend, H. J. (2004). Secondary flow in sharp open-channel bends. *Journal of Fluid Mechanics*, *498*, 353-380.
- Blanckaert, K., & De Vriend, H. J. (2005). Turbulence characteristics in sharp open-channel bends. *Physics of Fluids*, *17*(5), 055102.
- Buffington, J. M., & Montgomery, D. R. (2013). Geomorphic classification of rivers. *Fluvial Geomorphology*, Vol. 9, 730-767.
- Chao, W. A., Zheng, S. S., Wang, P. F., & Jun, H. O. (2015). Interactions between vegetation, water flow and sediment transport: A review. *Journal of Hydrodynamics, Ser. B*, *27*(1), 24-37.
- Cheviron, B., & Moussa, R. (2016). Determinants of modelling choices for 1-D free-surface flow and morphodynamics in hydrology and hydraulics: a review. *Hydrology and Earth System Sciences*, *20*(9), 3799-3830.
- Deltares. (2017a). *D-Flow 1D (SOBEK 3) Hydrodynamics Technical Reference Manual*. Delft: Deltares.
- Deltares. (2017b). *D-Flow Flexible Mesh in Delta Shell User Manual*. Delft: Deltares.
- Deltares. (2017c). *D-Flow1D in Delta Shell User Manual*. Delft: Deltares.
- Deltares. (2018a). *SOBEK Hydrodynamics, Rainfall Runoff and Real Time Control*. Delft: Deltares.
- Deltares. (2018b). *RGFGRID: Generation and manipulation of structured and unstructured grids*. Delft: Deltares.
- Dimitriadis, P., Tegos, A., Oikonomou, A., Pagana, V., Koukouvinos, A., Mamassis, N., . . . Efstratiadis, A. (2016). Comparative evaluation of 1D and quasi-2D hydraulic models based on benchmark and real-world applications for uncertainty assessment in flood mapping. *Journal of Hydrology*, *534*, 478-492.
- Duinmeijer, S. P. (2002). *Verification of Delft FLS*.
- Dury, G. H. (1976). Discharge prediction, present and former, from channel dimensions. *Journal of Hydrology*, *30*(3), 219-245.
- Fernandez-Nieto, E. D., Marin, J., & Monnier, J. (2010). Coupling superposed 1D and 2D shallow-water models: Source terms in finite volume schemes. *Computers & Fluids*, *39*(6), 1070-1082.

- Finaud-Guyot, P., Delenne, C., Guinot, V., & Llovel, C. (2011). 1D–2D coupling for river flow modeling. *Comptes Rendus Mécanique*, 339(4), 226-234.
- Fox, R. (2015). Retrieved from <https://slideplayer.com/slide/6357250/>
- Graf, W., & Blanckaert, K. (2002). Flow around bends in rivers. Capri. Retrieved from Hindered Settling: <https://hinderedsettling.com/page/2/>
- Helpdesk Water. (2018, 05 14). *Baseline*. Retrieved from Helpdesk Water: <https://www.helpdeskwater.nl/onderwerpen/applicaties-modellen/applicaties-per/watermanagement/watermanagement/baseline/>
- Jongbloed, J. W. (1996). Three-dimensional modelling of secondary flow in river bends.
- Kurstjens ecologisch adviesbureau & Bureau Strooming. (2013). *Projectplan: Beekherstel Vierlingsbeekse Molenbeek*. 's Hertogenbosch: Waterschap Aa en Maas.
- Manning, R. (1889). On the flow of water in open channels and pipes. *Transactions of the Institutions of Civil Engineers in Ireland*, 20, 166-195.
- McMillan, H. K., & Brasington, J. (2007). Reduced complexity strategies for modelling. *Geomorphology*, 90(3-4), 226–243.
- Morales-Hernández, M., Petaccia, G., Brufau, P., & García-Navarro, P. (2016). Conservative 1D–2D coupled numerical strategies applied to river flooding: The Tiber (Rome). *Applied Mathematical Modelling*, 40(3), 2087-2105.
- Mosselman, E. (2014). Bank erosion, planimetric changes and river training. Delft: TU Delft.
- Néelz, S., & Pender, G. (2013). *Benchmarking the Latest Generation of 2D Hydraulic Modelling Packages*. UK: DEFRA/Environment Agency.
- Philips, J., & Tadayon, S. (2006). *Selection of Manning's roughness coefficient for natural and constructed vegetated and non-vegetated channels, and vegetation maintenance plan guidelines for vegetated channels in Central Arizona*. Virginia: US Geological Survey.
- Pietrzak, J. (2017). *An Introduction to Oceanography for Civil and Offshore Engineers*. Delft: Delft University of Technology.
- Rosgen, D. L. (1994). A classification of natural rivers. *Catena*, 22(3), 169-199.
- Singh, V. (2003). On the theories of hydraulic geometry. *International journal of sediment research*, 18(3), 196-218.
- Stelling, G. S., & Duinmeijer, S. A. (2003). A staggered conservative scheme for every Froude number in rapidly varied shallow water flows. *International journal for numerical methods in fluids*, 43(12), 1329-1354.
- Sündermann, J., & Holz, K. P. (2012). *Mathematical Modelling of Estuarine Physics: Proceedings of an International Symposium Held at the German Hydrographic Institute Hamburg, August 24–26, 1978*. Springer Science & Business Media.
- Teng, J., Jakeman, A. J., Vaze, J., Croke, B. F., Dutta, D., & Kim, S. (2017). Flood inundation modelling: A review of methods, recent advances and uncertainty analysis. *Environmental Modelling & Software*, 90, 201-216.

- Uittenbogaard, R. E., Van Kester, J. T., & Stelling, G. S. (1992). *Implementation of Three Turbulence Models in TRISULA for Rectangular Horizontal Grids: Including 2DV-testcases*. Delft: Delft Hydraulics.
- Warner, T. T. (2010). *Numerical weather and climate prediction*. Cambridge University Press.
- Williams, G. P. (1986). River meanders and channel size. *Journal of hydrology*, 88(1-2), 147-164.
- Zijlema, M. (2015). *Computational Modelling of Flow and Transport*. Delft: Delft University of Technology.

Appendices

A. Secondary flow

Secondary flow is also called spiral or helical motion. It is a process that mainly occurs in river bends. Due to the curvature of the river, a cross-sectional pressure gradient occurs. This creates flow from the outer bend towards the inner bend. This causes a cross-stream circulation cell to occur (Jongbloed, 1996; Blanckaert & De Vriend, 2004). A year later, the latter authors published an article on an experiment they performed about turbulence characteristics in sharp open-channel bends (Blanckaert & De Vriend, 2005). In this research they showed that there occur more turbulent processes which are not incorporated in current turbulence closure models. Spiral motion has a key role for bank erosion and is therefore of importance to hydraulic modelling (Mosselman, 2014). This is depicted in the figure below.

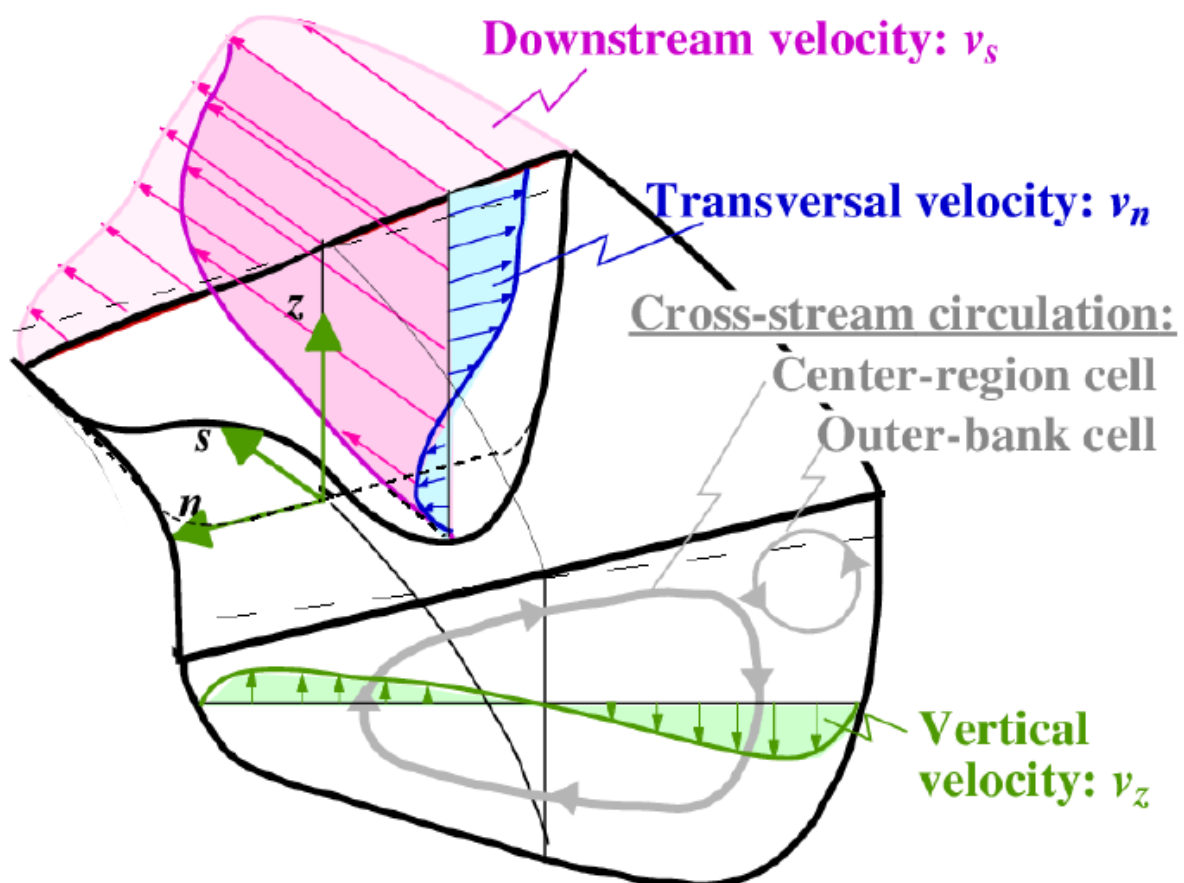


Figure A-1: River bend processes (Graf & Blanckaert, 2002)

B. Dimensionless numbers

From the flow equations, described in paragraph 3.1.2, dimensionless numbers can be derived that say something about the analyzed system. In comparing spatial scales this could point out some of the differences between these scales. The dimensionless numbers that will be analyzed here are the Reynolds number and the Froude number. These numbers can be derived by non-dimensionalizing the Navier-Stokes momentum equation. Assuming an incompressible flow, no Coriolis effect in rivers and no external sources or sinks, the following general equation of the Navier-Stokes equations is obtained:

$$\frac{\partial u}{\partial t} + (u * \nabla)u = -\frac{1}{\rho}\nabla p + \nu\nabla^2 u + g \quad B.1$$

The parameters are non-dimensionalized in the following way:

$$\nabla^* = \nabla L, u^* = u/U, t^* = t/(L/U), p^* = p/(\rho U^2), g^* = g/\hat{g}$$

where

$$L = \text{typical length scale [m]}$$

If these parameters are substituted into equation B.1 the following result is obtained:

$$\frac{U^2}{L} \frac{\partial u^*}{\partial t^*} + \frac{U^2}{L} (u^* * \nabla^*)u^* = -\frac{1}{\rho} \frac{\rho U^2}{L} \nabla^* p^* + \frac{\nu U}{L^2} \nabla^{*2} u^* + g^* \hat{g} \quad B.2$$

In this equation the factor U^2/L is present three of five terms. If all terms are divided by this term, we obtain the following equation:

$$\frac{\partial u^*}{\partial t^*} + (u^* * \nabla^*)u^* = -\nabla^* p^* + \frac{\nu}{UL} \nabla^{*2} u^* + \frac{L\hat{g}}{U^2} g^* \quad B.3$$

From this equation two dimensionless parameters can be derived, in the following way:

$$\frac{\partial u^*}{\partial t^*} + (u^* * \nabla^*)u^* = -\nabla^* p^* + \frac{1}{Re} \nabla^{*2} u^* + \frac{1}{Fr^2} g^* \quad B.4$$

This means these numbers are defined as following:

$$Re = \frac{UL}{\nu} \quad B.5$$

$$Fr = \frac{U}{\sqrt{gL}} \quad B.6$$

In both cases L is a typical length scale for the analyzed system. In the case of the Reynolds number, this is typically seen as the hydraulic radius of the system, denoted as R . In river or stream systems, this radius is calculated by dividing the flow area A by the wetted perimeter P . For most river cases, R is more or less equal to the river depth. But for this case, the comparison between two spatial scales, small differences can be important. Therefore, this assumption is not used in the equations.

In the case of the Froude number, this typical length scale is represented by the hydraulic depth of the channel, denoted as D . This is calculated by dividing the flow area A by the top width of the flow B . Furthermore, for simplicity and uniformity U will be replaced by u . Finally, the following equations are obtained:

$$Re = \frac{uR}{\nu} \quad B.7$$

$$Fr = \frac{u}{\sqrt{gD}} = \frac{u}{c} \quad B.8$$

where

$c = \text{wave celerity [m/s]}$

C. Grid criteria

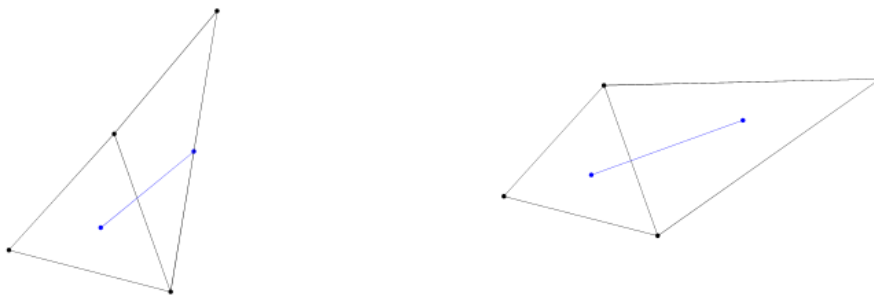
A computational grid should meet some criteria, of which the most important will be discussed here: the orthogonality and the smoothness.

Orthogonality

The orthogonality of a grid is defined as the cosine of the angle between a flow link and a net link. In the figure below, the black lines represent net links, the blue lines represent flow links. The cosine of an angle of 90° is 0, which corresponds with perfect orthogonality. Figure C-1b shows an example of perfect orthogonality.

Smoothness

The smoothness of a grid is defined as the ratio between two adjacent cells. In an ideal situation this value is 1, which means that both areas are equal. Figure C-1a gives an example of perfect smoothness.



(a) *Perfect smoothness, but poor orthogonality.*

(b) *Perfect orthogonality, but poor smoothness*

Figure C-1: Examples of smoothness and orthogonality (Deltares, 2017b)

It is obvious that the perfect situation is not schematized here. An example of a perfect situation is given below.

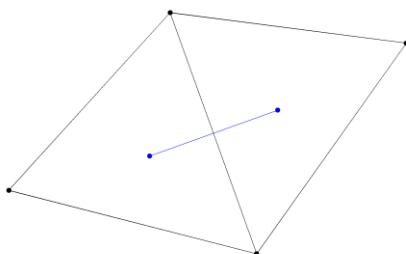


Figure C-2: Example of perfect smoothness and orthogonality (Deltares, 2017b)

In practice, the perfect situation is very hard to obtain in all locations. During this research a maximum value of 0.05 for orthogonality has been applied, both in the theoretical models as the case area model. The orthogonality is by far the most important of the two criteria, because the model cannot perform simulations when this parameter is too large. The smoothness is particular important in the flow areas, but is not problematic for simulations (Deltares, 2018b). Therefore, in the areas of interest, this parameter has been kept as low as possible.